The Dissertation Committee for Devin Alexander Matthews
certifies that this is the approved version of the following dissertation:

Non-orthogonal Spin-adaptation and Application to Coupled Cluster up to Quadruple Excitations

Committee:

John Stanton, Supervisor

Jennifer Brodbelt

Dmitrii Makarov

Peter Rossky

Robert van de Geijn

Non-orthogonal Spin-adaptation and Application to Coupled Cluster up to Quadruple Excitations

by

Devin Alexander Matthews, B.S.Ch.

DISSERTATION

Presented to the Faculty of the Graduate School of

The University of Texas at Austin

in Partial Fulfillment

of the Requirements

for the Degree of

DOCTOR OF PHILOSOPHY

THE UNIVERSITY OF TEXAS AT AUSTIN

August 2014

Dedicated to my wife Michelle and my children Alex and Anna.

Acknowledgments

I would like to thank Dr. John Stanton for being my mentor and advisor for nearly eight long years. I am forever grateful for the never-ending encouragement and guidance I have received, and the freedom I have enjoyed to pursue whatever crazy ideas I tend to come up with. I would also like to thank the members of the Stanton group past and present for their help and hospitality over the years. I would like to thank Drs. Jeff Hammond and Robert van de Geijn for almost turning me into a computer scientist. I also thank Drs. Josh Baraban and Greg Tschumper, and all of the CFOUR developers for beta-testing my CCSDT(Q) and CCSDTQ implementations. Lastly I would like to thank Dr. Jürgen Gauss for his pioneering work on closed-shell CCSDT.

My wife, Michelle, I would like to thank on a practical note for editing this manuscript, but also for her infinite patience with me throughout my undergraduate and graduate studies. I promise that when I graduate, I won't say, "...when I graduate..." anymore.

Non-orthogonal Spin-adaptation and Application to Coupled Cluster up to Quadruple Excitations

Publication No. __________________

Devin Alexander Matthews, Ph.D.
The University of Texas at Austin, 2014

Supervisor: John Stanton

The theory of non-orthogonal spin-adaptation for closed-shell molecular systems is presented, with an emphasis on application to the coupled cluster family of electronic structure methods. To aid in the derivation of efficient and compact working equations, a new diagrammatic interpretation of the Goldstone diagrams is derived which only requires a small number of the many distinct diagrams and which directly produces equations in a factored form in terms of "spin-summed" tensor elements. This diagrammatic interpretation is applied to coupled cluster methods with quadruple excitations (CCSDTQ), including coupled cluster with a perturbative correction for quadruple excitations (CCSDT(Q)) and to CCSDTQ gradients and properties. The advantages of the non-orthogonal spin-adaption with respect to simplification and factorization of the working equations and to efficient implementation are presented and discussed. Additionally, specific optimizations of the implementation for often-overlooked issues such as tensor transposition, disk access, and removal of redundant and/or unnecessary operations are detailed. The resulting algorithm is implemented for the CCSDTQ and CCSDT(Q) methods and compared to existing codes, where a one to two order-of-magnitude improvement in efficiency is observed. The new implementation is also used for calculations on several larger molecular systems to illustrate the scalability of the method.

Table of Contents

List of Tables

List of Figures

Chapter 1

Introduction

1.1 The Need for High Accuracy in Quantum Chemistry

Among the most successful electronic structure methods today are those based on the coupled cluster approximation.[1–6] Out of this general family, CCSD(T) (coupled cluster singles and doubles with perturbative triples),[7,8] has been so successful as to have been called the "gold standard" of electronic structure theory. However, the success of CCSD(T) is not universal. For calculations which require extreme accuracy – especially in the range of what is commonly called "sub-chemical" accuracy (e.g. < 1 kJ/mol for bond energies and other thermochemical quantities) – CCSD(T) by itself is insufficient even at the basis set limit.[9,10] Additionally, the presence of multi-reference character in the electronic wavefunction poses a formidable challenge for CCSD(T) as it is based on a truncated, single-reference description of the wavefunction.

In the first case, accuracy can be increased by using a method which provides a more rigorous accounting of the correlation energy, which for coupled cluster means moving to higher levels of excitation such as full triple and then quadruple excitations. In the second case, a truly multi-reference description of the wavefunction is perhaps the "right" way to approach the problem, but doing so within the coupled cluster framework (to maintain its extremely useful characteristics such as size extensivity) is not straightforward and is still an area of ongoing research.[11–19] However, the nature of coupled cluster suggests and practical experience[20–22] confirms that simply adding higher levels of excitation can (to a point) ameliorate multi-reference effects.

The need for extreme levels of accuracy is a very real problem in quantum chemistry, and is continually becoming more important as theory takes on a more predictive role, augmenting (and sometimes identifying problems with) experimental data. As larger and more complex molecular systems are studied, there are commonly many conformational structures which are very close in energy. Accurately ranking these (not necessarily chemically- or spectroscopically-similar) structures and then further accurately computing their structural properties is critical to describing the total system.[23–26] In a related field, extremely accurate determinations of the energy of minima and transition states is critical to obtaining good kinetic and thermodynamic predictions, even for well-isolated structures.[27–30] In an unrelated field, extreme accuracy in the description of the electronic wavefunction is necessary to accurately describe properties such as the nuclear quadrupole coupling moment, which has a strong dependence on the electronic structure. Accurate values of these constants are necessary to calculate useful predictive hyperfine spectra of molecular (or even atomic) systems.[31–33] Other electronic properties such as optical rotation are also heavily dependent on the quality of description of the electronic structure, requiring very accurate calculations to achieve convergence.[34,35]

1.2 Coupled Cluster Theory

Coupled cluster is a wavefunction-based method – that is, it provides a way to compute a wavefunction (which may be an approximation of the exact wavefunction) of a molecular system and, through the Schrödinger equation, defines the energy and other properties of the system. The specific wavefunction form prescribed by coupled cluster is an exponential excitation operator applied to some reference state,[1,2,36–38]

$$|\Psi_{CC}\rangle \quad = \quad e^{\hat{T}}|\Phi_0\rangle \tag{1.1}$$

The function $|\Phi_0\rangle$ is a single-particle wavefunction, i.e. it has no direct interaction between electrons (although it has indirect interactions for example through the self-consistent field procedure). The purpose of coupled cluster then is to account for this lack of electronic interaction, called electron correlation. While the electron correlation is usually only a small fraction of the total energy (about 10%), it is critical in quantitatively describing any molecular property. Furthermore, for high accuracy calculations, the correlation energy must be calculated to a very high accuracy itself, often to greater than 95%.

Fortunately, coupled cluster provides a roadmap for achieving this goal, in that the level of accuracy (and level of cost of course) of the calculation can be controlled by the cluster operator $\hat{T}$. In second-quantized terms, this operator annihilates electrons in orbitals (single-particle functions) which are occupied in the reference state $|\Phi_0\rangle$, and then creates an equal number in previously unoccupied (virtual) orbitals. The effect is to "excite" these electrons into higher orbitals. The total excitation operator can then be broken down into a sum over operators which excite a particular number of electrons simultaneously, up to a maximum number of excitations N which controls the accuracy,

$$\hat{T} = \sum_{k=1}^{N} \hat{T}_k \tag{1.2}$$

$$\hat{T}_k = \frac{1}{(k!)^2} \sum_{a_1 \dots a_k i_1 \dots i_k} t_{i_1 \dots i_k}^{a_1 \dots a_k} a_{a_1}^\dagger \dots a_{a_k}^\dagger a_{i_k} \dots a_{i_1} \tag{1.3}$$

These operators are defined in terms of second-quantized annihilation operators (a_p) and creation operators ($a_p^\dagger$), which perform the actual electron excitation, and a set of weights $t_{i_1 \dots i_k}^{a_1 \dots a_k}$ called amplitudes. The a indices run over virtual (unoccupied) orbitals and the i indices over occupied orbitals. The exponential nature of the wavefunction provides size extensivity,[36] meaning that the energy and wavefunction are separable in the limit of non-interacting fragments, and the implicit inclusion of some of the effects of higher-order excitations when the excitation operator $\hat{T}$ is truncated (i.e. $N < n_{elec}$, when $N = n_{elec}$ coupled cluster gives the complete correlation energy). The value of N defines the particular coupled cluster method, with $N = 2$ for CCSD, $N = 3$ for CCSDT, $N = 4$ for CCSDTQ etc.

Given the form of the wavefunction, the task is then to determine how to solve for the values of the amplitudes $t_{i_1 \dots i_k}^{a_1 \dots a_k}$ and then use them to compute the energy. Inserting the coupled cluster wavefunction into the Schrödinger equation gives,

$$\hat{H}e^{\hat{T}}|\Phi_0\rangle = E_{CC}e^{\hat{T}}|\Phi_0\rangle \tag{1.4}$$

It is possible to solve for the coupled cluster amplitudes by variationally minimizing the energy. However, since the wavefunction is defined in terms of an exponential operator, the expansion of the resulting equations does not terminate cleanly. Instead, the equations are solved by projection, where the inverse of the exponential operator is applied from the left, followed by some single-particle "bra" state. When this state is the reference, the energy is obtained,

$$\begin{aligned}\langle\Phi_0|e^{-\hat{T}}\hat{H}e^{\hat{T}}|\Phi_0\rangle &= \langle\Phi_0|e^{-\hat{T}}E_{CC}e^{\hat{T}}|\Phi_0\rangle \\ &= \langle\Phi_0|E_{CC}|\Phi_0\rangle \\ &= E_{CC}\end{aligned} \tag{1.5}$$

since the reference state is normalized. When the applied "bra" state is an excited state (i.e. one in which electrons have been moved from occupied to virtual orbitals), a set of coupled non-linear equations are obtained,

$$\begin{aligned}\langle\Phi_{i_1\ldots i_k}^{a_1\ldots a_k}|e^{-\hat{T}}\hat{H}e^{\hat{T}}|\Phi_0\rangle &= \langle\Phi_{i_1\ldots i_k}^{a_1\ldots a_k}|e^{-\hat{T}}E_{CC}e^{\hat{T}}|\Phi_0\rangle \\ &= \langle\Phi_{i_1\ldots i_k}^{a_1\ldots a_k}|E_{CC}|\Phi_0\rangle \\ &= 0\end{aligned} \tag{1.6}$$

since now the single-particles states are orthogonal. The "excited" single-particle states can be defined similarly to $\hat{T}$ by,

$$\langle\Phi_{i_1\ldots a_k}^{a_1\ldots a_k}| = \langle\Phi_0|a_{a_1}\ldots a_{a_k}a_{i_k}^{\dagger}\ldots a_{i_1}^{\dagger} \tag{1.7}$$

When as many states $\langle \Phi_{i_1 \ldots i_k}^{a_1 \ldots a_k}|$ are projected onto as there are $t_{i_1 \ldots i_k}^{a_1 \ldots a_k}$, then the equations define the amplitudes.

The combination of operators $e^{-\hat{T}} \hat{H} e^{\hat{T}}$ has special significance, as it essentially fills the role of the Hamiltonian in a non-symmetric analogue to the Schrödinger equation,

$$e^{-\hat{T}} \hat{H} e^{\hat{T}} |\Phi_0\rangle = E_{CC} |\Phi_0\rangle, \text{ but } \langle \Phi_0 | e^{-\hat{T}} \hat{H} e^{\hat{T}} \neq \langle \Phi_0 | E_{CC} \tag{1.8}$$

This combination is commonly referred to as $\bar{H}$, and is important also for the description of excited states, response properties, and so on. This operator has an interesting structure due to the expansion of the exponential operators. Using the Baker-Campbell-Hausdorff formula,

$$\begin{aligned} e^{-\hat{T}} \hat{H} e^{\hat{T}} &= \hat{H} + [\hat{H}, \hat{T}] + \frac{1}{2}[[\hat{H}, \hat{T}], \hat{T}] \\ &\quad + \frac{1}{6}[[[\hat{H}, \hat{T}], \hat{T}], \hat{T}] + \frac{1}{24}[[[[\hat{H}, \hat{T}], \hat{T}], \hat{T}], \hat{T}] \ldots \end{aligned} \tag{1.9}$$

The use of Wick's theorem[39] to calculate matrix elements results in "contractions" between pairs of annihilation and creation operators of the form,

$$\overbracket{a_a a_b^\dagger}, \quad \overbracket{a_i^\dagger a_j} \tag{1.10}$$

Looking at the operators in $\hat{T}$, it is clear that it may only be contracted with an operator on the left. However, an operator appearing to the left doesn't necessarily result in a contraction, so that two cases are possible,

$$\hat{X}\hat{T} \longrightarrow \textit{contracted} + \textit{uncontracted} \tag{1.11}$$

$$\hat{T}\hat{X} \longrightarrow \textit{uncontracted} \tag{1.12}$$

Thus, by applying the commutator, we retain only the contracted terms,

$$\begin{aligned} [\hat{X},\hat{T}] &= \hat{X}\hat{T}-\hat{T}\hat{X} \\ &= (contracted + uncontracted) - uncontracted \\ &= contracted \end{aligned} \tag{1.13}$$

The nested commutators in the CBH expansion select terms where $\hat{H}$ is contracted by at least one operator with each $\hat{T}$ to the right. Recognizing the $\hat{T}$ expansion as the Taylor expansion of the exponential, we can apply the much abbreviated notation,

$$\bar{H} = \left(\hat{H}e^{\hat{T}}\right)_c \tag{1.14}$$

where the subscript c denotes that each $\hat{T}$ must be contracted with $\hat{H}$. Since the Hamiltonian contains at most four operators and each one may only be contracted once, the expansion of the exponential terminates naturally at $\hat{T}^4$.

As an additional simplifying step, the Hamiltonian is converted to normal order (i.e. to a form where no contractions between operators within $\hat{H}$ are possible using Wick's theorem),

$$\hat{H} = \hat{T} + \hat{V} \rightarrow \hat{H}_N = \hat{F}_N + \hat{V}_N = \hat{H} - \langle\Phi_0|\hat{H}|\Phi_0\rangle \tag{1.15}$$

The $\hat{F}_N$ operator is the usual Fock matrix from self-consistent field (SCF) theory[40–43] and the expectation value $\langle\Phi_0|\hat{H}|\Phi_0\rangle$ is the SCF energy. The Hamiltonian can then be written quite simply using second-quantized operators as,

$$\hat{H}_N = \sum_{pq} f^p_q\{a^\dagger_p a_q\}_N + \frac{1}{4}\sum_{pqrs} v^{pq}_{rs}\{a^\dagger_p a^\dagger_q a_s a_r\}_N \tag{1.16}$$

where all indices are summed over both occupied and virtual orbitals, while $\{\ldots\}_N$ indicates that the enclosed operators are in normal order, i.e. no contractions are to be done between operators inside the braces. From this point, all operators are assumed to be in their normal ordered form (the $\hat{T}$ operator is already in normal-ordered form naturally). Finally, the equations for the energy and for the amplitudes may be represented schematically by using a tensor notation. Here, we write the Hamiltonian as $\mathbf{H} = \mathbf{F} + \mathbf{V} = \mathbf{F}' + \mathbf{D} + \mathbf{V}$ where the tensor $\mathbf{D}$ contains the diagonal elements of $\mathbf{F}$ (which for an SCF reference are sums of orbital energies), and the amplitudes as $\mathbf{T}$ (if amplitudes of a specific excitation level k are needed, they are represented as $\mathbf{T}_k$). It is implicitly understood that all terms must be contracted. The amplitude equations then become,

$$0 = \mathbf{F} + \mathbf{V} + \mathbf{FT} + \mathbf{VT} + \tfrac{1}{2}\mathbf{FT}^2 + \tfrac{1}{2}\mathbf{VT}^2 + \tfrac{1}{6}\mathbf{VT}^3 + \tfrac{1}{24}\mathbf{VT}^4 \tag{1.17}$$

$$\downarrow$$

$$-\mathbf{DT} = \mathbf{F} + \mathbf{V} + \mathbf{F}'\mathbf{T} + \mathbf{VT} + \tfrac{1}{2}\mathbf{FT}^2 + \tfrac{1}{2}\mathbf{VT}^2 + \tfrac{1}{6}\mathbf{VT}^3 + \tfrac{1}{24}\mathbf{VT}^4 \tag{1.18}$$

$$\downarrow$$

$$\mathbf{Z} \equiv \mathbf{F} + \mathbf{V} + \mathbf{F}'\mathbf{T} + \mathbf{VT} + \tfrac{1}{2}\mathbf{FT}^2 + \tfrac{1}{2}\mathbf{VT}^2 + \tfrac{1}{6}\mathbf{VT}^3 + \tfrac{1}{24}\mathbf{VT}^4 \tag{1.19}$$

and the energy equation is (including only terms which are non-zero after applying Wick's theorem),

$$E = \mathbf{FT} + \mathbf{VT} + \frac{1}{2}\mathbf{VT}^2 \tag{1.20}$$

where the $\mathbf{T}$ operators in this expression must not only be connected to the Hamiltonian (i.e. at least one operator contracted), they must be fully contracted with it (such fully-contracted expression are commonly referred to as "closed").

The procedure for obtaining the coupled cluster energy is then: first, solve the amplitude equations by first setting $\mathbf{T} = -\mathbf{D}^{-1}(\mathbf{F} + \mathbf{V})$, then iteratively solve for $\mathbf{Z}$, obtain a new $\mathbf{T}$ as $-\mathbf{D}^{-1}\mathbf{Z}$, and repeat until the change in $\mathbf{T}$ is small enough, and second, calculate the energy from the converged $\mathbf{T}$.

1.3 Diagrammatic Form of the Coupled Cluster Equations

Using Wick's theorem to calculate the individual matrix elements in equation (1.5) and equation (1.6) is straightforward but tedious. The overall factor of unique terms is most commonly 1, with the presence of identically contracted $\hat{T}$ operators sometimes bringing this down to $\frac{1}{2}$ or $\frac{1}{4}$. On the other hand, the numerical factor on terms generated by Wick's theorem is a product of the factor from the expansion of $e^{\hat{T}}$ and any factors from equation (1.3) or equation (1.16). For terms from a combination like $\frac{1}{2}\mathbf{V}\mathbf{T}_1^2\mathbf{T}_3$, the Wick's theorem prefactor is $\frac{1}{2} \cdot \frac{1}{4} \cdot \frac{1}{6^2} = \frac{1}{288}$, meaning that for each unique term, there are 288 (assuming a final factor of 1) different contractions which must be enumerated.

An alternative method of generating the matrix elements is by the use of diagrams.[1,2,44–46] In this method, a graphical representation of the Hamiltonian and $\hat{T}$ operators is manipulated to represent individual terms of the final equations, with a one-to-one correspondence between (topologically) unique

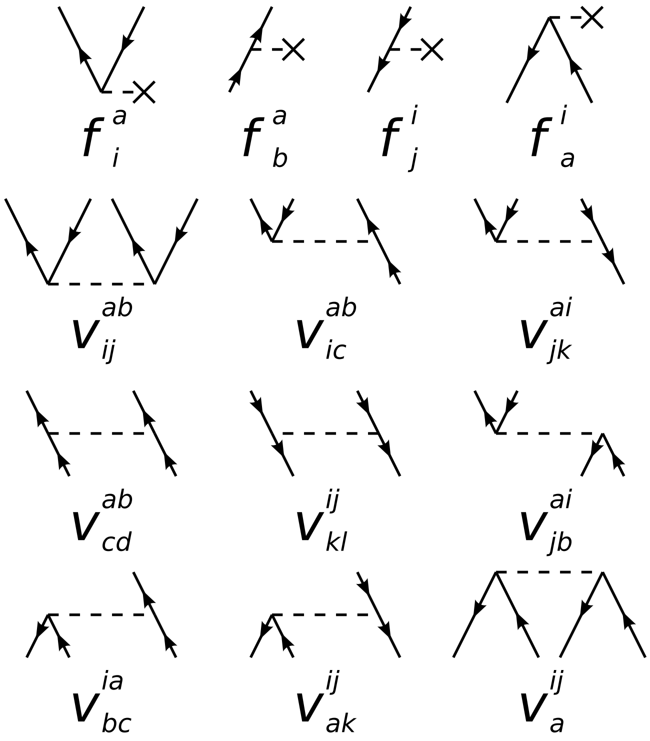

Figure 1.1: The normal-ordered Hamiltonian in the Brandow diagrammatic representation.

diagrams and unique terms. The most common form of diagrams are the Brandow (also called antisymmetrized Goldstone) diagrams.[46] In this form, the Hamiltonian is represented by a collection of 13 "vertices", as depicted in figure 1.1.

The operators in the diagrammatic form are represented by horizontal lines, called vertices. These vertices have one or more semi-vertical lines emanating from them, corresponding to the component second-quantized operators, or, referring to the tensor elements such as v^{pq}_{rs} and $t^{a_1 \ldots a_k}_{i_1 \ldots i_k}$, corresponding to the tensor indices. Upward-directed lines, as indicated by arrows, refer to

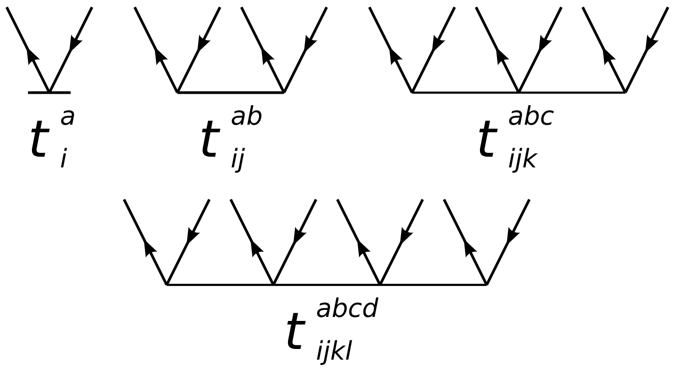

Figure 1.2: The cluster operator in the Brandow diagrammatic representation.

operators and indices over virtual orbitals (labeled in this work with the letters $abcdefgh$), while downward-directed lines refer to occupied orbitals (labeled with the letters $ijklmnop$). Additionally, lines which are directed away from the vertex (i.e. upward and above, or downward and below) correspond to creation operators or upper indices of tensors, while inward-directed lines correspond to annihilation operators or lower tensor indices. Thus, it can be seen that the 13 diagrams in figure 1.1 correspond to all possible assignments of the $pqrs$ operators/indices of the Hamiltonian to either the virtual or occupied orbital set. The coupled cluster amplitudes can be represented similarly as shown in figure 1.2, where the vertices are distinguished from the Hamiltonian by a solid rather than a dashed line.

Matrix elements can be constructed by taking the vertices of all operators in the expression, placing them in top-to-bottom order as they appear in the expression left-to-right, and then connecting lines on the bottom of higher vertices with lines on the top of lower ones. The lines must be contracted such that virtual (upward) lines are connected with virtual lines and occupied with occupied. Furthermore, lines which are left uncontracted must match the single-particle states on the left and right of the matrix element. For example, a matrix element with states $\langle\Phi_{ij}^{ab}|\ldots|\Phi_k^c\rangle$ would need two virtual and two occupied uncontracted lines extending above the diagram (for the left state) and one virtual and one occupied line extending below. These uncontracted lines are called "external" lines, and are labeled with the same letters as the indices on the single-particle states. Lines which are contracted between two vertices are given a single label (in connection with Wick's theorem, this corresponds to summation over both lines and a Kronecker delta).

There are often multiple ways to contract the lines of the vertices together within the restrictions given. Some of the possibilities are identical, since the anticommutation of the second-quantized operators results in antisymmetry of the lines on a given vertex. For example, considering the diagram for v_{ij}^{ab}, both the pair of virtual lines and the pair of occupied lines may be switched with the only result being a change in sign of the tensor element, i.e. $v_{ij}^{ab} = -v_{ij}^{ba} = -v_{ji}^{ab} = v_{ji}^{ba}$. The same is true for the remaining Hamiltonian elements and for the amplitudes, although for $\hat{T}_3$ and higher permutations of three or more lines/indices are also possible. So, the diagrams which must be considered are those that are *topologically distinct*, that is diagrams which are not related by a permutation of lines on the vertices. Since the order and position of the contracted lines is not important, the diagrams may simply be classified by the number of occupied and virtual lines contracted between each

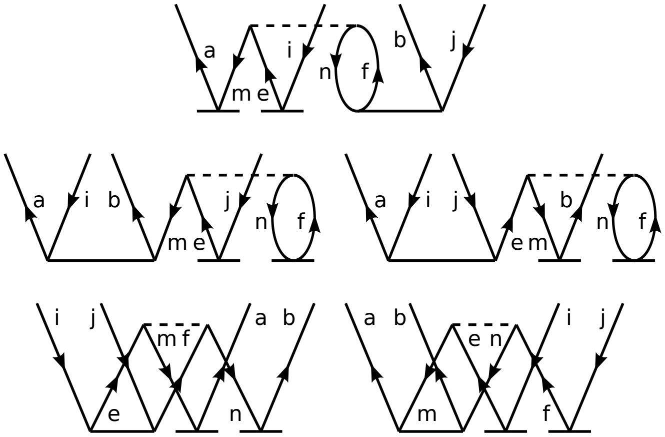

Figure 1.3: Topologically unique diagrams for the matrix element $\langle\Phi_{ij}^{ab}|\frac{1}{2}\hat{H}_N\hat{T}_2\hat{T}_1^2|\Phi_0\rangle$.

pair of vertices. To illustrate this point, the topologically unique diagrams for the matrix element $\langle\Phi_{ij}^{ab}|\frac{1}{2}\hat{H}_N\hat{T}_2\hat{T}_1^2|\Phi_0\rangle$ are given in figure 1.3. Note that since the single-particle state on the right, $|\Phi_0\rangle$, is the (Fermi) vacuum, there are no lines extending downward from the diagrams. This is the case for all of the diagrams in the amplitude equations. Since the coupled cluster energy also has $\langle\Phi_0|$ on the left, it can't have any external lines at all, leading to only "closed" diagrams.

To produce equations from the diagrams, a set of rules is used to interpret the diagrams. These rules determine which tensor elements are needed, what numerical factors and sign the term has, which indices should be summed over, and what other operations must be applied to the expression. The rules for the Brandow diagrams are:[46]

R1. Each vertex contributes a tensor element $X_{all-in-labels}^{all-out-labels}$, where the identity of X is determined by the type of the line. Dashed lines are Hamiltonian elements, solid lines are cluster amplitudes, and wavy lines are intermediates.

R2. Each set of n identical lines (lines of the same type, going the same direction, between the same vertices) gives a factor of $\frac{1}{n!}$.

R3. The overall sign is equal to $(-1)^{l+h}$, where l is the number of loops (a path which either goes from one point along contracted lines returning to that same point, or from an external line to another external line on the same side) and h is the number of occupied (hole) lines.

R4. Each set of n identically-connected vertices from an exponential expansion (e.g. the coupled cluster amplitudes) gives a factor of $\frac{1}{n!}$.

R5. Contracted lines are summed over all spin-orbitals.

R6. External lines of the same type (*in/out*, *hole/particle*) which appear on different vertices are antisymmetrized.

Using these rules, we find for the value of the first diagram in figure 1.3,

$$-P(ab)P(ij)\sum_{efmn} v_{ef}^{mn} t_{ni}^{fb} t_{m}^{a} t_{i}^{e} \tag{1.21}$$

Rule 1 determines the tensor elements, while rule 2 does not apply in this case. Rule 3 gives a sign of -1 since there are three loops and four occupied lines. Rule 4, even though there are two $\hat{T}_1$ vertices from the exponential, has no effect, since the vertices are not connected the same way (so that we are implicitly counting both the identical cases of “$t_m^a t_i^e$” and “$t_i^e t_m^a$” each with the proper factor of $\frac{1}{2}$). Rule 5 gives the summation of the contracted $efmn$ indices. Finally, rule 6 gives the factors $P(ab)P(ij)$, where for example $P(pq)X[\ldots p \ldots q \ldots] = X[\ldots p \ldots q \ldots] - X[\ldots q \ldots p \ldots]$. These factors ensure the antisymmetry of the matrix element. Similarly, we can derive the equations for all of the diagrams giving

$$\begin{aligned}\langle \Phi_{ij}^{ab} | \frac{1}{2} \hat{H}_N \hat{T}_2 \hat{T}_1^2 | \Phi_0 \rangle &= -P(ab)P(ij) \sum_{efmn} v_{ef}^{mn} t_{ni}^{fb} t_m^a t_i^e - P(ij) \sum_{efmn} v_{ef}^{mn} t_{im}^{ab} t_i^e t_n^f \\ &\quad -P(ab) \sum_{efmn} v_{ef}^{mn} t_{ij}^{ae} t_m^b t_n^f + \frac{1}{4} P(ab) \sum_{efmn} v_{ef}^{mn} t_{ij}^{ef} t_m^a t_n^b \\ &\quad + \frac{1}{4} P(ij) \sum_{efmn} v_{ef}^{mn} t_{mn}^{ab} t_i^e t_j^f \qquad (1.22)\end{aligned}$$

where the terms in the RHS are given in the same order as the diagrams. Note that the last two terms now have numerical factors: a $\frac{1}{2}$ from rule 2 since either two virtual or two occupied lines run from the Hamiltonian to $\hat{T}_2$, and a factor of $\frac{1}{2}$ from rule 4 since there are two identically-connected $\hat{T}_1$ vertices. The entire amplitude equations are not given here as Brandow diagrams or spin-orbital equations (as the equations above are, since each label runs over both spin-α and spin-β orbitals). Instead, a new form of diagrammatic interpretation will be derived for the case of a closed-shell system, where spin may be removed from the equations.

1.4 Quadruple Excitations

Given the need for very high accuracy in quantum chemical calculations, and the possibility of the coupled cluster method to attain this through systematic improvement of the wavefunction description (increasing N), the obvious question is then, "What level of excitation is sufficient?" For thermodynamic and kinetic problems, experience with protocols such as HEAT[47–49] and W4[50–52] show that full quadruple excitations (CCSDTQ)[53] are "essentially exact" for most problems of chemical interest. CCSDTQ calculations on biradical systems (perhaps the most commonly encountered and practically important class of multi-reference problem) such as ozone and C_2[20–22,54–56] show that again, CCSDTQ gives a highly accurate description of the electronic correlation despite still being based on a single-reference description. What about those cases that need a still more accurate description of correlation? Previous studies of excitations beyond quadruples show that, in general, the additional contribution of pentuple excitations (CCSDTQP) is small, not only compared to the CCSDTQ contribution, but can even be smaller than the hextuple excitations (CCSDTQPH) in some cases.[22] Thus, if one were to be really serious about wringing out the last drop of correlation energy, one should go two levels of excitation further. In terms of computational cost, though, this requires going from an $\mathscr{O}(n^{10})$ method (CCSDTQ), where n scales with the system size, to a whopping $\mathscr{O}(n^{14})$ method (CCSDTQPH). What's more, non-iterative approximations to CCSDTQ such as CCSDT(Q) and CCSDT(Q)$_\Lambda$[57,58] often gain nearly the same level of accuracy as full CCS-

DTQ with "only" an $\mathscr{O}(n^9)$ cost. As $\mathscr{O}(n^9 - n^{10})$ is already at (or beyond) the limit of computational feasibility even for small molecules and basis sets, it is clear that CCSDTQ and its approximations are the most accurate practical electronic structure methods available for non-trivial problems. The combination of extreme accuracy and (relative) computational savings for CCSDT(Q) et al. presents the opportunity to establish a new "platinum standard" for electronic structure calculations.

Since CCSDTQ is so important to high-accuracy calculations, it is naturally desirable to have an efficient computer implementation. Here I present such an implementation and describe how both the use of a non-orthogonally spin-adapted representation (for closed-shell cases) and a focus on optimization of the program architecture provide for highly efficient yet modular and (in terms of code complexity and maintainability) manageable code.

Chapter 2

Non-orthogonal Spin-adaptation

In this chapter, the usual rules for interpreting coupled cluster diagrams in terms of spin-orbital Hamiltonian and amplitude elements are translated to an algebraic equation using permutation operators. The relationship between the spin-orbital and "orbital" or spin-free amplitudes (described below), also written in terms of algebraic permutations, is then used, along with several important theorems, to rearrange the spin-orbital equation into an orbital one. The orbital equation is then further manipulated to expose two types of special permutation operators, denoted spin-summation operators, which can be used to factorize and simplify the equation. Lastly, the resulting algebraic equation is translated back into diagrammatic rules which can be used to generate compact, efficient equations in terms of orbital amplitudes and Hamiltonian elements.

2.1 From Spin-orbital to Orbital

The amplitudes, Hamiltonian elements, and diagrammatic rules presented in the previous chapter are all in what is called the spin-orbital representation. In this representation, each orbital label, whether it runs over occupied or virtual orbitals or both, encompasses orbitals with both spin-α (or spin up) and spin-β (spin-down) spin functions augmenting a spatial part. The product or the spin and spatial (orbital) functions is the total spin-orbital function, of which there are an equal number of α and β spin in total. However, there may be an unequal number of α and β orbitals which are occupied in the single-particle reference function, and the spatial parts may be different for the α and β spin functions, for example in UHF calculations[43] (also called DODS – different orbitals for different spins). In this case, the α and β spin-orbitals functions are completely different and must be handled separately. The spin-orbital functions are still separable, though, and the spin parts may be integrated over separately when forming matrix elements. Due to the spin-selection rules of the spin-independent Hamiltonian, only matrix elements which conserve both the number of α and β spin electrons are non-zero. The amplitudes may have non-zero total spin, but the spin-projection quantum number must be zero, so that again there must be an equal number of α and β annihilation and, separately, creation operators. Exceptions to this rule do sometimes occur: for example in coupled cluster equation-of-motion theory (CC-EOM), where an excitation operator is used which may ionize or attach an electron (so that the spin-projection quantum number is $\pm\frac{1}{2}$)[59] or change the total spin of the wavefunction (i.e. a spin-projection quantum number of ± 1).[60]

The spin-orbital tensors such as v^{pq}_{rs} and the amplitudes may then be broken up into several “spin cases” with the spin combinations that integrate

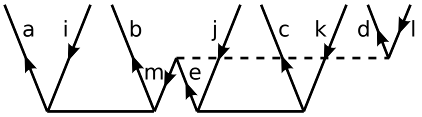

Figure 2.1: Typical spin-orbital diagram in the CCSDTQ amplitude equations.

to 0 excluded. For example,

$$v_{ij}^{ab} \rightarrow \left\{ v_{ij}^{ab},\, v_{i\bar{j}}^{a\bar{b}},\, v_{\bar{i}\bar{j}}^{\bar{a}\bar{b}} \right\} \tag{2.1}$$

where α orbitals are written as usual but β orbitals are written with an overbar. This is referred to as the spin-integrated representation, and for the working equations requires the expansion of each term into several terms over all valid combinations of spin cases. Both the spin-orbital and spin-integrated tensor elements have the same antisymmetry of the labels (since the annihilation and creation operators anticommute regardless of spin), so that it is not necessary to consider for example a full six spin cases for v_{ij}^{ab}, but only the three shown. However, more spin cases are needed for example for v_{ci}^{ab} since $v_{c\bar{i}}^{a\bar{b}}$ and $v_{\bar{c}i}^{\bar{a}b}$ are not related by antisymmetry, and for v_{bj}^{ai} the full six spin cases are in fact all distinct. The expansion of spin-orbital equations into spin-integrated ones can introduce a significant amount of complexity. For example, the diagram shown in figure 2.1 expands as (for only the $z_{ij\bar{k}\bar{l}}^{ab\bar{c}\bar{d}}$ spin case),

(spin-orbital)

$$-P(ab/c/d)P(i/jk/l)\sum_{em} v^{md}_{el} t^{ab}_{im} t^{ec}_{jk} \tag{2.2}$$

$$\downarrow$$

$$\begin{aligned}
&-P(ab)P(cd)\left\{P(kl)\sum_{em} v^{m\bar{d}}_{e\bar{l}} t^{\bar{c}b}_{\bar{k}m} t^{ea}_{ji} + P(ij)\sum_{\bar{e}\bar{m}} v^{\bar{m}a}_{\bar{e}i} t^{b\bar{c}}_{j\bar{m}} t^{\bar{e}\bar{d}}_{\bar{k}\bar{l}}\right\} \\
&-P(ij)P(kl)\left\{P(cd)\sum_{em} v^{m\bar{d}}_{e\bar{l}} t^{ab}_{mj} t^{e\bar{c}}_{i\bar{k}} + P(ab)\sum_{\bar{e}\bar{m}} v^{\bar{m}a}_{\bar{e}i} t^{\bar{c}\bar{d}}_{\bar{k}\bar{m}} t^{\bar{e}b}_{\bar{l}j}\right\} \\
&-P(ab)P(kl)\sum_{e\bar{m}} v^{\bar{m}b}_{\bar{l}e} t^{\bar{c}\bar{d}}_{\bar{k}\bar{m}} t^{ea}_{ji} - P(cd)P(ij)\sum_{\bar{e}m} v^{m\bar{d}}_{j\bar{e}} t^{ab}_{im} t^{\bar{e}\bar{c}}_{\bar{l}\bar{k}} \\
&-P(ab)P(cd)P(ij)P(kl)\left\{\sum_{em} v^{ma}_{ei} t^{\bar{d}b}_{\bar{l}m} t^{e\bar{c}}_{j\bar{k}} + \sum_{\bar{e}\bar{m}} v^{\bar{m}\bar{d}}_{\bar{e}\bar{l}} t^{b\bar{c}}_{j\bar{m}} t^{a\bar{e}}_{i\bar{k}}\right. \\
&\left. + \sum_{e\bar{m}} v^{\bar{m}a}_{\bar{l}e} t^{b\bar{d}}_{j\bar{m}} t^{e\bar{c}}_{i\bar{k}} + \sum_{\bar{e}m} v^{m\bar{d}}_{j\bar{e}} t^{\bar{c}b}_{\bar{k}m} t^{a\bar{e}}_{i\bar{l}}\right\}
\end{aligned} \tag{2.3}$$

(spin-integrated)

Doing the expansion for all spin cases for all 198 diagrams in the CCSDTQ amplitude equations, and then implementing the result is a daunting proposition in terms of complexity, tedium, and possibility of error.

If the number of occupied α and β orbitals are the same, and the same spatial orbitals are used for both spin functions, then some interesting and useful relationships arise between the spin-integrated spin cases, though. The most useful relationship is spin-reversal symmetry, where the value of a tensor element is unchanged on interchange of α and β spin functions, for example,

$$v^{ab}_{ij} = v^{\bar{a}\bar{b}}_{\bar{i}\bar{j}} \tag{2.4}$$

$$t^{ab\bar{c}}_{ij\bar{k}} = t^{\bar{a}\bar{b}c}_{\bar{i}\bar{j}k} \tag{2.5}$$

This reduces the number of independent spin cases by roughly $\frac{1}{2}$, and similarly the complexity of the equations by a similar amount. However, it is possible to go further. Spin cases with all indices of the same spin can be formed by antisymmetrizing spin cases of mixed spin, for example,

$$\begin{aligned} v_{ij}^{ab} &= v_{i\bar{j}}^{a\bar{b}} - v_{j\bar{i}}^{a\bar{b}} = v_{i\bar{j}}^{a\bar{b}} - v_{i\bar{j}}^{b\bar{a}} && (2.6) \\ t_{ijkl}^{abcd} &= t_{ijk\bar{l}}^{abc\bar{d}} - t_{ijl\bar{k}}^{abc\bar{d}} - t_{ilk\bar{j}}^{abc\bar{d}} - t_{ljk\bar{i}}^{abc\bar{d}} \\ &= t_{ij\bar{k}\bar{l}}^{ab\bar{c}\bar{d}} - t_{ik\bar{j}\bar{l}}^{ab\bar{c}\bar{d}} - t_{kj\bar{i}\bar{l}}^{ab\bar{c}\bar{d}} - t_{il\bar{k}\bar{j}}^{ab\bar{c}\bar{d}} - t_{lj\bar{k}\bar{i}}^{ab\bar{c}\bar{d}} + t_{kl\bar{i}\bar{j}}^{ab\bar{c}\bar{d}} && (2.7) \end{aligned}$$

Using this relation, the number of spin cases for the Hamiltonian, $\hat{T}_1$, $\hat{T}_2$, and $\hat{T}_3$ is reduced to one, and for $\hat{T}_4$ to two ($t_{ijk\bar{l}}^{abc\bar{d}}$ and $t_{ij\bar{k}\bar{l}}^{ab\bar{c}\bar{d}}$).

This is still not the end, however, as it is possible to use tensor elements which have no spin functions at all.[1,2,61] These quantities are called orbital tensor elements, also called spin-free, and sometimes skeleton, quantities. These tensor elements are distinguished in this work by an inverted chevron (a hacek) over the quantity, for example $\check{v}_{ij}^{ab}$. The spin-integrated tensor elements, even those of mixed spin, are formed from the orbital elements by antisymmetrization of the same-spin indices, for example,

$$\begin{aligned} v_{ij}^{ab} &= \check{v}_{ij}^{ab} - \check{v}_{ji}^{ba} && (2.8) \\ t_{ijk\bar{l}}^{abc\bar{d}} &= \check{t}_{ijkl}^{abcd} - \check{t}_{ijkl}^{abdc} - \check{t}_{ijkl}^{adcb} - \check{t}_{ijkl}^{dbca} + \check{t}_{ijkl}^{bcad} + \check{t}_{ijkl}^{cabd} && (2.9) \\ t_{ij\bar{k}\bar{l}}^{ab\bar{c}\bar{d}} &= \check{t}_{ijkl}^{abcd} - \check{t}_{ijkl}^{bacd} - \check{t}_{ijkl}^{abdc} + \check{t}_{ijkl}^{badc} && (2.10) \end{aligned}$$

The relationship for the one-particle operators (F and $\hat{T}_1$) is trivial, as well as for the mixed-spin cases of the two-particle Hamiltonian and $\hat{T}_2$.

In this way, only using the all-same-spin relationship above suffices to give directly the orbital form for CCSD. For CCSDT and CCSDTQ, however, the orbital relationship is somewhat more complicated. The orbital quantities do not have antisymmetry of their labels, since anticommutation of the creation and annihilation operators is only fixed after re-addition of the spin functions. They do have a different kind of symmetry, though, in that interchange of columns of indices (i.e. simultaneously interchanging labels in the same positions in the top and bottom labels) gives the same result with no change in sign. This column symmetry relates to the indistinguishability of electron excitations regardless of spin. Thus, the amplitudes have symmetries like,

$$\check{t}_{ijk}^{abc} = \check{t}_{ikj}^{acb} = \check{t}_{kji}^{cba} = \check{t}_{jik}^{bac} = \check{t}_{jki}^{bca} = \check{t}_{kij}^{cab} \tag{2.11}$$

$$\check{t}_{ijkl}^{abcd} = \check{t}_{ijlk}^{abdc} = \check{t}_{kjil}^{cbad} = \check{t}_{jlik}^{bdac} = \ldots \tag{2.12}$$

Lastly, because the orbital amplitudes are specific to a closed-shell reference function, the final correlated wavefunction is guaranteed to be a pure singlet state. For this reason, the orbital form is also known as the non-orthogonally spin-adapted formalism. The “non-orthogonal” qualifier refers to the fact that the excited one-particle functions produced by applying the orbital amplitude operator are not orthogonal to one another. Additionally, the excited functions are actually linearly dependent for triple excitations and higher, so that the orbital amplitude elements for $\hat{T}_3$ and $\hat{T}_4$ are not uniquely or numerically well-determined. Applying the antisymmetrization operations necessary to get the spin-integrated spin cases removes these indeterminacies, so that the spin-integrated (and of course spin-orbital) equations are numerically well-determined. Controlling the numerical effect of this indeterminacy in the orbital equations will be discussed in a later section.

The use of the orbital quantities instead of the spin-integrated ones has the potential to produce much simpler and easier to implement equations. But, it is tedious to do a direct expansion of the spin-orbital or spin-integrated equations to the orbital ones, and from there it is necessary to factor the result in an obscure way to obtain the most compact representation. This "optimal" orbital form has been used for some time for CCD and CCSD,[62–64] but for CCSDT and especially CCSDTQ, the techniques of the following sections are critical for deriving useful equations.

2.2 Goldstone Diagrams and their Limitations

While the majority of the work on Goldstone diagrams has been formulated and applied in the area of many-body perturbation theory,[36,44,45] it is the goal of the present work to apply Goldstone diagrammatics, and as an extension our new spin-summed diagrams, to more general theories, especially including higher-order coupled cluster. The main differences in applying Goldstone diagrams in this case are: 1) the coupled cluster amplitude equations involve open diagrams instead of only closed energy diagrams, and 2) the vertices are not limited to two-body quantities. These differences, especially the second, require some reformulation of the traditional rules for interpreting Goldstone diagrams, and also require some explanation of the relationship

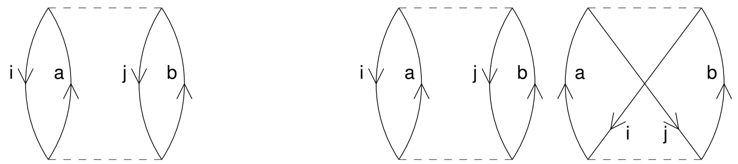

(a) Brandow (b) Goldstone

Figure 2.2: Diagrams for the MBPT[2] energy.

between the three- and higher-body spin-free quantities and their explicitly spin-labeled relatives.

Before going into detail on these points, however, let us first review some of the basic theory of Goldstone diagrams, as it relates to the other diagrammatic techniques. For the essentials of diagrammatic methods in quantum chemistry in general the reader is referred to the books of Shavitt and Bartlett,[38] Szabo and Ostlund,[65] and the review of Crawford and Schaefer.[37] As a first example, take the simplest (non-zero correction to HF) many-body perturbation theory, MBPT[2] (also called MP2). The Brandow and Goldstone diagrams for the MPBT[2] energy are given in figure 2.2.

The integrals (dashed line) in the Brandow diagrams are the usual antisymmetrized two-electron elements of the Hamiltonian, $\langle pq||rs\rangle \equiv v^{pq}_{rs}$. In the Goldstone diagrams, however, the orbital (or spin-free) integrals, $\langle pq|rs\rangle \equiv \check{v}^{pq}_{rs}$ are used, with the relationship $v^{pq}_{rs} = \check{v}^{pq}_{rs} - \check{v}^{qp}_{rs}$. While the orbital integrals do not have any antisymmetric permutational symmetry, they still have a “column” symmetry $\check{v}^{pq}_{rs} = \check{v}^{qp}_{sr}$ since simultaneous excitations commute regardless of spin. This symmetry is a fundamental feature of the orbital integrals, but also coupled cluster amplitudes or any other quantity expressed in the orbital representation. Relative to the Brandow representation, the Goldstone formulation introduces an additional diagram, since the interchange of two lines on either vertex produces a topologically distinct diagram (i.e. $\check{v}_{ij}^{ab} \neq \pm\check{v}_{ji}^{ab}$). It should be noted that the second Goldstone diagram can be produced from the first by a permutation of lines on either the top or bottom vertex, and permutation of either the hole or particle lines due to the aforementioned symmetry. Also, both Goldstone diagrams, when interpreted as Brandow diagrams, are equal. This is the case in general, so that each Goldstone diagram corresponding to a Brandow diagram is equal to all the others when itself interpreted as a Brandow diagram. This illustrates the fact that the Brandow representation is not unique, which will be important when interpreting the Brandow diagrams using our new spin-summation rules.

The traditional rules for interpreting Goldstone diagrams state that (omitting the energy denominators for simplicity),[38]

R1′. Each vertex contributes an orbital tensor element: $\check{X}_{all-in-labels}^{all-out-labels}$, where $\check{X}$ is determined by the type of line – dashed for V, solid for $\hat{T}$, wavy for intermediates, etc.

R2′. Each closed loop contributes an overall factor of 2.

R3′. The overall sign is equal to $(-1)^{l+h}$, where l is the number of closed loops and h is the number of hole lines.

R4′. If the diagram is symmetric with respect to a left-right reflection, the overall factor is multiplied by $\frac{1}{2}$.

R5′. Internal lines are summed over all spatial orbitals.

Applying these to the diagrams of figure 2.2 gives,

$$E = \sum_{abij} \check{v}^{ab}_{ij} (2\check{v}^{ij}_{ab} - \check{v}^{ji}_{ab}) \tag{2.13}$$

Evaluating the Brandow diagram with the appropriate rules (given explicitly below) gives, in terms of explicitly spin-integrated quantities,

$$\begin{aligned} E &= \frac{1}{4} \sum_{abij} v^{ab}_{ij} v^{ij}_{ab} + \sum_{a\bar{b}i\bar{j}} v^{a\bar{b}}_{i\bar{j}} v^{i\bar{j}}_{a\bar{b}} + \frac{1}{4} \sum_{\bar{a}\bar{b}\bar{i}\bar{j}} v^{\bar{a}\bar{b}}_{\bar{i}\bar{j}} v^{\bar{i}\bar{j}}_{\bar{a}\bar{b}} \\ &= \frac{1}{2} \sum_{abij} v^{ab}_{ij} v^{ij}_{ab} + \sum_{a\bar{b}i\bar{j}} v^{a\bar{b}}_{i\bar{j}} v^{i\bar{j}}_{a\bar{b}} \\ &= \frac{1}{2} \sum_{abij} (\check{v}^{ab}_{ij} - \check{v}^{ba}_{ij})(\check{v}^{ij}_{ab} - \check{v}^{ji}_{ab}) + \sum_{abij} \check{v}^{ab}_{ij} \check{v}^{ij}_{ab} \\ &= \sum_{abij} \check{v}^{ab}_{ij} (2\check{v}^{ij}_{ab} - \check{v}^{ji}_{ab}) \end{aligned} \tag{2.14}$$

since in the closed shell case we have $v^{pq}_{rs} = v^{\bar{p}\bar{q}}_{\bar{r}\bar{s}} = v^{p\bar{q}}_{r\bar{s}} - v^{q\bar{p}}_{r\bar{s}} = \check{v}^{pq}_{rs} - \check{v}^{qp}_{rs}$. This gives precisely the same result as using the Goldstone representation, as it must.

These same rules also hold for open diagrams containing only one- and two-body vertices, such as in the coupled cluster singles and double model (CCSD). As an example, take the "ring" part of the $\hat{T}_2 \times V \rightarrow \hat{T}_2$ equations, whose various diagrams are given in figure 2.3.

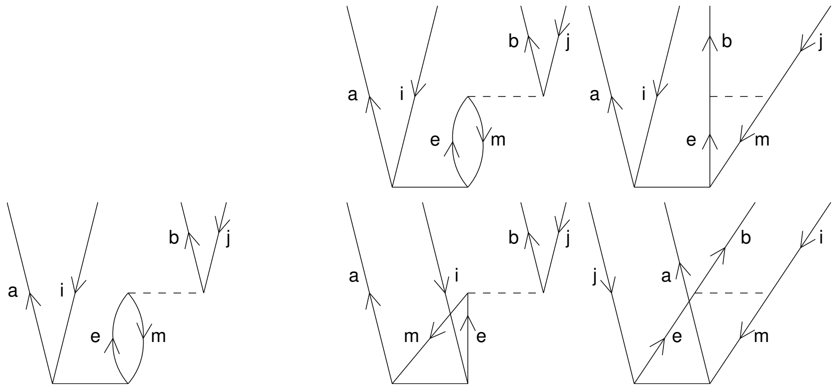

(a) Brandow

(b) Goldstone

Figure 2.3: Diagrams for the "ring" part of $\hat{T}_2 \times V \rightarrow \hat{T}_2$.

A straightforward interpretation of the Goldstone diagrams in figure 2.3 gives the following (labeling the result as $\check{z}_{ij}^{ab}$):

$$\begin{aligned}
\check{z}_{ij}^{ab} &= (1 + P_{bj}^{ai}) \sum_{em} \left\{ 2\check{t}_{im}^{ae} \check{v}_{ej}^{mb} - \check{t}_{im}^{ae} \check{v}_{ej}^{bm} - \check{t}_{im}^{ea} \check{v}_{ej}^{mb} - \check{t}_{im}^{eb} \check{v}_{ej}^{am} \right\} \\
&= (1 + P_{bj}^{ai}) \sum_{em} \left\{ \frac{1}{2} (2\check{t}_{im}^{ae} - \check{t}_{im}^{ea})(2\check{v}_{ej}^{mb} - \check{v}_{ej}^{bm}) \right. && (2.15) \\
&\qquad \left. -(\frac{1}{2} + P_b^a) \check{t}_{im}^{ea} \check{v}_{ej}^{bm} \right\} && (2.16)
\end{aligned}$$

where P_y^x exchanges the groups of labels x and y simultaneously. The factor $(1 + P_{bj}^{ai})$ replaces the usual antisymmetrization operators in the Brandow representation, and gives the result the proper permutational symmetry. While not generally listed with the canonical set of Goldstone diagram evaluation rules, this need for this permutation factor is well understood in CCSD. The second factorization is the optimal form,[62–64] and while it may seem bizarre, it is in fact a general feature of many non-orthogonally spin-adapted diagrams.

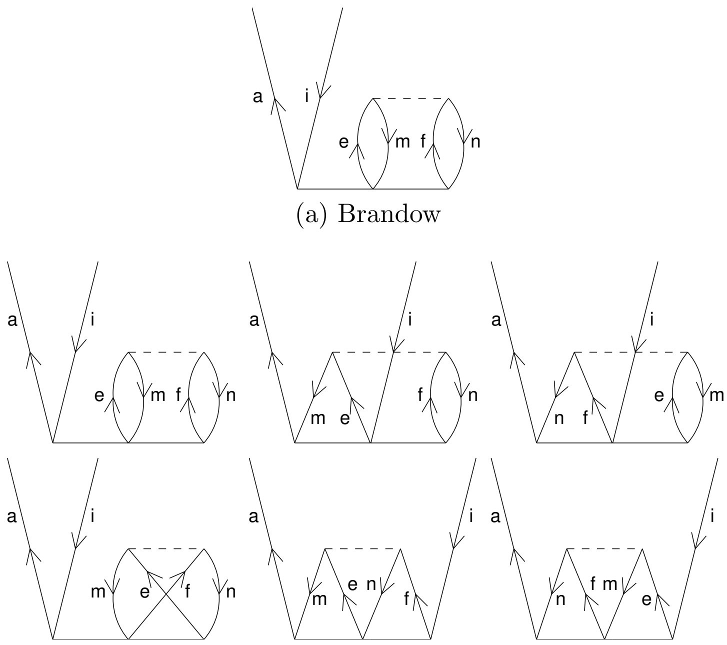

(a) Brandow

(b) “Goldstone”

Figure 2.4: Diagrams for $\hat{T}_3 \times V \rightarrow \hat{T}_1$.

The spin-integrated equations can be obtained fairly easily from the Brandow diagram to give for the spin case $z^{a\bar{b}}_{i\bar{j}} = \check{z}^{ab}_{ij}$,

$$\begin{aligned} z^{a\bar{b}}_{i\bar{j}} &= \sum_{em} t^{ae}_{im} v^{m\bar{b}}_{e\bar{j}} + \sum_{\bar{e}\bar{m}} t^{a\bar{e}}_{i\bar{m}} v^{\bar{m}\bar{b}}_{\bar{e}\bar{j}} - \sum_{e\bar{m}} t^{e\bar{b}}_{i\bar{m}} v^{a\bar{m}}_{e\bar{j}} \\ &+ \sum_{em} t^{\bar{b}e}_{\bar{j}m} v^{ma}_{ei} + \sum_{\bar{e}\bar{m}} t^{\bar{b}\bar{e}}_{\bar{j}\bar{m}} v^{\bar{m}a}_{\bar{e}i} - \sum_{\bar{e}m} t^{\bar{e}a}_{\bar{j}m} v^{\bar{b}m}_{\bar{e}i} \end{aligned} \tag{2.17}$$

which is again the same as the equation derived from the Goldstone diagrams after expansion and conversion of the spin-integrated quantities.

When the diagram contains higher than two-particle vertices, however, the rules as stated above are not sufficient. For example, take the term $\hat{T}_3 \times V \rightarrow \hat{T}_1$ from the CCSDT equations. The six diagrams given in figure 2.4b are the "most correct" set of Goldstone diagrams obtainable from permutation of lines on the amplitude or integral vertices relative to some Brandow diagram. Only diagrams which are unique with respect to the permutation symmetry of the orbital quantities are retained, but there are still diagrams which are relatable to each other by relabeling of the contracted indices. The total contribution from these diagrams is,

$$\check{z}_i^a = \sum_{mnef} \check{v}_{ef}^{mn} \left(4\check{t}_{imn}^{aef} - 2\check{t}_{min}^{aef} - 2\check{t}_{nmi}^{aef} - 2\check{t}_{inm}^{aef} + \check{t}_{mni}^{aef} + \check{t}_{nim}^{aef} \right) \tag{2.18}$$

The corresponding spin-integrated equation for $z_i^a = z_{\bar{i}}^{\bar{a}} = \check{z}_i^a$ is,

$$z_i^a = \frac{1}{4} \sum_{mnef} v_{ef}^{mn} t_{imn}^{aef} + \sum_{m\bar{n}e\bar{f}} v_{e\bar{f}}^{m\bar{n}} t_{im\bar{n}}^{ae\bar{f}} + \frac{1}{4} \sum_{\bar{m}\bar{n}\bar{e}\bar{f}} v_{\bar{e}\bar{f}}^{\bar{m}\bar{n}} t_{i\bar{m}\bar{n}}^{a\bar{e}\bar{f}}. \tag{2.19}$$

Expanding the above in terms of orbital amplitudes and integrals gives,

$$\check{z}_i^a = \frac{1}{2} \sum_{mnef} \check{v}_{ef}^{mn} \left(4\check{t}_{imn}^{aef} - 2\check{t}_{min}^{aef} - 2\check{t}_{nmi}^{aef} - 2\check{t}_{inm}^{aef} + \check{t}_{mni}^{aef} + \check{t}_{nim}^{aef} \right) \tag{2.20}$$

which is the same as equation (2.18), but with an extra factor of $\frac{1}{2}$. Rearranging the Goldstone diagrams to try and produce a plane of symmetry to invoke rule 4′ fails to correct the situation, as does adding more or removing some of the Goldstone diagrams. Additionally, even for this relatively simple case, enumerating the correct set of Goldstone diagrams (correct since they produce the proper equation apart from a factor) is difficult to get right without knowing the answer beforehand and tedious even if one does know. These difficulties, combined with the need for extra permutation factors for open diagrams (as was seen in the CCSD example), clearly show the need for modifications to the usual Goldstone evaluation rules.

2.3 Non-orthogonally Spin-adapted Diagrams

The Goldstone rules, while quite useful for many-body perturbation theory, CCSD, and other two-body theories, are not sufficiently general for CCSDT and CCSDTQ diagrammatics. Furthermore, the Goldstone rules require the enumeration of all unique Goldstone diagrams, of which there are quite a few for each Brandow diagram in CCSDTQ. The resulting equations must also be factorized by hand after applying the Goldstone rules to obtain a compact, efficient set of equations. So, it would be desirable to derive a diagrammatic interpretation which, 1) requires only the Brandow diagrams or only a very few additional diagrams, 2) produces compact, already-factored orbital equations, and 3) can be unambiguously applied to any order of coupled cluster and other many-body theories.

Rather than use the MBPT Goldstone rules as a starting point, the approach taken here is to start with the spin-orbital interpretation of the Brandow diagrams, and then use the basic ideas of the Goldstone diagrams, that the spin-orbital quantities are related to the orbital ones by antisymmetrization and that summation over closed loops gives a factor of 2 due to summation over both spins, to directly derive "non-orthogonally spin-adapted diagrammatics". The Brandow diagrammatic rules are given by rules R1-R6 in section §1.3.

Since the orbital quantities are related to the spin-orbital and spin-integrated ones by antisymmetry, this antisymmetry then forms the relationship between the two diagrammatics. To formalize the issue, consider the set of permutations of indices on a vertex v, $\{P_v(pq)\}$, where p and q run over all indices out of either the top (*out*) or bottom (*in*) labels of v. Each of these permutations exchanges the indicated labels, but only on the given vertex. Since the relevant transformations describe antisymmetry of either *in* (annihilation) or *out* (creation) lines (operators), we must also associate with each $P_v(pq)$ a minus sign and restrict p and q to be either both *in* or both *out* labels. Of course pairwise permutations are idempotent, such that,

$$P_v(pq)^2 = 1 \tag{2.21}$$

Additionally, each label p has, due to the column symmetry of the orbital quantities, a column-symmetric partner p^*. The column-symmetric partner is simply the label in the same column when all labels are written out, e.g. $v^{...p...q...}_{...p*...q*...}$. Then, since $v^{...p...q...}_{...p*...q*...} = v^{...q...p...}_{...q*...p*...}$ we have,

$$\begin{aligned} P_v(pq) &= P_v(p^*q^*) && (2.22) \\ P_v(pq)P_v(p^*q^*) &= 1 && (2.23) \end{aligned}$$

Instead of giving unity, the product of a permutation with its column-symmetric partner (or equivalently itself) can also be written as a symmetric double permutation,

$$P_v(pq)P_v(p^*q^*) = P_v(pq)S_v(^{p\ \ q}_{p*\, q*}) \tag{2.24}$$

where the symmetric permutation interchanges both sets of labels simultaneously. The same can also be done when the labels are on different vertices, which provides a way to enforce the column symmetry of a tensor contraction product.

Given a spin-orbital diagram, all of the related orbital Goldstone diagrams are obtained by an antisymmetrization operation built up from the set of column-symmetry-unique permutations. This antisymmetrization operation, however, generally contains permutations which involve more than two indices. In the general case the unique permutations of more than two out of n indices can be formed from the set of two-index permutations $P \equiv \{P(pq)\}_{p<q=1}^{n}$ by taking only ordered products,

$$\begin{aligned} \tilde{P}^k &\equiv \{P(i_{p_1} i_{q_1}) P(i_{p_2} i_{q_2}) \ldots P(i_{p_k} i_{q_k}) \,| \\ &\qquad\qquad p_1 < p_2 < \ldots < p_k \wedge p_l < q_l \forall l\}_{p_1 \ldots p_k, q_1 \ldots q_k = 1}^{n} \qquad (2.25) \\ \mathscr{A}_P &\equiv \{\tilde{P}^k\}_{k=0}^{n-1} \qquad (2.26) \end{aligned}$$

The special case $\tilde{P}^0 = \{1\}$ even if P is the empty set. All of the permutations of n objects are then given by $\mathscr{A}_P$ (see theorem 1 in the appendix).

In manipulating sets of permutations and their antisymmetrizers, it is quite helpful to be able to separate the permutations of a set of indices into those of some disjoint partitioning. In particular, the total antisymmetrizer can be written as a product of subset antisymmetrizers and a special partial antisymmetrizer which contains permutations between the subsets (see theorem 2),

$$\mathscr{A}_P = \mathscr{A}_{P_1} \mathscr{A}_{P_2} \tilde{\mathscr{A}}_{P_1 - P_2}$$

$$= \tilde{\mathscr{A}}_{P_1-P_2}\mathscr{A}_{P_1}\mathscr{A}_{P_2} \tag{2.27}$$

where $\mathscr{A}_{P_1}$ is the antisymmetrizer for the indices in set 1 (of size n_1, and similarly for set 2 of size n_2), while the special antisymmetrizer $\tilde{\mathscr{A}}_{P_1-P_2}$ is given by,

$$\begin{aligned} \tilde{\tilde{P}}^k_{1-2} &\equiv \{P(i_{p_1}i_{q_1})\dots P(i_{p_k}i_{q_k})\,|\,p_1 < \dots < p_k \wedge q_1 < \dots < q_k \\ &\qquad \wedge p_l < q_l \forall\, l\}^{n_1,n_1+n_2}_{p_1\dots p_k=1,q_1\dots q_k=n_1+1} \qquad (2.28) \\ \tilde{\mathscr{A}}_{P_1-P_2} &\equiv \{\tilde{\tilde{P}}^k_{1-2}\}^{min\{n_1,n_2\}}_{k=0} \qquad (2.29) \end{aligned}$$

To simplify the derivation of the new rules, it suffices to consider only diagrams of one or two vertices. This is not restrictive since the factorization of the target equations into unary and binary terms can be performed at the spin-orbital diagram stage, and then the resulting diagrams in terms of intermediates transformed into orbital equations.

Since diagrams of only one vertex are trivial (this corresponds to simply adding or assigning one quantity to another), we can consider only the general two-vertex diagram of figure 2.5. Each vertex v in this form has: $n_{a;v}$ $particle-out$ (particle being synonymous with virtual or unoccupied) and $n_{i;v}$ $hole-in$ (hole meaning occupied) lines which extend upward and $n_{b;v}$ $particle-in$ and $n_{j;v}$ $hole-out$ lines which extend downward, to give n_v total lines. The upper vertex is labeled A and the lower B. Usually, the operators will be number-conserving such that $n_{a;v}+n_{j;v} = n_{b;v}+n_{i;v}$, and it will simplify the discussion to make this assumption at first. Of the labels on each vertex, the first $n_e \leqslant$

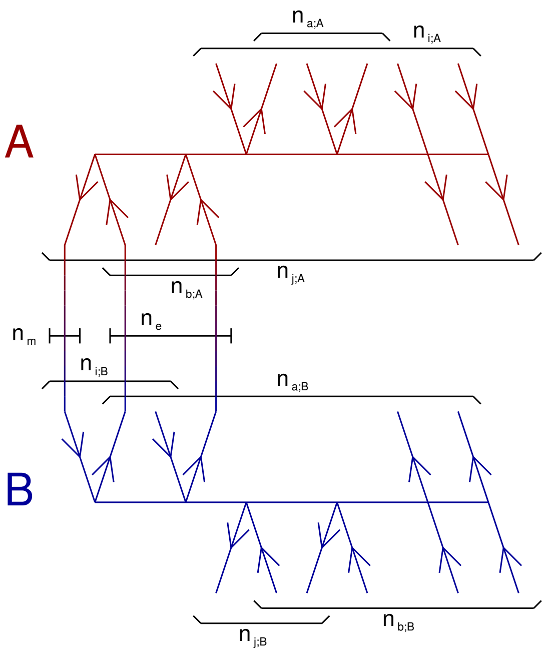

Figure 2.5: General form of a two-vertex Brandow diagram and the grouping of lines into various sets. The "extra" lines on the right may be either hole or particle lines.

$min(n_{b;A}, n_{a;B})$ of the $particle-in$ vertices on A and the $particle-out$ vertices on B are contracted together as are the first $n_m \leqslant min(n_{j;A}, n_{i;B})$ of the $hole-out$ and $hole-in$ vertices on A and B respectively. The individual labels are conveniently called $a_{1;A} \ldots a_{n_{a;A};A}$, $e_1 \ldots e_{n_e}$, etc. The possible permutations of the labels relevant to antisymmetry are then:

$$\begin{aligned}
P_{o;A} &\equiv \{P_A(a_{k;A}a_{l;A})\}_{k<l=1}^{n_{a;A}} \cup \{P_A(j_{k;A}j_{l;A})\}_{k<l=1}^{n_{j;A}} \\
&\quad \cup\{P_A(a_{k;A}j_{l;A})\}_{k,l=1}^{n_{a;A},n_{j;A}} \qquad (2.30) \\
P_{i;A} &\equiv \{P_A(b_{k;A}b_{l;A})\}_{k<l=1}^{n_{b;A}} \cup \{P_A(i_{k;A}i_{l;A})\}_{k<l=1}^{n_{i;A}} \\
&\quad \cup\{P_A(b_{k;A}i_{l;A})\}_{k,l=1}^{n_{b;A},n_{i;A}} \qquad (2.31)
\end{aligned}$$

and similarly for B. Since there are an equal number of out and in vertices, the column symmetry of the orbital quantities means that each permutation in $P_{o;A}$ is related to a permutation in $P_{i;A}$ and vice versa, for example $P_A(a_{1;A}a_{2;A}) \leftrightarrow P_A(a^*_{1;A}a^*_{2;A}) = P_A(i_{1;A}b_{1;A})$ for $A^{a_1a_2}_{i_1b_1}$. Only one set is needed to produce distinct Goldstone diagrams and we can arbitrarily choose $P_A \equiv P_{o;A}$. The final set of permutations P_A and its unique products form the relationship between the spin-orbital and orbital quantities,

$$\begin{aligned}
A^{pq\ldots}_{rs\ldots} &= \sum_{k=0}^{n_A-1} \tilde{P}^k_A \breve{A}^{pq\ldots}_{rs\ldots} \\
&= \mathscr{A}_A \breve{A}^{pq\ldots}_{rs\ldots} \qquad (2.32)
\end{aligned}$$

where the application of the set $\tilde{P}^k_A$ sums over each element applied to the object in turn.

Besides permutations of the two diagram vertices, we must also consider permutations of the external labels. To use the language defined above, the external lines can be considered to belong also to a third C vertex, with sets of permutations defined similarly to A and B (except of course no lines are contracted). Rule 6 gives permutations (and products of permutations since multiple indices may be antisymmetrized) between labels of the same type on different vertices, conveniently denoted by,

$$
\begin{aligned}
P_{Brandow} &\equiv P_{a;Brandow} \cup P_{b;Brandow} \cup P_{i;Brandow} \cup P_{j;Brandow} \\
&= \{P(a_{k;A}a_{l;B})\}_{k=1,l=n_e+1}^{n_{a;A},n_{a;B}} \cup \{P(b_{k;A}b_{l;B})\}_{k=n_e+1,l=1}^{n_{b;A},n_{b;B}} \cup \\
&\quad \{P(i_{k;A}i_{l;B})\}_{k=n_m+1,l=1}^{n_{i;A},n_{i;B}} \cup \{P(j_{k;A}j_{l;B})\}_{k=1,l=n_m+1}^{n_{j;A},n_{j;B}} \qquad (2.33) \\
\tilde{\mathscr{A}}_{Brandow} &\equiv \{\tilde{\tilde{P}}_{a;Brandow}^{k}\}_{k=0}^{min\{n_{a;A},n_{a;B}-n_e\}} \otimes \\
&\quad \{\tilde{\tilde{P}}_{b;Brandow}^{k}\}_{k=0}^{min\{n_{b;A}-n_e,n_{b;B}\}} \otimes \\
&\quad \{\tilde{\tilde{P}}_{i;Brandow}^{k}\}_{k=0}^{min\{n_{i;A}-n_m,n_{i;B}\}} \otimes \\
&\quad \{\tilde{\tilde{P}}_{j;Brandow}^{k}\}_{k=0}^{min\{n_{j;A},n_{j;B}-n_m\}} \qquad (2.34)
\end{aligned}
$$

The permutations here are not labeled with a vertex subscript because they affect the labeling of all vertices (including the external “vertex” C).

Armed with the relationship between the spin-orbital (ABC) and orbital ($\breve{A}\breve{B}\breve{C}$) quantities and an explicit form for the Brandow antisymmetrization operator, we can now write a preliminary relationship between the two diagrammatics,

$$
\begin{aligned}
C &= \tilde{\mathscr{A}}_{Brandow} F_s F_e F_h F_p \sum AB \qquad (2.35) \\
&\updownarrow \\
\mathscr{A}_C \breve{C} &= \tilde{\mathscr{A}}_{Brandow} F_s F_e F_h F_p F_c \sum \mathscr{A}_A \mathscr{A}_B \breve{A}\breve{B} \qquad (2.36)
\end{aligned}
$$

F_h and F_p are the factors for identical contracted hole and particle lines, respectively, from rule 2. F_s is the sign factor from rule 3, and F_e is the exponential factor from rule 4. The summation from rule 5 goes over spin-orbitals in the first equation, but over spatial orbitals in the second, with the additional factor F_c accounting for the factor of 2 for each closed loop. The indices on A, B, and C and on the summation are implicit in the following derivation.

The first logical thing to do is to somehow remove the antisymmetrization operation on $\check{C}$ so that an equation for a specific orbital tensor "orbital case" (i.e. a specific ordering of the *out* and *in* labels since there is no antisymmetry) can be obtained. The antisymmetrizer $\mathscr{A}_C$ mixes different orderings of labels on $\check{C}$, for example $v^{ab}_{ci} = \check{v}^{ab}_{ci} - \check{v}^{ba}_{ci}$, where the labels are of the same type. These two orderings correspond to the same orbital quantity since the a and b labels run over the same set of spatial orbitals. However, $\mathscr{A}_c$ also contains permutations which mix labels of different types, for example, $v^{ai}_{bj} = \check{v}^{ai}_{bj} - \check{v}^{ai}_{jb}$, where now the different permutations are completely unrelated orbital quantities. In particular, the different "types" of orbital quantities related to the same spin-orbital one can be classified by a number n_s which counts the number of hole labels and particle labels in the same column (this is also the number of external loops when C is viewed as a diagram itself). For example, $\check{v}^{ai}_{bj}$ has $n_s = 0$ while $\check{v}^{ai}_{jb}$ has $n_s = 2$.

Using theorem 4, $\mathscr{A}_C$ can be split into several parts, each of which applies to a specific n_s value,

$$\mathscr{A}_{a;C}\mathscr{A}_{j;C}\tilde{\mathscr{A}}_{\substack{a\\i}-\substack{j\\i};C}\tilde{\mathscr{A}}_{\substack{a\\b}-\substack{j\\b};C}\check{C}_{n_s} = \tilde{\mathscr{A}}_{Brandow}F_sF_eF_hF_pF_c\sum\left(\mathscr{A}_A\mathscr{A}_B\check{A}\check{B}\right)_{n_s} \quad (2.37)$$

where for example $\mathscr{A}_{a;C}$ antisymmetrizes the $particle - out$ labels on $\check{C}$ and $\tilde{\mathscr{A}}_{\substack{a\\i}-\substack{j\\i};C}$ exchanges $hole - in$ labels partnered with $particle - in$ labels and those partnered with $hole - out$ labels (on $\check{C}$). The notation $(\ldots)_{n_x}$ means that only permutations which give external labels consistent with the given value of n_s are retained ($\tilde{\mathscr{A}}_{Brandow}$ can not change n_s). The antisymmetrization operators on the LHS can be cleaned up somewhat by inserting the identity as $(n_{\substack{a\\i};C}!n_{\substack{j\\i};C}!n_{\substack{a\\b};C}!n_{\substack{j\\b};C}!)^{-1}\mathscr{A}_{\substack{a\\i};C}\mathscr{A}_{\substack{j\\i};C}\mathscr{A}_{\substack{a\\b};C}\mathscr{A}_{\substack{j\\b};C}$ which is possible since for example $\mathscr{A}_{a;C}\mathscr{A}_{\substack{a\\i};C} = \mathscr{A}_{a;C}(n_{\substack{a\\i};C}!)^{-1}$. Now, we can simplify by using theorem 2,

$$\begin{aligned}
\mathscr{A}_{a;C}\mathscr{A}_{j;C}\tilde{\mathscr{A}}_{\substack{a\\i}-\substack{j\\i};C}\tilde{\mathscr{A}}_{\substack{a\\b}-\substack{j\\b};C}\check{C}_{n_s} &= \frac{\mathscr{A}_{a;C}\mathscr{A}_{j;C}\mathscr{A}_{\substack{a\\i};C}\mathscr{A}_{\substack{j\\i};C}\mathscr{A}_{\substack{a\\b};C}\mathscr{A}_{\substack{j\\b};C}\tilde{\mathscr{A}}_{\substack{a\\i}-\substack{j\\i};C}\tilde{\mathscr{A}}_{\substack{a\\b}-\substack{j\\b};C}}{n_{\substack{a\\i};C}!n_{\substack{j\\i};C}!n_{\substack{a\\b};C}!n_{\substack{j\\b};C}!}\check{C}_{n_s} \\
&= \frac{\mathscr{A}_{a;C}\mathscr{A}_{j;C}\mathscr{A}_{i;C}\mathscr{A}_{b;C}}{n_{\substack{a\\i};C}!n_{\substack{j\\i};C}!n_{\substack{a\\b};C}!n_{\substack{j\\b};C}!}\check{C}_{n_s} \qquad (2.38)
\end{aligned}$$

On the RHS a similar trick can be applied, by inserting additional antisymmetrizers so that the Brandow antisymmetrizer becomes,

$$\begin{aligned}
&\tilde{\mathscr{A}}_{Brandow} \\
&= \frac{\tilde{\mathscr{A}}_{Brandow}\mathscr{A}_{a;A}\mathscr{A}_{j;A}\mathscr{A}_{i;A/m}\mathscr{A}_{b;A/e}\mathscr{A}_{a;B/e}\mathscr{A}_{j;B/m}\mathscr{A}_{i;B}\mathscr{A}_{b;B}}{n_{a;A}!n_{j;A}!(n_{i;A}-n_m)!(n_{b;A}-n_e)!(n_{a;B}-n_e)!(n_{j;B}-n_m)!n_{i;B}!n_{b;B}!} \\
&= \frac{\mathscr{A}_{a;C}\mathscr{A}_{j;C}\mathscr{A}_{i;C}\mathscr{A}_{b;C}}{n_{a;A}!n_{j;A}!(n_{i;A}-n_m)!(n_{b;A}-n_e)!(n_{a;B}-n_e)!(n_{j;B}-n_m)!n_{i;B}!n_{b;B}!} \qquad (2.39)
\end{aligned}$$

Both the LHS and the RHS now have the same set of antisymmetrizers applied, so that a single orbital case of $\check{C}$ can be extracted from both sides by removing this antisymmetrization step. Of course, the equation obtained this way is not unique, and that is the root of the indeterminacy of the orbital tensor elements. However, the equation is valid when the antisymmetrizers are re-applied, and is unique when the procedure here is followed, so that the orbital quantities obtained this way can be considered the “canonical” form. After removing the antisymmetrizers, the orbital equation becomes,

$$\check{C} = \frac{n_{\substack{a\\i};C}!\,n_{\substack{j\\i};C}!\,n_{\substack{a\\b};C}!\,n_{\substack{j\\b};C}!\,F_s F_e F_h F_p F_c \sum \left(\mathscr{A}_A \mathscr{A}_B \check{A}\check{B}\right)_{\check{C}}}{n_{a;A}!\,n_{j;A}!\,(n_{i;A}-n_m)!\,(n_{b;A}-n_e)!\,(n_{a;B}-n_e)!\,(n_{j;B}-n_m)!\,n_{i;B}!\,n_{b;B}!} \tag{2.40}$$

where now $\check{C}$ is has a definite ordering of the labels, and the notation $(\ldots)_{\check{C}}$ retains only contributions which match this ordering.

At this point, the equation is very similar to the usual Goldstone interpretation, in that the antisymmetrizers $\mathscr{A}_A\mathscr{A}_B$ produce the unique Goldstone diagrams (with some over-counting which cancels the factorials). However, with the equation in a formal representation, the antisymmetrizers can be manipulated further to expose the desired compact, factorized result directly. In order to proceed we must first do two things: first, while the antisymmetrizers produce all of the Goldstone diagrams from some initial diagram determined by the label ordering of $\check{A}\check{B}$, it will prove advantageous to choose this initial ordering carefully as the one which has the maximal number of closed loops, and second, starting from this ordering we will subdivide the labels on each fragment into three groups, c, x, and u. The c labels are contracted labels whose partner label is also contracted on both vertices. The x labels are either contracted with an uncontracted partner or *vice versa* on at least one vertex. The u labels are uncontracted with uncontracted partners. Choosing a well-defined initial ordering is important since these classifications depend on that ordering. For some Brandow diagrams, there will be more than one

Goldstone diagram with the maximal number of closed loops. At this point it suffices to choose any of these, although it will be shown below that the final interpretation will depend equally on each of these representative diagrams.

The antisymmetrizers $\mathscr{A}_A$ and $\mathscr{A}_B$ can be decomposed into different partitions of these groups using theorem 2. The first step is to remove the redundant permutations over c and x labels, since a permutation of these labels on $\check{A}$ is the same as permutation on $\check{B}$ followed by relabeling the contracted labels. This gives,

$$\begin{aligned}
\check{C} &= \frac{n_{\substack{a\\i};C}!n_{\substack{j\\i};C}!n_{\substack{a\\b};C}!n_{\substack{j\\b};C}!F_sF_eF_hF_pF_c\sum\left(\mathscr{A}_A\mathscr{A}_{cx;B}\mathscr{A}_{u;B}\tilde{\mathscr{A}}_{cx-u;B}\check{A}\check{B}\right)_{\check{C}}}{n_{a;A}!n_{j;A}!(n_{i;A}-n_m)!(n_{b;A}-n_e)!(n_{a;B}-n_e)!(n_{j;B}-n_m)!n_{i;B}!n_{b;B}!} \\
&= \frac{n_{\substack{a\\i};C}!n_{\substack{j\\i};C}!n_{\substack{a\\b};C}!n_{\substack{j\\b};C}!F_sF_e max\{F_h,F_p\}F_c}{n_{a;A}!n_{j;A}!(n_{i;A}-n_m)!(n_{b;A}-n_e)!(n_{a;B}-n_e)!(n_{j;B}-n_m)!n_{i;B}!n_{b;B}!}\times \\
&\quad \sum\left(\mathscr{A}_A\mathscr{A}_{u;B}\tilde{\mathscr{A}}_{cx-u;B}\check{A}\check{B}\right)_{\check{C}} \qquad (2.41)
\end{aligned}$$

Since the number of cx labels is the greater of the the number of contracted hole and particle lines, then $\mathscr{A}_{cx;B}\rightarrow n_{cx}!$ cancels either F_h or F_p. $\mathscr{A}_A$ can also be decomposed, but this time it is better to break it into c and xu groups,

$$\begin{aligned}
\check{C} &= \frac{n_{\substack{a\\i};C}!n_{\substack{j\\i};C}!n_{\substack{a\\b};C}!n_{\substack{j\\b};C}!F_sF_e max\{F_h,F_p\}F_c}{n_{a;A}!n_{j;A}!(n_{i;A}-n_m)!(n_{b;A}-n_e)!(n_{a;B}-n_e)!(n_{j;B}-n_m)!n_{i;B}!n_{b;B}!}\times \\
&\quad \sum\left(\mathscr{A}_{xu;A}\mathscr{A}_{c;A}\tilde{\mathscr{A}}_{c-xu;A}\mathscr{A}_{u;B}\tilde{\mathscr{A}}_{cx-u;B}\check{A}\check{B}\right)_{\check{C}} \qquad (2.42)
\end{aligned}$$

The next step is to use the rather esoteric form of theorem 3, though its purpose will become clear after some more manipulation,

$$\begin{aligned}
\check{C} &= \frac{n_{\substack{a\\i};C}!n_{\substack{j\\i};C}!n_{\substack{a\\b};C}!n_{\substack{j\\b};C}!F_sF_e max\{F_h,F_p\}F_c}{n_{a;A}!n_{j;A}!(n_{i;A}-n_m)!(n_{b;A}-n_e)!(n_{a;B}-n_e)!(n_{j;B}-n_m)!n_{i;B}!n_{b;B}!}\times \\
&\quad \sum\left(\mathscr{A}_{xu;A}\mathscr{A}_{u;B}\mathscr{A}_{c;A}\tilde{\mathscr{A}}_{c-xu;A}\tilde{\mathscr{A}}_{cx-u;B}\check{A}\check{B}\right)_{\check{C}} \\
&= \frac{n_{\substack{a\\i};C}!n_{\substack{j\\i};C}!n_{\substack{a\\b};C}!n_{\substack{j\\b};C}!F_sF_e max\{F_h,F_p\}F_c}{n_{a;A}!n_{j;A}!(n_{i;A}-n_m)!(n_{b;A}-n_e)!(n_{a;B}-n_e)!(n_{j;B}-n_m)!n_{i;B}!n_{b;B}!}\times \\
&\quad \sum\left(\mathscr{A}_{xu;A}\mathscr{A}_{xu;B}\mathscr{A}_{c;A}\tilde{\mathscr{A}}_{c-xu;A}\frac{n_{u;B}!}{(n_x+n_{u;B})!}\tilde{\mathscr{A}}_{cx-u;B}\check{A}\check{B}\right)_{\check{C}} \\
&= \frac{n_{\substack{a\\i};C}!n_{\substack{j\\i};C}!n_{\substack{a\\b};C}!n_{\substack{j\\b};C}!F_sF_e max\{F_h,F_p\}F_c}{n_{a;A}!n_{j;A}!(n_{i;A}-n_m)!(n_{b;A}-n_e)!(n_{a;B}-n_e)!(n_{j;B}-n_m)!n_{i;B}!n_{b;B}!}\times \\
&\quad \sum\left(\mathscr{A}_{xu;A}\mathscr{A}_{xu;B}\mathscr{A}_{c;A}\tilde{\mathscr{A}}_{c-xu;A}\sum_{k=0}^{min\{n_c,n_{u;B}\}}\frac{k!}{(n_x+k)!}\tilde{\tilde{P}}^k_{c-u;B}\check{A}\check{B}\right)_{\check{C}} \qquad (2.43)
\end{aligned}$$

The second equality is obtained by inserting $\frac{n_{u;B}!}{(n_x+n_{u;B})!}\mathscr{A}_{x;B}\tilde{\mathscr{A}}_{x-u;B}$ and using theorem 2. Before finally dealing with $\mathscr{A}_{xu}$ and the factorials in the denominator, we can use the factorials in the numerator to build a useful operator. Since this equation is only "really" valid after re-application of the antisymmetrizers $\mathscr{A}_{a;C}\mathscr{A}_{j;C}\mathscr{A}_{i;C}\mathscr{A}_{b;C}$, then the fact that these contain all of the permutations in, for example, $\mathscr{A}_{\substack{a\\i};C}$ allows us to "reconstitute" these antisymmetrizers on the RHS,

$$\begin{aligned}
\check{C} &= \frac{\mathscr{A}_{\substack{a\\i};C}\mathscr{A}_{\substack{j\\i};C}\mathscr{A}_{\substack{a\\b};C}\mathscr{A}_{\substack{j\\b};C}F_sF_e max\{F_h,F_p\}F_c}{n_{a;A}!n_{j;A}!(n_{i;A}-n_m)!(n_{b;A}-n_e)!(n_{a;B}-n_e)!(n_{j;B}-n_m)!n_{i;B}!n_{b;B}!}\times \\
&\quad \sum\left(\mathscr{A}_{xu;A}\mathscr{A}_{xu;B}\mathscr{A}_{c;A}\tilde{\mathscr{A}}_{c-xu;A}\sum_{k=0}^{min\{n_c,n_{u;B}\}}\frac{k!}{(n_x+k)!}\tilde{\tilde{P}}^k_{c-u;B}\check{A}\check{B}\right)_{\check{C}} \qquad (2.44)
\end{aligned}$$

But, since we are now applying the same permutations twice, we can use equation (2.24) to change this into a symmetrizer,

$$\begin{aligned}
\check{C} &= \frac{\mathscr{S}_C F_s F_e max\{F_h, F_p\} F_c}{n_{a;A}! n_{j;A}! (n_{i;A} - n_m)! (n_{b;A} - n_e)! (n_{a;B} - n_e)! (n_{j;B} - n_m)! n_{i;B}! n_{b;B}!} \times \\
&\quad \sum \left(\mathscr{A}_{xu;A} \mathscr{A}_{xu;B} \mathscr{A}_{c;A} \tilde{\mathscr{A}}_{c-xu;A} \sum_{k=0}^{min\{n_c, n_{u;B}\}} \frac{k!}{(n_x + k)!} \tilde{\tilde{P}}^k_{c-u;B} \check{A} \check{B} \right)_{\check{C}} \qquad (2.45)
\end{aligned}$$

where the symmetrizer $\mathscr{S}_C$ is defined as,

$$\begin{aligned}
S_C &\equiv S_{{}^a_i;C} \cup S_{{}^j_i;C} \cup S_{{}^a_b;C} \cup S_{{}^j_b;C} \\
&= \left\{ S_C\left({}^{a_k\, a_l}_{a^*_k\, a^*_l}\right) \,|\, a^*_k \in i \;\wedge\; a^*_l \in i \right\}_{k<l=1}^{n_{a;C}} \cup \\
&\quad \left\{ S_C\left({}^{j_k\, j_l}_{j^*_k\, j^*_l}\right) \,|\, j^*_k \in i \;\wedge\; j^*_l \in i \right\}_{k<l=1}^{n_{j;C}} \cup \\
&\quad \left\{ S_C\left({}^{a_k\, a_l}_{a^*_k\, a^*_l}\right) \,|\, a^*_k \in b \;\wedge\; a^*_l \in b \right\}_{k<l=1}^{n_{a;C}} \cup \\
&\quad \left\{ S_C\left({}^{j_k\, j_l}_{j^*_k\, j^*_l}\right) \,|\, j^*_k \in b \;\wedge\; j^*_l \in b \right\}_{k<l=1}^{n_{j;C}} \qquad (2.46) \\
\mathscr{S}_C &\equiv \left\{ \tilde{S}^k_{{}^a_i;C} \right\}_{k=0}^{n_{{}^a_i;C}-1} \otimes \left\{ \tilde{S}^k_{{}^j_i;C} \right\}_{k=0}^{n_{{}^j_i;C}-1} \otimes \\
&\quad \left\{ \tilde{S}^k_{{}^a_b;C} \right\}_{k=0}^{n_{{}^a_b;C}-1} \otimes \left\{ \tilde{S}^k_{{}^j_b;C} \right\}_{k=0}^{n_{{}^j_b;C}-1} \qquad (2.47)
\end{aligned}$$

This symmetrization step is quite important as it ensures the column symmetry of $\check{C}$, which is extremely useful in practical implementation of non-orthogonally spin-adapted methods (and of course is assumed in this diagrammatic derivation).

The last simplification to make is to deal with the factorials in the denominator and the antisymmetrizers $\mathscr{A}_{xu;A}$ and $\mathscr{A}_{xu;B}$. The antisymmetrizers have three types of permutations: 1) permutations of external labels of the same type (or who have partners of the same type), 2) permutations of external labels which are not of the same type, and so which change n_s, and 3) permutations involving partially contracted labels (labels from the set x). Since the factor of $n_{a;A}!$ could be canceled by antisymmetrizer $\mathscr{A}_{a;A}$ and so on for each factor, we must examine which permutations from $\mathscr{A}_{xu;A}$ are "missing" to form $\mathscr{A}_{a;A}\mathscr{A}_{j;A}\mathscr{A}_{i;A/m}\mathscr{A}_{b;A/e}$ and similarly for B. Additionally, if a factor of $n_x!$ is multiplied and divided in the sum over k then, as careful analysis shows, it is actually simpler to relate the xu antisymmetrizers for both vertices into the daunting string of operators, $\mathscr{A}_{a;A}\mathscr{A}_{j;A}\mathscr{A}_{i;A/m}\mathscr{A}_{b;A/e}\mathscr{A}_{a;B/e}\mathscr{A}_{j;B/m}\mathscr{A}_{i;B}\mathscr{A}_{b;B}\mathscr{A}_{x}$, which can simultaneously cancel all of the remaining factorials. Since permutations of type 2) and permutations in 3) which, due to the column symmetry of $\check{C}$ also change n_s can be ignored, the "only" remaining permutations needed to cancel the factors are $\mathscr{A}_{\substack{a\\i};A}\mathscr{A}_{\substack{a\\b};A}\mathscr{A}_{\substack{j\\i};A}\mathscr{A}_{\substack{j\\b};A}\mathscr{A}_{\substack{a\\i};A}\mathscr{A}_{\substack{j\\i};A}\mathscr{A}_{\substack{a\\b};A}\mathscr{A}_{\substack{j\\b};A}\mathscr{A}_{\substack{a\\i};x}\mathscr{A}_{\substack{j\\i};x}\mathscr{A}_{\substack{a\\b};x}\mathscr{A}_{\substack{j\\b};x}$ where the $\mathscr{A}_{\ldots;x}$ antisymmetrizers permute labels which are of the upper type on $\check{A}$ and whose column-symmetric partners in $\check{C}$ are of the lower type on $\check{B}$.

This seemingly complicated set of antisymmetrizers is actually quite simple when examined diagrammatically, as it simply antisymmetrizes pairs of external labels of the same combined type ($\substack{a\\i}$, $\substack{j\\i}$, etc.) which are either on the same vertex or both partially contracted. In essence these are "identical" external pairs. Since these permutations are lacking in $\mathscr{A}_{xu;A}\mathscr{A}_{xu;B}$, they must be inserted as an identity with the corresponding factors $n_{\substack{a\\i};A}!$ etc. in the denominator (this can be done since all of these permutations are in $\mathscr{A}_{a;C}\mathscr{A}_{j;C}\mathscr{A}_{i;C}\mathscr{A}_{b;C}$). However, these need not remain in the denominator for long as they also exactly cancel the over-counting (i.e. symmetrization of already symmetric pairs of labels) in $\mathscr{S}_C$. These can then be removed, and a "unique" symmetrizer $\tilde{\mathscr{S}}_C$ inserted instead, which only symmetrizes pairs of external labels of the same type where either the *in* and/or the *out* labels are on different vertices. The final expression for the non-orthogonally spin-adapted tensor element is,

$$\begin{aligned}
\check{C} &= \tilde{\mathscr{S}}_C F_s F_e max\{F_h, F_p\} F_c \times \\
&\quad \sum \left(\mathscr{A}_{c;A} \tilde{\mathscr{A}}_{c-xu;A} \sum_{k=0}^{min\{n_c, n_{u;B}\}} \binom{n_x + k}{k}^{-1} \tilde{\tilde{P}}^k_{c-u;B} \check{A}\check{B} \right)_{\check{C}} \\
&= \tilde{\mathscr{S}}_C F_s F_e max\{F_h, F_p\} F_c \sum SS_A \widetilde{SS}_B \check{A}\check{B} \qquad (2.48)
\end{aligned}$$

where the restriction that the result matches the orbital case of $\check{C}$ is implicit from this point.

The sign factor F_s is determined for the initial diagrammatic ordering of $\check{A}\check{B}$, as the individual permutations in the expression above carry their own sign change factors. The factor of $max\{F_h, F_p\} = (n_c!)^{-1}$ is also determined once for the initial ordering, as further permutations will change the topology (and hence the "instantaneous" value of n_c), but the over-counting factor which led to this term is fixed by the initial ordering. The factor F_e is independent of permutation. However, the additional closed loop factor F_c *does* depend on the permutation of $\check{A}\check{B}$ and so will be affected by the permutations above. The way in which this factor varies can be determined easily, though, since we chose the initial ordering of $\check{A}\check{B}$ with the maximal number of closed loops. Thus, each individual permutation in SS_A or $\widetilde{SS}_B$ necessarily reduces the number of loops by one, and hence F_c by a factor of two. When there are multiple closed loops, SS_A or $\widetilde{SS}_B$ by itself will continue to reduce the number of loops with additional compound permutations, until all closed loops are gone and these operators run out of permutations. But, when permutations from both operators are applied simultaneously, the result may not reduce the number of loops. This occurs when the permutations from both operators permute the same contracted label (or its partner). Then, the first permutation breaks the loop, but the second then simply moves one end of the new broken loop to the other vertex. If the ends of the loop (the external labels) are of the same type, then this gives a relabeling of the result (with a change in sign!). If not, then this changes the result to a different value of n_s, and so these permutations are discarded. Note that in the first case, even though the orbital case is different due to the relabeling, we could simply have considered the initial $\check{A}\check{B}$ to be relabeled so that the result still is the desired orbital case of $\check{C}$, so these contributions must be kept. Also, in the second case, even though the permutations are discarded, the orbital case they describe would have opposite sign from what the permutations give since the number of loops is not in fact decreased.

In truth, however, some combinations of cross permutations which, individually, change n_s may combine so that the net effect on n_s is zero. In this case, an orbital case of a certain number of closed loops is transformed to another of the same number of closed loops. If such permutations exist applied to the initial ordering, then there are multiple Goldstone diagrams with the same number of closed loops. In this case, though, the spin-summation operators above can be applied to each maximal orbital case separately, with the permutations which relate them ignored as if they led to orbital cases of different n_s.

So, while the effect of F_c can be incorporated easily into either SS_A or $\widetilde{SS}_B$ by itself, simultaneously incorporating into both operators creates additional permutational cross products which must be handled. This expression can be conveniently factorized ignoring these cross terms for now with the *spin-summed* quantities $\check{A}_{SS}$ and $\check{B}_{\widetilde{SS}}$, defined as,

$$\begin{aligned}
\check{A}_{SS} &= F_c SS_A \check{A} \\
&= \sum_{k=0}^{min\{n_c,n_x+n_{u;A}\}} \sum_{l=0}^{n_c-1} F_c \tilde{\tilde{P}}^k_{c-xu;A} \tilde{P}^l_{c;A} \check{A} \\
&= \left\{ \prod_{k=1}^{n_c} \left(2 + \sum_{i=k+1}^{n_c} P(c_k c_i) + \sum_{i=1}^{n_x+n_{u;A}} P(c_k x u_i) \right) \right\} \check{A} \qquad (2.49) \\
\check{B}_{\widetilde{SS}} &= F_c \widetilde{SS}_B \check{B} \\
&= \sum_{k=0}^{min\{n_c,n_{u;B}\}} 2^{min\{n_c,n_{u;B}\}-k} \binom{n_x+k}{k}^{-1} \tilde{\tilde{P}}^k_{c-u;B} \check{B} \qquad (2.50)
\end{aligned}$$

where c is the set of contracted labels (which is the same for $\check{A}$ and $\check{B}$) and xu is all other labels on $\check{A}$ (the same as $x \cup u_A$). The factorized expression is now,

$$\check{C} = \tilde{\mathscr{S}} \frac{F_s F_e}{n_c! 2^{min\{n_c,n_{u;B}\}}} \sum \check{A}_{SS} \check{B}_{\widetilde{SS}} + \text{real cross terms} - \text{extra cross terms} \qquad (2.51)$$

After permutations from SS_A and/or $\widetilde{SS}_B$ have been applied, the remaining permutations are the same as those of $SS_A\widetilde{SS}_B\check{A}\check{B}$ in the new permutation, since these are those that further reduce the number of closed loops. Thus, the cross terms arise from simultaneous permutations of SS_A and $\widetilde{SS}_B$ (the "real" cross terms) can be written in terms of the same equation above applied to a different orbital case of $\check{A}\check{B}$. Likewise, the "extra" cross terms which arise from the forced factorization into $\check{A}_{SS}$ and $\check{B}_{\widetilde{SS}}$ are of the same form, but with an additional factor of $\frac{1}{2}$ due to the inclusion of F_c in both parts. So, for each extra cross term, we must subtract a suitable term with the proper factors of 2 and $\binom{n_x + k}{k}^{-1}$. Since each cross permutation does not actually decrease the number of loops (and hence change the sign), this means that for an odd permutation from SS_A (since $\widetilde{SS}_B$ has already broken all the closed loops) we must *add* the corresponding orbital case (evaluated itself using the same rules above), or for an even permutation from SS_A, we must *subtract* the orbital case. When the permutations involve external labels of the same type, then we must add in the same term, but now with an additional factor of 2 and permuting the external labels. The orbital case which is added may itself have cross terms, so that by recursively decomposing the equation in this way considerable effort is saved. The final procedure for forming the compact, factored non-orthogonally spin-adapted equations can be summarized in the following rules:

R1$''$. Each vertex contributes an orbital tensor element: $\check{X}^{all-out-labels}_{all-in-labels}$, where $\check{X}$ is determined by the type of line – dashed for V, solid for $\hat{T}$, wavy for intermediates, etc.

R2″. One vertex is spin-summed as $\check{A}_{SS}$ and the other as $\check{B}_{\widetilde{SS}}$. For each set of permutations on $\check{A}$ and $\check{B}$ which only involve the same contracted labels, add the equation for the resulting orbital case multiplied by the proper factors from SS_A and $\widetilde{SS}_B$, and a minus sign if the permutation from SS_A is even. If the external labels in the permutations are of the same type, then add the resulting orbital case again multiplied by 2 and with the external labels permuted to match $\check{C}$.

R3″. The overall sign is equal to $(-1)^{l+h}$, where l is the number of closed loops and h is the number of hole lines.

R4″. Apply a factor of $\frac{1}{l!}$ where l is the number of closed loops.

R5″. Each set of n identically-connected vertices from an exponential expansion (e.g. the coupled cluster amplitudes) gives a factor of $\frac{1}{n!}$.

R6″. Internal lines are summed over all spatial orbitals.

R7″. Pairs of external lines of the same type, which either go *in* or *out* on different vertices are symmetrized.

R8″. Apply a factor of $2^{-min\{l,e\}}$, where l is the number of closed loops and e is the number of external pairs of lines on $\check{B}$.

where these rules must be applied to every "maximal" Goldstone diagram.

For writing the final non-orthogonally spin-adapted equations down, a combined notation for $\check{A}_{SS}$ and $\check{B}_{\widetilde{SS}}$ with index labels is adopted which shows directly how to compute the spin-summed quantity. First, zero or more sets of labels (and their partners) are topped with a hacek (ˇ). For $\check{A}_{SS}$, each label in c is topped, while for $\check{B}_{\widetilde{SS}}$ the set of all c labels is topped with a single hacek, but only if there are any u labels. Then, some set of labels is topped with a chevron (ˆ), or this may be omitted in which case all remaining indices are assumed to be as if they were so decorated. For $\check{A}_{SS}$ this is all remaining labels (xu), and for $\check{B}_{\widetilde{SS}}$ this is only the u labels. For example, one might have,

$$\check{A}_{SS} = \check{A}^{\check{m}\check{n}ab}_{\check{e}\check{f}gj} = \check{A}^{\check{m}\check{n}\widehat{ab}}_{\check{e}\check{f}\widehat{gj}} \tag{2.52}$$

$$\check{B}_{\widetilde{SS}} = \check{B}^{\widecheck{ef}g\hat{c}}_{\widecheck{mn}i\hat{k}} \tag{2.53}$$

The procedure for spin-summation is then: 1) for the first group of labels $\check{i}$ (of size $\check{n}$) topped with a hacek, apply the permutation operator,

$$\sum_{k=0}^{min\{\check{n},\hat{n}\}} 2^{min\{\check{n},\hat{n}\}-k} \binom{n_x + k}{k}^{-1} \tilde{\check{P}}^{k}_{\check{i}-\hat{i}} \tag{2.54}$$

where $\hat{i}$ are all $\hat{n}$ indices either topped with a chevron *or* indices other than $\check{i}$ topped with a hacek and n_x is the number of indices initially without either decoration, 2) remove the hacek from $\check{i}$, and 3) repeat from 1) until no more suitable indices remain. Using the examples above, this gives,

$$\begin{aligned} \check{A}^{\check{m}\check{n}\widehat{ab}}_{\check{e}\check{f}\widehat{gj}} &= (2 + P(na) + P(nb))\,(2 + P(mn) + P(ma) + P(mb)) \times \\ &\quad \check{A}^{mnab}_{efgj} \end{aligned} \tag{2.55}$$

$$\check{B}^{\widecheck{ef}g\hat{c}}_{\widecheck{mn}i\hat{k}} = (2 + \frac{1}{2}P(ec) + \frac{1}{2}P(fc))\check{B}^{efgc}_{mnik} \tag{2.56}$$

Using this notation, the equations can be written without the need to explicitly include complicated permutation operators and numerical factors.

It should be noted that the above definition of the spin-summed quantities is not quite correct for diagrams where $\check{A}$ does not have any x or u indices. In this case, the last "haceked" index group should still give a factor of two, but the definition above gives $2^{min\{\check{n},\hat{n}\}} = 1$. Thus, vertices which are "fully spin-summed" (i.e. each index is topped with a hacek) should be multiplied by an additional factor of 2. The need for this caveat is an unfortunate side-affect of treating the two types of spin-summation with the same notation. It should also be noted that the same derivation as above could be applied with $\check{A}$ and $\check{B}$ reversed. That is, ending up with $\check{A}_{\widetilde{SS}}$ and $\check{B}_{SS}$. In some situations it may be desirable to make this switch so that the resulting equations are simpler. Generally, this would be when only one vertex has any u labels, in which case this vertex should be the spin-summed vertex with SS instead of $\widetilde{SS}$.

2.4 Examples

The rules given in the previous section are hard to absorb on a first (or even third) reading, and are best illustrated by example. In this section, several such examples are given which span a range of diagrammatic topologies and which exemplify the nuances of the non-orthogonal spin-adaptation rules.

The first example is the MBPT[2] energy diagram, which was given in figure 2.2. Both Goldstone diagrams in part c do not need to be used, since the first diagram has more closed loops than the second. Thus only this diagram needs to be evaluated using the rules. The sign from rule 3″ is positive, since there are two loops and two hole lines. Rules 5″, 7″, and 8″ have no effect, while rule 4″ gives a factor of $\frac{1}{2}$. Rule 6″ gives a sum over spatial orbitals $efmn$. Finally, the real meat of the diagram is given by rules 1″ and 2″ which give, in total (and remembering the factor of 2 since $\check{v}^{\check{i}\check{j}}_{\check{a}\check{b}}$ is fully spin-summed),

$$\frac{1}{2}\sum_{efmn} \check{v}^{ab}_{ij}\check{v}^{\check{i}\check{j}}_{\check{a}\check{b}} = \sum_{efmn} \check{v}^{ab}_{ij}\left(2\check{v}^{ij}_{ab} - \check{v}^{ji}_{ab}\right) \tag{2.57}$$

which is of course the same as derived using the Goldstone or Brandow diagrams.

The second example, the ring part of $\hat{T}_2 \times V \to \hat{T}_2$, has also already been derived using Goldstone and Brandow diagrams. The diagrams are given in figure 2.3. Again, only the first diagram in part c is required. Taking either $\check{v}$ as $\check{A}$ and $\check{t}$ as $\check{B}$ or *vice versa* results in a factor of $\frac{1}{2}$ from rules $3'' - 5''$ and $8''$, a sum over em from rule 6″, and now a symmetrizer of $\left(1 + P^{ai}_{bj}\right)$ from rule 7″. Rules 1″ and 2″ give the spin-summation, for a total result of,

$$\frac{1}{2}\left(1 + P^{ai}_{bj}\right)\sum_{em}\left\{\check{v}^{\check{m}b}_{\check{e}j}\check{t}^{\check{e}a}_{\check{m}i} - \left(1 + 2P^{i}_{j}\right)\check{v}^{mb}_{je}\check{t}^{ea}_{im}\right\}$$

The use of the non-orthogonally spin-adapted rules directly gives the factored, "optimal" form, without the need for any manual intervention.

The third example is $\hat{T}_3 \times V \to \hat{T}_1$, whose diagrams are given in 2.4. Using the first diagram in part c and taking $\check{v}$ as $\check{B}$ and $\check{t}$ as $\check{A}$, we can see that rules 3″-8″ simply give a summation $\sum_{efmn}$ and factor of $\frac{1}{2}$. Rules 1″ and

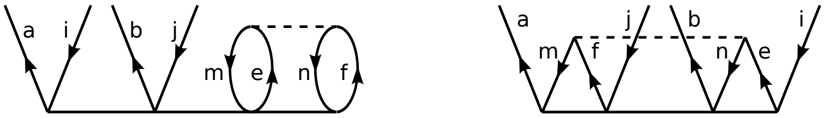

(a) Primary orbital case

(b) Secondary orbital case

Figure 2.6: Diagrams for $\hat{T}_4 \times V \rightarrow \hat{T}_2$.

$2''$ then give the very simple form,

$$\frac{1}{2}\sum_{efmn} \check{v}^{mn}_{ef} \check{t}^{\check{e}\check{f}a}_{\check{m}\check{n}i} = \frac{1}{2}\sum_{mnef} \check{v}^{mn}_{ef} \left(4\check{t}^{aef}_{imn} - 2\check{t}^{aef}_{min} - 2\check{t}^{aef}_{nmi} - 2\check{t}^{aef}_{inm} + \check{t}^{aef}_{mni} + \check{t}^{aef}_{nim}\right) \tag{2.58}$$

again exactly as it should be (including the factor of $\frac{1}{2}$ missing in the Goldstone approach). If instead we were to choose $\check{v}$ as $\check{A}$ and $\check{t}$ as $\check{B}$, we would find that now rule $8''$ gives a factor of $\frac{1}{2}$, while rules $1''$ and $2''$ give the total result,

$$\begin{aligned} \frac{1}{4}\sum_{efmn} \check{v}^{\check{m}\check{n}}_{\check{e}\check{f}} \check{t}^{\widecheck{ef}a}_{\widecheck{mn}i} &= \frac{1}{4}\sum_{mnef} \left(4\check{v}^{mn}_{ef} - 2\check{v}^{mn}_{fe}\right)\left(2\check{t}^{aef}_{imn} - \check{t}^{aef}_{min} - \check{t}^{aef}_{nmi}\right) \\ &= \frac{1}{2}\sum_{mnef} \check{v}^{mn}_{ef} \Big(4\check{t}^{aef}_{imn} - 2\check{t}^{aef}_{min} \\ &\qquad -2\check{t}^{aef}_{nmi} - 2\check{t}^{aef}_{inm} + \check{t}^{aef}_{mni} + \check{t}^{aef}_{nim}\Big) \end{aligned} \tag{2.59}$$

for this diagram, there is not much difference in the complexity of the equations, whichever choice is made.

For more complicated diagrams, however, there may be a significant difference. Consider the contribution of $\hat{T}_4 \times V \rightarrow \hat{T}_2$ whose diagrammatic form is given in figure 2.6. If we choose $\check{v} = \check{B}$ and $\check{t} = \check{A}$, then following the rules gives again a simple result,

$$\frac{1}{2}\sum_{efmn} \check{v}^{mn}_{ef} \check{t}^{\check{e}\check{f}ab}_{\check{m}\check{n}ij} \tag{2.60}$$

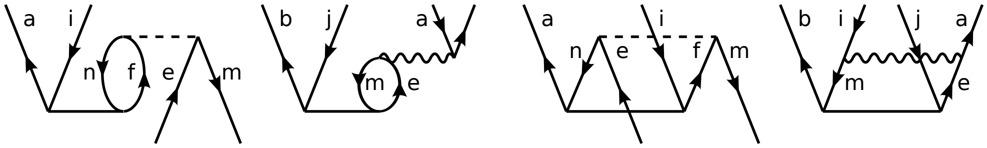

(a) Primary orbital cases

(b) Secondary orbital cases

Figure 2.7: Factorized diagrams for the ring part of $\frac{1}{2}\hat{T}_2^2 \times V \rightarrow \hat{T}_2$.

However, if instead we were to choose $\check{v} = \check{A}$ and $\check{t} = \check{B}$, we would arrive at the considerably more complicated form,

$$\frac{1}{8} \sum_{efmn} \left\{ \check{v}^{\check{m}\check{n}}_{\check{e}\check{f}} \check{t}^{\widecheck{ef}ab}_{\underset{\smile}{mn}ij} + \left(1 + 2P^i_j\right) \check{v}^{mn}_{fe} \check{t}^{efab}_{ijmn} \right\} \tag{2.61}$$

The second term in this expression arises because we have permutations on $\check{A}$ $(P(mn))$ and on $\check{B}$ $(P(mi)P(nj))$ which involve the same set of contracted labels. Thus by rule $2''$ we must add the resulting orbital case (shown in figure 2.6b), and since the external labels ij are of the same type, include a third term which is twice a permutation of this. Of course, the end result is identical, but the first choice of spin-summation requires only one tensor contraction and is considerably more compact. So, to reiterate what was stated at the end of the previous section, when only one vertex has any u labels, then this vertex should be the spin-summed vertex with SS_A instead of $\widetilde{SS}_B$.

Next consider a slight extension of the $\hat{T}_2 \times V \rightarrow \hat{T}_2$ ring example given earlier. The non-linear term (also only the ring part) $\frac{1}{2}\hat{T}_2^2 \times V \rightarrow \hat{T}_2$ can be factored as $\tilde{W} = \frac{1}{2}\hat{T}_2 \times V$, $\hat{T}_2 \times \tilde{W} \rightarrow \hat{T}_2$. The two diagrams for this example are given in figure 2.7. Using the rules we come up with the fairly simple form for $\tilde{\check{W}}_{ie}^{am}$,

$$\tilde{\check{W}}_{ie}^{am} = \frac{1}{2} \sum_{fn} \left\{ \check{t}_{\check{n}i}^{\check{f}a} \check{v}_{\check{f}e}^{\check{n}m} - \check{t}_{in}^{fa} \check{v}_{ef}^{nm} \right\} \tag{2.62}$$

The second term in this expression is another orbital case (by rule 2″) of $\tilde{W}$, name $\tilde{\check{W}}_{ei}^{am}$ which is given by the secondary diagram,

$$\tilde{\check{W}}_{ei}^{am} = -\sum_{fn} \check{t}_{in}^{fa} \check{v}_{ef}^{nm} \tag{2.63}$$

Since this orbital case is required explicit along with the "primary" case (as will be seen in the next equation), there is actually very little overhead in computing the second term in $\tilde{\check{W}}_{ie}^{am}$ since it can simply be copied from $\tilde{\check{W}}_{ei}^{am}$ without needing to do another actual tensor contraction. The second diagram gives the contribution to $\hat{T}_2$, and was examined with integrals instead of intermediates (the result is the same) using the Goldstone approach in a previous section. Using the non-orthogonally spin-adapted rules it is,

$$\frac{1}{2} \left(1 + P_{bj}^{ai}\right) \sum_{em} \left\{ \check{t}_{\check{m}j}^{\check{e}b} \tilde{\check{W}}_{\check{e}i}^{\check{m}a} - \left(1 + 2P_{j}^{i}\right) \check{t}_{jm}^{eb} \tilde{\check{W}}_{ie}^{ma} \right\} \tag{2.64}$$

The secondary spin case of $\tilde{W}$ is used in the second term, which corresponds to the secondary orbital case of the $\hat{T}_2 \times \tilde{W}$ diagram. This time the secondary orbital case is not useful on its own, and so a real second contraction is needed.

This factorized form is common in the non-orthogonally spin-adapted equations, as can be seen by examining the ring diagram for $\hat{T}_4 \times V \rightarrow \hat{T}_4$, whose diagrams are given in figure 2.8. As one might expect, applying the non-orthogonally spin-adapted rules gives a result very similar in form to that

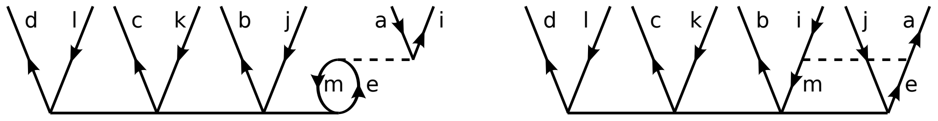

(a) Primary orbital case (b) Example secondary orbital case

Figure 2.8: Diagrams for the ring part of $\hat{T}_4 \times V \rightarrow \hat{T}_4$.

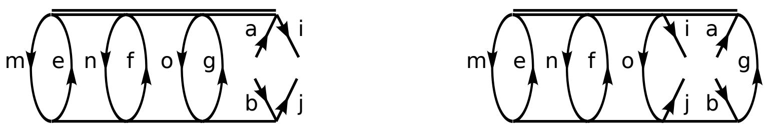

(a) Primary orbital case (b) Secondary orbital case

Figure 2.9: Diagrams for the ring part of $\hat{\Lambda}_4 \times \hat{T}_4 \rightarrow \Gamma$.

for $\hat{T}_2$,

$$\begin{aligned}\tfrac{1}{2}\left(1 + P^{ai}_{bj} + P^{ai}_{ck} + P^{ai}_{dl}\right) \textstyle\sum_{em} \Big\{ & \check{t}^{\check{e}bcd}_{\check{m}jkl} \check{v}^{\check{m}a}_{\check{e}i} - \left(1 + 2P^{i}_{j}\right) \check{t}^{ebcd}_{jmkl} \check{v}^{ma}_{ie} \\ & - \left(1 + 2P^{i}_{k}\right) \check{t}^{ebcd}_{kjml} \check{v}^{ma}_{ie} - \left(1 + 2P^{i}_{l}\right) \check{t}^{ebcd}_{ljkm} \check{v}^{ma}_{ie} \Big\} \end{aligned} \tag{2.65}$$

Now there are three "secondary" orbital cases which must be added, since m may be transposed with either j, k, or l. Applying a symmetrization operator (essentially, using $\mathscr{S}_C$ instead of $\tilde{\mathscr{S}}_C$), simplifies the expression a bit,

$$\begin{aligned}\tfrac{1}{2}\left(1 + P^{ai}_{dl} + P^{bj}_{dl} + P^{ck}_{dl}\right)\left(1 + P^{ai}_{ck} + P^{bj}_{ck}\right)\left(1 + P^{ai}_{bj}\right) \times \\ \textstyle\sum_{em} \left\{ \tfrac{1}{6} \check{t}^{\check{e}bcd}_{\check{m}jkl} \check{v}^{\check{m}a}_{\check{e}i} - \tfrac{1}{2}\left(1 + 2P^{i}_{j}\right) \check{t}^{ebcd}_{jmkl} \check{v}^{ma}_{ie} \right\} \end{aligned} \tag{2.66}$$

and exposes the structure of the equivalent $\hat{T}_2 \times V \rightarrow \hat{T}_2$ term.

As the previous diagram generalizes the form of $\hat{T}_2 \times V \rightarrow \hat{T}_2$ diagram (or equivalently with $\tilde{W}$), we can also generalize in one way the intermediate diagram $\tilde{W} = \frac{1}{2}\hat{T}_2 \times V$. Besides being an intermediate in the coupled cluster

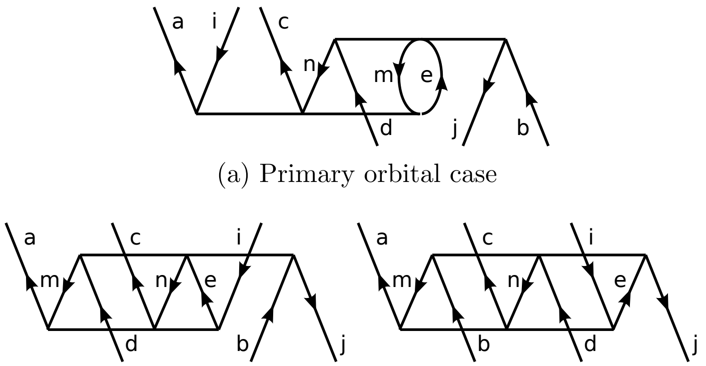

(a) Primary orbital case

(b) Secondary orbital cases

Figure 2.10: More complicated diagrams.

amplitude equations, we can replace V with $\hat{\Lambda}_2$ (and remove the $\frac{1}{2}$) and get one of the contributions (the ring contribution, of course) to the two-particle density Γ. Extending this by taking $\hat{T}_2 \rightarrow \hat{T}_4$ and $\hat{\Lambda}_2 \rightarrow \hat{\Lambda}_4$, we arrive at the equivalent contribution from CCSDTQ, whose diagrams are given in figure 2.9. Following the rules gives,

$$\frac{1}{12} \sum_{efgmno} \left\{ \check{\lambda}^{\check{m}\check{n}\check{o}i}_{\check{e}\check{f}\check{g}a} \check{t}^{e\widecheck{fg}b}_{\widecheck{mno}j} - 3\check{\lambda}^{\check{m}\check{n}oi}_{\check{e}\check{f}ag} \check{t}^{efgb}_{mnjo} \right\} \tag{2.67}$$

Unlike the case in the CCSDTQ amplitudes, here the three permutations which give a second orbital case are all identical through relabeling of the contracted labels (although this is similar to the fully symmetrized form). Also, in the secondary orbital case, there is still some spin-summation of $\hat{\Lambda}$. But, since there are no u labels left on either vertex there is not a third layer of orbital cases. Also note that $\check{t}^{e\widecheck{fg}b}_{\widecheck{mno}j} = \check{t}^{efg\check{b}}_{mno\check{j}}$, so that only the "normal" spin-summed amplitudes are needed.

Of course, ring type diagrams are not the only complicated cases made easier by the non-orthogonally spin-adapted rules. Consider the case of figure 2.10, which now has c, x, and u labels on both vertices (which we will simply label as $\check{A}$ and $\check{B}$ as in the previous section). The rules now call for a non-trivial spin-summation of $\check{B}$ as well as two distinct secondary orbital cases to be added,

$$-\frac{1}{2}\sum_{emn}\left\{\check{A}^{\check{m}nj}_{\check{e}db}\check{B}^{\check{e}c\hat{a}}_{\check{m}n\hat{i}}-\frac{1}{2}\left(1+2P^{a}_{c}\right)\check{A}^{mnj}_{deb}\check{B}^{eca}_{inm}-\frac{1}{2}\check{A}^{mnj}_{bde}\check{B}^{eca}_{inm}\right\}$$

The second added orbital case is again another "useful" case of the tensor product, so that this requires two unique contractions and one addition. Note that the presence of x labels in $\check{B}_{\widehat{SS}}$ necessitates the additional factors of $\frac{1}{2}$ on the added orbital cases. Despite the nuances introduced by having all three types of labels on each vertex, the overall structure and complexity of this expression is very similar to the others already presented.

A closely related diagram is given in figure 2.11. The only change is to take the bj labels on $\check{A}$ and make them upwards-pointing, but now we find that there are two "maximal loop" diagrams, and four secondary orbital cases. Both of these primary diagrams must be considered, and the rules must be applied to each independently. The total result is,

$$\begin{aligned}&-\tfrac{1}{2}\left(1+P^{ai}_{bj}\right)\textstyle\sum_{emn}\left\{\check{A}^{\check{m}nb}_{\check{e}dj}\check{B}^{\check{e}c\hat{a}}_{\check{m}n\hat{i}}-\tfrac{1}{2}\left(1+2P^{a}_{c}\right)\check{A}^{mnb}_{dej}\check{B}^{eca}_{inm}\right.\\&\left.-\tfrac{1}{2}\left(1+2P^{a}_{b}\right)\check{A}^{mnb}_{jde}\check{B}^{eca}_{inm}\right\}-\tfrac{1}{2}\left(1+P^{ai}_{bj}\right)\textstyle\sum_{emn}\left\{\check{A}^{\check{m}nc}_{\check{e}jd}\check{B}^{\check{e}b\hat{a}}_{\check{m}n\hat{i}}\right.\\&\left.-\tfrac{1}{2}\left(1+2P^{a}_{b}\right)\check{A}^{mnc}_{jed}\check{B}^{eba}_{inm}-\tfrac{1}{2}\left(1+2P^{a}_{c}\right)\check{A}^{mnc}_{dje}\check{B}^{eba}_{inm}\right\}\end{aligned}\qquad(2.68)$$

These are all "real" contractions now as each describes a simple permutation of the same final orbital case. This diagram is actually possible for a certain

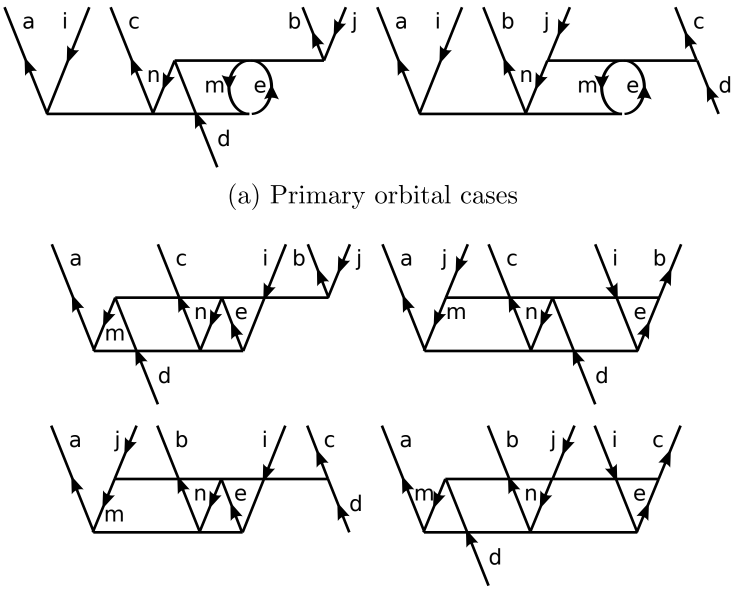

(a) Primary orbital cases

(b) Secondary orbital cases

Figure 2.11: More more complicated diagrams.

factorization of CCSDTQ, where a three-body intermediate with the shape of $\breve{A}$ is used. However, factorizations of this type are inefficient, not only because of the large number of contractions needed for this diagram, but because the three downward lines of the intermediate must come from the two-particle Hamiltonian V. Then, an alternate factorization would be to split the whole diagram on the other side of the V vertex to give an intermediate with one downward index. This alternate factorization will always have a leading-order asymptotic cost a factor of $\mathscr{O}(n^2)$ less. These contributions have also been evaluated using the Goldstone approach as an additional check, and the reduction in complexity, even though the final, factorized result is itself not particularly simple, is enormous. The form given here is also not at all obvious from the

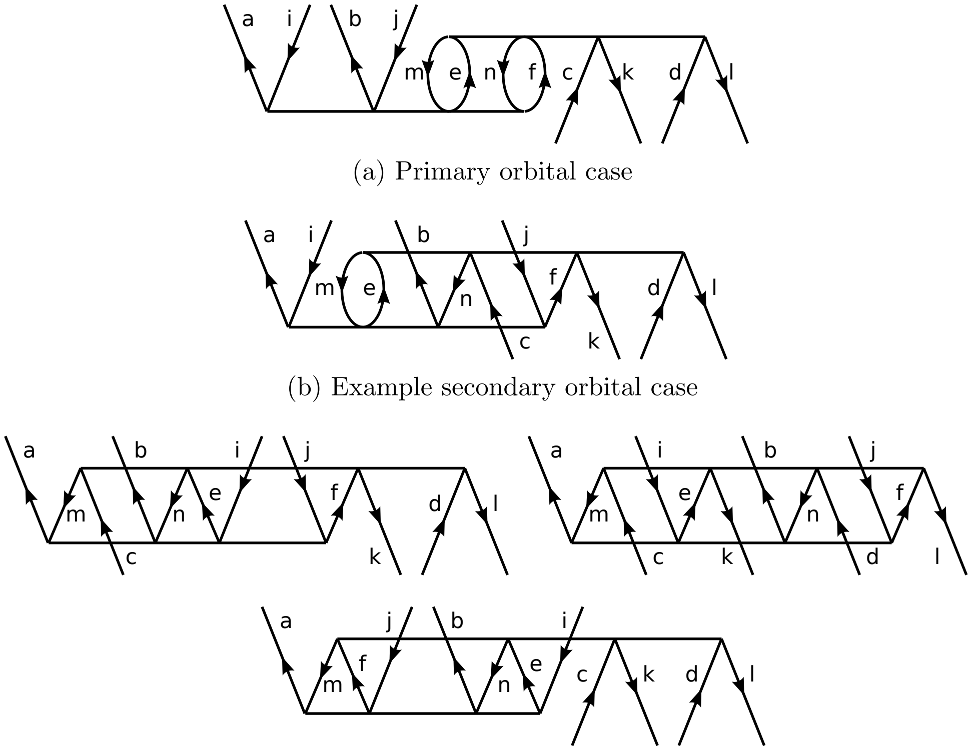

(a) Primary orbital case

(b) Example secondary orbital case

(c) Tertiary orbital cases

Figure 2.12: Very complicated diagrams.

Goldstone equations, so that it would be quite difficult to arrive at the same result without the rules derived above or a deep familiarity with these types of equations.

As a last example, let us consider the deceptively simple-looking diagram in figure 2.12. The complexity of this diagram comes from the fact that the secondary orbital cases, which must be added to correct the cross terms, themselves have a very complicated structure which involves yet another layer of orbital cases (and additional factors from the presence of x labels). However, judiciously following the rules, recursively applying them to the "lower" orbital cases, one arrives at,

$$
\begin{aligned}
&\tfrac{1}{8}\textstyle\sum_{efmn}\Big\{\check{A}^{\check{m}\check{n}kl}_{\check{e}\check{f}cd}\check{B}^{\widecheck{ef}ab}_{\widecheck{mn}ij} \\
&-4\left[\tfrac{1}{2}\check{A}^{\check{m}nkl}_{\check{e}cfd}\check{B}^{\check{e}fa\hat{b}}_{\check{m}in\hat{j}}-\tfrac{1}{6}\left(1+2P^{a}_{b}\right)\left(\check{A}^{mnkl}_{cefd}\check{B}^{efab}_{jinm}+\check{A}^{mnkl}_{fced}\check{B}^{efab}_{jinm}\right)-\tfrac{1}{6}\check{A}^{mnkl}_{dcfe}\check{B}^{efab}_{jinm}\right] \\
&-4\left[\tfrac{1}{2}\check{A}^{\check{m}nkl}_{\check{e}dcf}\check{B}^{\check{e}fa\hat{b}}_{\check{m}in\hat{j}}-\tfrac{1}{6}\left(1+2P^{a}_{b}\right)\left(\check{A}^{mnkl}_{decf}\check{B}^{efab}_{jinm}+\check{A}^{mnkl}_{fdce}\check{B}^{efab}_{jinm}\right)-\tfrac{1}{6}\check{A}^{mnkl}_{cdef}\check{B}^{efab}_{jinm}\right] \\
&-4\left[\tfrac{1}{2}\check{A}^{\check{m}nkl}_{\check{e}cfd}\check{B}^{\check{e}f\hat{a}b}_{\check{m}j\hat{i}n}-\tfrac{1}{6}\left(1+2P^{a}_{b}\right)\left(\check{A}^{mnkl}_{cefd}\check{B}^{efab}_{ijmn}+\check{A}^{mnkl}_{fced}\check{B}^{efab}_{ijmn}\right)-\tfrac{1}{6}\check{A}^{mnkl}_{dcfe}\check{B}^{efab}_{ijmn}\right] \\
&-4\left[\tfrac{1}{2}\check{A}^{\check{m}nkl}_{\check{e}dcf}\check{B}^{\check{e}f\hat{a}b}_{\check{m}j\hat{i}n}-\tfrac{1}{6}\left(1+2P^{a}_{b}\right)\left(\check{A}^{mnkl}_{decf}\check{B}^{efab}_{ijmn}+\check{A}^{mnkl}_{fdce}\check{B}^{efab}_{ijmn}\right)-\tfrac{1}{6}\check{A}^{mnkl}_{cdef}\check{B}^{efab}_{ijmn}\right] \\
&-\left(1+2P^{a}_{b}\right)\left(\check{A}^{mnkl}_{fced}\check{B}^{efab}_{ijmn}+\check{A}^{mnkl}_{cefd}\check{B}^{efab}_{ijmn}+\check{A}^{mnkl}_{decf}\check{B}^{efab}_{ijmn}+\check{A}^{mnkl}_{fdce}\check{B}^{efab}_{ijmn}\right) \\
&-\check{A}^{mnkl}_{cdef}\check{B}^{efab}_{ijmn}-\check{A}^{mnkl}_{dcfe}\check{B}^{efab}_{ijmn}+2\left(1+2P^{a}_{b}\right)\check{A}^{mnkl}_{fecd}\check{B}^{efab}_{ijmn}\Big\}
\end{aligned}
\tag{2.69}
$$

In the sixth and seven lines of the expression, note that the even permutation from SS_A part of rule $2''$ finally takes effect.

Some terms in this expression are identical after relabeling of the contracted labels. Also, the parts in square brackets correspond to the total equation for one of the secondary orbital cases. Lastly, many terms are equivalent under permutations of pairs of external labels, so that by applying the total symmetrizer instead of $\tilde{\mathscr{S}}_C$, relabeling the contracted labels, and inserting "lower" orbital cases without expansion, we get the much simpler expression,

$$
\begin{aligned}
&\tfrac{1}{8}\left(1+P^{ai}_{bj}\right)\left(1+P^{ck}_{dl}\right)\textstyle\sum_{efmn}\Big\{\tfrac{1}{4}\check{A}^{\check{m}\check{n}kl}_{\check{e}\check{f}cd}\check{B}^{\widecheck{ef}ab}_{\widecheck{mn}ij}+4(\check{A}\check{B})^{abkl}_{cjid} \\
&-\left(1+2P^{a}_{b}\right)(\check{A}\check{B})^{abkl}_{jcid}-\tfrac{1}{2}(\check{A}\check{B})^{abkl}_{cdij}+\tfrac{1}{2}\left(1+2P^{a}_{b}\right)(\check{A}\check{B})^{abkl}_{jicd}\Big\}
\end{aligned}
\tag{2.70}
$$

The orbital cases such as $(\check{A}\check{B})^{abkl}_{jicd}$ are of course understood to be the diagram(s) of $\check{A}$ and $\check{B}$ which give the listed ordering by permutation from the primary orbital case, and not simply P^i_j applied to the above.

2.5 Summary

The previous sections show that, using the properties of simple pairwise permutations, that the rules for interpreting coupled cluster diagrams in terms of spin-orbital quantities can instead be transformed into rules for generating compact, efficient equations in terms of orbital quantities. While the new rules are not as simple to understand or apply as the spin-orbital ones, they are still vastly more expedient than a direct translation of the spin-orbital equations into orbitals ones, or the derivation of the orbital equations by using Goldstone diagrams (both of which require non-obvious factorizations of the result).

Luckily, most of the diagrams encountered in the coupled cluster amplitude equations (as well as the $\hat{\Lambda}$ and density equations, discussed in the next chapter), do not trigger some of the trickier aspects of non-orthogonal spin-adaptation. In fact, the rules given above can be simplified considerably for this use, as long as certain (necessarily sub-optimal) factorizations are avoided. However, the simplification of the rules only enhances their benefit, as the translation from spin-orbital or factorization of Goldstone equations is still quite complex for CCSDT and CCSDTQ. Additionally, it is hoped that by deriving the rules in the most general case, that perhaps the theory of non-orthogonal spin-adaptation can be applied in new areas of chemical physics.

Chapter 3

Application of Non-orthogonal Spin-adaptation to CCSDTQ and CCSDT(Q)

In this chapter, the theory of non-orthogonal spin-adaptation, as developed and discussed in the previous chapter, is applied to the specific case of coupled cluster with single, double, triple, and quadruple excitations (CCSDTQ). Some simplifications of the diagrammatic rules and spin-summed amplitudes (as generated by the SS_A or $\widetilde{SS}_B$ operators) are given, since the coupled cluster amplitude equations avoid some of the complications which arose in the previous chapter. The equations in terms of spin-summed orbital amplitudes and Hamiltonian elements are surprisingly compact and simple.

Additionally, an approximate method, CCSDT(Q), which treats the effect of quadruple excitations using perturbation theory is presented and discussed. The results of the previous chapter apply equally well in this case, as the diagrams which are necessary for CCSDT(Q) are either already necessary for CCSDTQ or are quite similar.

Lastly, the calculation of the "$\hat{\Lambda}$" equations and density matrix for CCSDTQ, which are important for calculating the gradient of the energy and other molecular properties are presented and discussed. Again, since these equations can be represented diagrammatically, the non-orthogonally spin-adapted rules can be used to generate compact and efficient equations.

3.1 Spin-summation

The spin-summed amplitudes are formed by relatively simple linear combinations of the orbital (or for successive spin-summations, the previously spin-summed) amplitudes. Additionally, due to the column symmetry of the amplitudes, the permutations may be performed entirely on either the top or bottom indices. Some examples are,

$$\begin{aligned}
\check{t}^{\breve{a}b}_{\check{i}j} &= 2\check{t}^{ab}_{ij} - \check{t}^{ab}_{ji} \\
&= 2\check{t}^{ab}_{ij} - \check{t}^{ba}_{ij} \qquad (3.1) \\
\check{t}^{\breve{a}bcd}_{\check{i}jkl} &= 2\check{t}^{abcd}_{ijkl} - \check{t}^{abcd}_{jikl} - \check{t}^{abcd}_{kjil} - \check{t}^{abcd}_{ljki} \\
&= 2\check{t}^{abcd}_{ijkl} - \check{t}^{bacd}_{ijkl} - \check{t}^{cbad}_{ijkl} - \check{t}^{dbca}_{ijkl} \qquad (3.2) \\
\check{t}^{\breve{a}\check{b}cd}_{\check{i}\check{j}kl} &= 2\check{t}^{\breve{a}bcd}_{\check{i}jkl} - \check{t}^{\breve{a}bcd}_{\check{i}kjl} - \check{t}^{\breve{a}bcd}_{\check{i}lkj} \\
&= 2\check{t}^{\breve{a}bcd}_{\check{i}jkl} - \check{t}^{\breve{a}cbd}_{\check{i}jkl} - \check{t}^{\breve{a}dcb}_{\check{i}jkl} \\
&= 2\check{t}^{a\check{b}cd}_{i\check{j}kl} - \check{t}^{a\check{b}cd}_{k\check{j}il} - \check{t}^{a\check{b}cd}_{l\check{j}ki} \\
&= 2\check{t}^{a\check{b}cd}_{i\check{j}kl} - \check{t}^{c\check{b}ad}_{i\check{j}kl} - \check{t}^{d\check{b}ca}_{i\check{j}kl} \qquad (3.3)
\end{aligned}$$

Other types of spin-summation, as required by the rules of the previous chapter, all reduce to this kind of “simple” spin-summation for the case of the coupled cluster amplitude equations. For example,

$$\check{t}^{\widecheck{ab}c}_{\widecheck{ij}k} = \check{t}^{ab\check{c}}_{ij\check{k}} \tag{3.4}$$

$$\check{t}^{\widecheck{abc}d}_{\widecheck{ijk}l} = \check{t}^{abc\check{d}}_{ijk\check{l}} \tag{3.5}$$

Also, the equations can be factorized and the resulting diagrams interpreted with $\check{A}$ and $\check{B}$ (in the notation of the previous chapter) chosen so that spin-summations such as $\check{t}^{\check{a}b\hat{c}}_{\check{i}j\hat{k}}$ and $\check{t}^{\widecheck{ab}cd}_{\check{i}jkl}$ are not required. Thus, only the spin-summations $\check{t}^{\check{a}b}_{\check{i}j}$, $\check{t}^{\check{a}bc}_{\check{i}jk}$, $\check{t}^{\check{a}\check{b}c}_{\check{i}\check{j}k}$, $\check{t}^{\check{a}bcd}_{\check{i}jkl}$, $\check{t}^{\check{a}\check{b}cd}_{\check{i}\check{j}kl}$, and $\check{t}^{\check{a}\check{b}\check{c}d}_{\check{i}\check{j}\check{k}l}$ (only for CCSDT(Q)) are required.

Several properties of spin-summation are evident from the above examples and from the symmetry of the orbital quantities: first, the order of successive spin-summations is arbitrary, second, spin-summed quantities retain column symmetry separately among the spin-summed and non-spin-summed indices, and third, additional spin-summations permute the new spin-summed index with only non-spin-summed indices. A consequence of the last property is that the final spin-summation step is always just a multiplication by 2, since no non-spin-summed indices remain. Combining this with the second property shows that both the fully spin-summed and "almost" spin-summed (i.e. only one column of non-spin-summed indices) quantities have the full symmetry of the starting orbital quantity.

During the computation, it is sometimes necessary to spin-sum an orbital quantity (for example, the amplitudes) in place, and then later return it to its non-spin-summed form. For one- and two-body quantities ($\hat{T}_2$ and V), this "de-spin-summation" is simple and well-determined, for example,

$$\check{t}_{ij}^{ab} = \frac{2}{3}\check{t}_{\check{i}j}^{\breve{a}b} + \frac{1}{3}\check{t}_{\check{j}i}^{\breve{a}b} \tag{3.6}$$

However, for three- and higher-body quantities this transformation is not unique. Mathematically this is due to the fact that the transformation can be represented in terms of a singular matrix. Physically, this represents the fact that the orbital quantities are incompletely defined relative to the spin-integrated ones (for example, the value of the sum $\check{t}_{ijk}^{abc}+\check{t}_{jik}^{abc}+\check{t}_{kji}^{abc}+\check{t}_{ikj}^{abc}+\check{t}_{jki}^{abc}+\check{t}_{kij}^{abc}$ is arbitrary), while the spin-summed quantities are well-defined. It is still possible to regenerate the orbital quantities from the spin-summed ones, though, since each definite choice of equivalent orbital coefficients has a definite transformation from the spin-summed quantity. These transformations can be generated by taking the Moore-Penrose pseudo-inverse of the spin-summation transformation matrix, and then shifting all entries by a constant. Judicious choice of the constant to maximize the sparsity of the resulting transformation matrix minimizes the number of terms in the de-spin-summation relation. Possible de-spin-summation relations for all three- and four-body spin-summation cases are given by (using the amplitudes as an example),

$$\begin{aligned}
\check{t}_{ijk}^{abc} &= \frac{5}{8}\check{t}_{\check{i}jk}^{\breve{a}bc} + \frac{1}{4}\check{t}_{\check{j}ik}^{\breve{a}bc} + \frac{1}{4}\check{t}_{\check{k}ji}^{\breve{a}bc} - \frac{1}{8}\check{t}_{\check{i}kj}^{\breve{a}bc} \\
&= \frac{1}{4}\check{t}_{\check{i}\check{j}k}^{\breve{a}\check{b}c} - \frac{1}{12}\check{t}_{\check{j}\check{k}i}^{\breve{a}\check{b}c} - \frac{1}{12}\check{t}_{\check{k}\check{i}j}^{\breve{a}\check{b}c} \qquad (3.7) \\
\check{t}_{ijkl}^{abcd} &= \frac{101}{360}\check{t}_{\check{i}jkl}^{\breve{a}bcd} - \frac{1}{16}\left\{\check{t}_{\check{j}ikl}^{\breve{a}bcd} + \check{t}_{\check{k}jil}^{\breve{a}bcd} + \check{t}_{\check{l}jki}^{\breve{a}bcd}\right\} - \frac{19}{144}\left\{\check{t}_{\check{i}kjl}^{\breve{a}bcd} + \check{t}_{\check{i}lkj}^{\breve{a}bcd} + \check{t}_{\check{i}jlk}^{\breve{a}bcd}\right\} \\
&\quad -\frac{19}{160}\left\{\check{t}_{\check{k}ijl}^{\breve{a}bcd} + \check{t}_{\check{l}ikj}^{\breve{a}bcd} + \check{t}_{\check{j}kil}^{\breve{a}bcd} + \check{t}_{\check{l}jik}^{\breve{a}bcd} + \check{t}_{\check{j}lki}^{\breve{a}bcd} + \check{t}_{\check{k}jli}^{\breve{a}bcd}\right\}
\end{aligned}$$

$$-\frac{1}{40}\left\{\check{t}^{\check{a}bcd}_{\check{j}ilk}+\check{t}^{\check{a}bcd}_{\check{k}lij}+\check{t}^{\check{a}bcd}_{\check{l}kji}\right\}+\frac{89}{1440}\left\{\check{t}^{\check{a}bcd}_{\check{i}klj}+\check{t}^{\check{a}bcd}_{\check{i}ljk}\right\} \tag{3.8}$$

$$\begin{aligned} = \;& \frac{67}{480}\check{t}^{\check{a}\check{b}cd}_{\check{i}\check{j}kl}-\frac{1}{32}\check{t}^{\check{a}\check{b}cd}_{\check{j}\check{i}kl}-\frac{7}{96}\check{t}^{\check{a}\check{b}cd}_{\check{i}\check{j}lk}+\frac{9}{160}\check{t}^{\check{a}\check{b}cd}_{\check{j}\check{i}lk}+\frac{17}{480}\left\{\check{t}^{\check{a}\check{b}cd}_{\check{k}\check{l}ij}+\check{t}^{\check{a}\check{b}cd}_{\check{l}\check{k}ji}\right\} \\ & -\frac{13}{480}\left\{\check{t}^{\check{a}\check{b}cd}_{\check{k}\check{i}jl}+\check{t}^{\check{a}\check{b}cd}_{\check{j}\check{k}il}+\check{t}^{\check{a}\check{b}cd}_{\check{l}\check{i}kj}+\check{t}^{\check{a}\check{b}cd}_{\check{j}\check{l}ki}\right\}+\frac{1}{96}\left\{\check{t}^{\check{a}\check{b}cd}_{\check{k}\check{l}ji}+\check{t}^{\check{a}\check{b}cd}_{\check{l}\check{k}ij}\right\} \\ & -\frac{1}{160}\left\{\check{t}^{\check{a}\check{b}cd}_{\check{l}\check{j}ik}+\check{t}^{\check{a}\check{b}cd}_{\check{i}\check{l}jk}+\check{t}^{\check{a}\check{b}cd}_{\check{k}\check{j}li}+\check{t}^{\check{a}\check{b}cd}_{\check{i}\check{k}lj}\right\} \\ & +\frac{1}{24}\left\{\check{t}^{\check{a}\check{b}cd}_{\check{l}\check{i}jk}+\check{t}^{\check{a}\check{b}cd}_{\check{j}\check{l}ik}+\check{t}^{\check{a}\check{b}cd}_{\check{k}\check{i}lj}+\check{t}^{\check{a}\check{b}cd}_{\check{j}\check{k}li}\right\} \end{aligned} \tag{3.9}$$

$$\begin{aligned} = \;& \frac{7}{96}\check{t}^{\check{a}\check{b}\check{c}d}_{\check{i}\check{j}\check{k}l}+\frac{1}{480}\left\{\check{t}^{\check{a}\check{b}\check{c}d}_{\check{j}\check{i}\check{k}l}+\check{t}^{\check{a}\check{b}\check{c}d}_{\check{k}\check{j}\check{i}l}+\check{t}^{\check{a}\check{b}\check{c}d}_{\check{l}\check{j}\check{k}i}+\check{t}^{\check{a}\check{b}\check{c}d}_{\check{i}\check{k}\check{j}l}+\check{t}^{\check{a}\check{b}\check{c}d}_{\check{i}\check{l}\check{k}j}+\check{t}^{\check{a}\check{b}\check{c}d}_{\check{i}\check{j}\check{l}k}\right\} \\ & +\frac{11}{480}\left\{\check{t}^{\check{a}\check{b}\check{c}d}_{\check{k}\check{i}\check{l}j}+\check{t}^{\check{a}\check{b}\check{c}d}_{\check{l}\check{i}\check{j}k}+\check{t}^{\check{a}\check{b}\check{c}d}_{\check{j}\check{l}\check{i}k}+\check{t}^{\check{a}\check{b}\check{c}d}_{\check{l}\check{k}\check{i}j}+\check{t}^{\check{a}\check{b}\check{c}d}_{\check{j}\check{k}\check{l}i}+\check{t}^{\check{a}\check{b}\check{c}d}_{\check{k}\check{l}\check{j}i}\right\} \\ & +\frac{1}{32}\left\{\check{t}^{\check{a}\check{b}\check{c}d}_{\check{j}\check{i}\check{l}k}+\check{t}^{\check{a}\check{b}\check{c}d}_{\check{k}\check{l}\check{i}j}+\check{t}^{\check{a}\check{b}\check{c}d}_{\check{l}\check{k}\check{j}i}\right\} \end{aligned} \tag{3.10}$$

3.2 CCSDTQ

As discussed previously, the parameter N, which represents the maximum number of simultaneous electron excitations in the $\hat{T}$ operator, is the principal factor that controls the accuracy of the coupled cluster method (for a given molecular basis set). To describe the effects of quadruple excitations, which are necessary for very high accuracy, the coupled cluster equations must be derived for $N = 4$. In this case, the cluster operator is,

$$\hat{T} = \hat{T}_1 + \hat{T}_2 + \hat{T}_3 + \hat{T}_4 \tag{3.11}$$

Inserting this into the schematic equation for the coupled cluster amplitude and energy equations (equation (1.19) and equation (1.20)) we get,

$$\begin{aligned}\mathbf{Z}_1 \;&=\; \mathbf{F} + (\mathbf{F}-\mathbf{D})\mathbf{T}_1 + \mathbf{F}\mathbf{T}_2 + \mathbf{V}\mathbf{T}_1 + \mathbf{V}\mathbf{T}_2 + \mathbf{V}\mathbf{T}_3 + \frac{1}{2}\mathbf{F}\mathbf{T}_1^2 \\ &\quad + \frac{1}{2}\mathbf{V}\mathbf{T}_1^2 + \mathbf{V}\mathbf{T}_1\mathbf{T}_2 + \frac{1}{6}\mathbf{V}\mathbf{T}_1^3\end{aligned} \tag{3.12}$$

$$\begin{aligned}\mathbf{Z}_2 \;&=\; \mathbf{V} + (\mathbf{F}-\mathbf{D})\mathbf{T}_2 + \mathbf{F}\mathbf{T}_3 + \mathbf{V}\mathbf{T}_1 + \mathbf{V}\mathbf{T}_2 + \mathbf{V}\mathbf{T}_3 + \mathbf{V}\mathbf{T}_4 \\ &\quad + \mathbf{F}\mathbf{T}_1\mathbf{T}_2 + \frac{1}{2}\mathbf{V}\mathbf{T}_1^2 + \mathbf{V}\mathbf{T}_1\mathbf{T}_2 + \mathbf{V}\mathbf{T}_1\mathbf{T}_3 + \frac{1}{2}\mathbf{V}\mathbf{T}_2^2 + \frac{1}{6}\mathbf{V}\mathbf{T}_1^3 \\ &\quad + \frac{1}{2}\mathbf{V}\mathbf{T}_1^2\mathbf{T}_2 + \frac{1}{24}\mathbf{V}\mathbf{T}_1^4\end{aligned} \tag{3.13}$$

$$\begin{aligned}\mathbf{Z}_3 \;&=\; (\mathbf{F}-\mathbf{D})\mathbf{T}_3 + \mathbf{F}\mathbf{T}_4 + \mathbf{V}\mathbf{T}_2 + \mathbf{V}\mathbf{T}_3 + \mathbf{V}\mathbf{T}_4 + \mathbf{F}\mathbf{T}_1\mathbf{T}_3 + \frac{1}{2}\mathbf{F}\mathbf{T}_2^2 \\ &\quad + \mathbf{V}\mathbf{T}_1\mathbf{T}_2 + \mathbf{V}\mathbf{T}_1\mathbf{T}_3 + \mathbf{V}\mathbf{T}_1\mathbf{T}_4 + \frac{1}{2}\mathbf{V}\mathbf{T}_2^2 + \mathbf{V}\mathbf{T}_2\mathbf{T}_3 + \frac{1}{2}\mathbf{V}\mathbf{T}_1^2\mathbf{T}_2 \\ &\quad + \frac{1}{2}\mathbf{V}\mathbf{T}_1^2\mathbf{T}_3 + \frac{1}{2}\mathbf{V}\mathbf{T}_1\mathbf{T}_2^2 + \frac{1}{6}\mathbf{V}\mathbf{T}_1^3\mathbf{T}_2\end{aligned} \tag{3.14}$$

$$\begin{aligned}\mathbf{Z}_4 \;&=\; (\mathbf{F}-\mathbf{D})\mathbf{T}_4 + \mathbf{V}\mathbf{T}_3 + \mathbf{V}\mathbf{T}_4 + \mathbf{F}\mathbf{T}_1\mathbf{T}_4 + \mathbf{F}\mathbf{T}_2\mathbf{T}_3 + \mathbf{V}\mathbf{T}_1\mathbf{T}_3 \\ &\quad + \frac{1}{2}\mathbf{V}\mathbf{T}_2^2 + \mathbf{V}\mathbf{T}_1\mathbf{T}_4 + \mathbf{V}\mathbf{T}_2\mathbf{T}_3 + \mathbf{V}\mathbf{T}_2\mathbf{T}_4 + \frac{1}{2}\mathbf{V}\mathbf{T}_3^2 + \frac{1}{2}\mathbf{V}\mathbf{T}_1^2\mathbf{T}_3 \\ &\quad + \frac{1}{2}\mathbf{V}\mathbf{T}_1\mathbf{T}_2^2 + \frac{1}{2}\mathbf{V}\mathbf{T}_1^2\mathbf{T}_4 + \mathbf{V}\mathbf{T}_1\mathbf{T}_2\mathbf{T}_3 + \frac{1}{6}\mathbf{V}\mathbf{T}_2^3 + \frac{1}{6}\mathbf{V}\mathbf{T}_1^3\mathbf{T}_3 \\ &\quad + \frac{1}{4}\mathbf{V}\mathbf{T}_1^2\mathbf{T}_2^2\end{aligned} \tag{3.15}$$

$$E_{CC} \;=\; \mathbf{F}\mathbf{T}_1 + \mathbf{V}\mathbf{T}_2 + \mathbf{V}\mathbf{T}_1^2 \tag{3.16}$$

The coupled cluster energy does not depend directly on the $\hat{T}_3$ and $\hat{T}_4$ amplitudes. Rather, the solution of the equations in a larger space alters the converged values of the $\hat{T}_1$ and $\hat{T}_2$ amplitudes and hence the energy.

The individual terms in this equation can be represented diagrammatically as previously discussed, and using the diagrammatic interpretation of the previous chapter, explicit non-orthogonally spin-adapted equations can be derived for the case of a closed-shell molecule. One additional step must be inserted, however, in that the equations must be factorized. Since the equations are non-linear, many $\hat{T}$ operators may be involved simultaneously. When the working equations are derived directly from this form, the computational effort needed to evaluate the individual terms may be much greater than the cost of an efficient implementation. For example, in the equations above, the term $\mathbf{VT}_2^3$ produces, among other contributions, this part (the spin-orbital equation is given here, but the cost is asymptotically the same in the non-orthogonally spin-adapted form),

$$z_{ijkl}^{abcd} \leftarrow -\sum_{efmn} v_{ef}^{mn} t_{im}^{ab} t_{jk}^{ec} t_{nl}^{fd} \tag{3.17}$$

This term involves summation over four contracted labels for each of the elements of z_{ijkl}^{abcd}, which itself has eight more labels. If the number of orbitals spanned by each label is on the order of n, then this is a $\mathscr{O}(n^{12})$cost. But, it was claimed that CCSDTQ has only an $\mathscr{O}(n^{10})$ cost! The resolution to this is to break the equation into a series of steps, where at each step only two tensors are combined to form an intermediate. The intermediate from the first step is then used in the second step and so on until at the final step the result is obtained. The equation above can be factored as, for example,

$$\begin{aligned} z_{ijkl}^{abcd} &\leftarrow \sum_{e} t_{jk}^{ec} I_{iel}^{abd} && (3.18)\\ I_{iel}^{abd} &= -\sum_{m} t_{im}^{ab} I_{el}^{md} && (3.19)\\ I_{el}^{md} &= \sum_{fn} v_{ef}^{mn} t_{nl}^{fd} && (3.20) \end{aligned}$$

These individual steps now scale as $\mathscr{O}(n^9)$, $\mathscr{O}(n^7)$, and $\mathscr{O}(n^6)$, respectively.

The factorization given is not unique, however (see for example the alternate factorization of Kucharski and Bartlett).[66] In general, for a term with m tensors, there are $\frac{m!(m-1)!}{2^m}$ ways to do the factorization. Also, the factorization must be done for each term in the amplitude equations. The factorizations used should then satisfy certain “sanity checks”. First, each factorized term should scale as $\mathscr{O}(n^{10})$ or less. Second, intermediates which are as large or larger (in terms of storage space) than the cluster amplitudes should be avoided. Additionally, to maximize the efficiency of the resulting equations, intermediates of the same size and shape should be combined between as many terms as possible so that many terms can be computed as a linear combination. The scaling and the storage size of intermediates should also be minimized as much as possible beyond the limits above (especially the number of terms with the maximal scaling of $\mathscr{O}(n^{10})$ should be minimized). Luckily, a fairly simple heuristic which produces very efficient factorizations has been developed, which is to use intermediates which “look like” elements of the coupled cluster transformed Hamiltonian, $\bar{H}$, which has tensor elements of the same type as $\hat{H}$, but relabeled as $f \rightarrow F$ and $v \rightarrow W$. By this, it is meant that an intermediate, say I^{ab}_{ie}, should contain only contributions which are part of the transformed Hamiltonian element of the same type, namely W^{ab}_{ic}. Additionally, intermediates are built starting with the smallest ones first, i.e. first the one-particle intermediates are built with terms from F^a_i, F^i_j, F^a_b, and F^i_a, then intermediates with terms from W^{ij}_{kl}, then W^{ij}_{ak} and W^{ia}_{jk}, then W^{ai}_{bj}, etc. (since there are generally many fewer occupied orbitals than virtual ones). Since these intermediates are “$\bar{H}$-like”, they are labeled by $\tilde{W}$ (or $\tilde{\tilde{W}}$ when two intermediates of the same type are needed), and when all terms from the corresponding $\bar{H}$ element have been included, then the actual elements W may simply be used.

This method of factorization has been applied to the CCSDTQ equations, and the result in terms of binary tensor operations has been evaluated diagrammatically using the non-orthogonally spin-adapted rules. The energy equation is the same as previously given

$$E_{CC} = 2\sum_{em} \check{f}_e^m \check{t}_m^e + \sum_{efmn} \check{v}_{\check{e}f}^{\check{m}n} \check{\tau}_{mn}^{ef} \tag{3.21}$$

The amplitude equations are

$$\begin{aligned} \check{z}_i^a \quad = \quad & \check{f}_i^a + \sum_e (1-\delta_{ae}) \check{f}_e^a \check{t}_i^e - \sum_m \check{F}_i^m \check{t}_m^a + \sum_{em} \check{v}_{\check{e}i}^{\check{m}a} \check{t}_m^e + \sum_{em} \check{F}_e^m \check{t}_{\check{m}i}^{\check{e}a} \\ & + \sum_{efm} \check{v}_{ef}^{ma} \check{\tau}_{\check{m}i}^{\check{e}f} - \sum_{emn} \check{W}_{\check{e}i}^{\check{m}n} \check{t}_{mn}^{ea} + \frac{1}{2} \sum_{efmn} \check{v}_{ef}^{mn} \check{t}_{\check{m}\check{n}i}^{\check{e}\check{f}a} \end{aligned} \tag{3.22}$$

$$\begin{aligned} \check{z}_{ij}^{ab} \quad = \quad & \left(1 + P_{bj}^{ai}\right) \left\{ \frac{1}{2} \check{v}_{ij}^{ab} + \sum_e \check{v}_{ie}^{ab} \check{t}_j^e - \sum_m \tilde{\check{W}}_{ij}^{am} \check{t}_m^b + \sum_e \check{F}_e^a \check{t}_{ij}^{eb} \right. \\ & - \sum_m \check{F}_i^m \check{t}_{mj}^{ab} + \frac{1}{2} \sum_{em} \tilde{\check{W}}_{\check{e}i}^{\check{m}a} \check{t}_{\check{m}j}^{\check{e}b} - \left(\frac{1}{2} + P_b^a\right) \sum_{em} \tilde{\check{W}}_{ie}^{ma} \check{t}_{jm}^{eb} \\ & + \frac{1}{2} \sum_{mn} \check{W}_{ij}^{mn} \check{\tau}_{mn}^{ab} + \frac{1}{2} \sum_{ef} \check{v}_{ef}^{ab} \check{\tau}_{ij}^{ef} + \frac{1}{2} \sum_{efmn} \check{F}_e^m \check{t}_{\check{m}ij}^{\check{e}ab} \\ & \left. + \sum_{efm} \check{W}_{ef}^{am} \check{t}_{\check{m}ij}^{\check{f}eb} - \sum_{emn} \check{W}_{ej}^{mn} \check{t}_{\check{m}in}^{\check{e}ab} + \frac{1}{4} \sum_{efmn} \check{v}_{ef}^{mn} \check{t}_{\check{m}\check{n}ij}^{\check{e}\check{f}ab} \right\} \end{aligned} \tag{3.23}$$

$$\begin{aligned} \check{z}_{ijk}^{abc} \quad = \quad & \left(1 + P_{ck}^{ai} + P_{ck}^{bj}\right) \left(1 + P_{bj}^{ai}\right) \left\{ \sum_e \tilde{\check{W}}_{ej}^{ab} \check{t}_{ik}^{ec} - \sum_m \check{W}_{ij}^{am} \check{t}_{mk}^{bc} \right. \\ & + \frac{1}{2} \sum_e \check{F}_e^a \check{t}_{ijk}^{ebc} - \frac{1}{2} \sum_m \check{F}_i^m \check{t}_{mjk}^{abc} + \frac{1}{4} \sum_{em} \check{W}_{\check{e}i}^{\check{m}a} \check{t}_{\check{m}jk}^{\check{e}bc} \\ & - \left(\frac{1}{2} + P_b^a\right) \sum_{em} \check{W}_{ie}^{ma} \check{t}_{jmk}^{ebc} + \frac{1}{2} \sum_{mn} \check{W}_{ij}^{mn} \check{t}_{mnk}^{abc} + \frac{1}{2} \sum_{ef} \check{W}_{ef}^{ab} \check{t}_{ijk}^{efc} \end{aligned}$$

$$
\begin{aligned}
&+\frac{1}{6}\sum_{em}\check{F}_{e}^{m}\check{t}_{\check{m}ijk}^{\check{e}abc}+\frac{1}{2}\sum_{efm}\check{W}_{ef}^{am}\check{t}_{\check{m}ijk}^{\check{f}ebc}-\frac{1}{2}\sum_{emn}\check{W}_{ej}^{mn}\check{t}_{\check{m}ink}^{\check{e}abc}\Bigg\}
\end{aligned}
\tag{3.24}
$$

$$
\begin{aligned}
\check{z}_{ijkl}^{abcd} \;=\;& \left(1+P_{dl}^{ai}+P_{dl}^{bj}+P_{dl}^{ck}\right)\left(1+P_{ck}^{ai}+P_{ck}^{bj}\right)\left(1+P_{bj}^{ai}\right)\times \\
&\Bigg\{\frac{1}{2}\sum_{e}\check{W}_{ej}^{ab}\check{t}_{ikl}^{ecd}-\frac{1}{2}\sum_{m}\check{W}_{ij}^{am}\check{t}_{mkl}^{bcd}+\frac{1}{6}\sum_{e}\check{F}_{e}^{a}\check{t}_{ijkl}^{ebcd} \\
&-\frac{1}{6}\sum_{m}\check{F}_{i}^{m}\check{t}_{mjkl}^{abcd}+\frac{1}{12}\sum_{ef}\check{W}_{\check{e}i}^{\check{m}a}\check{t}_{\check{m}jkl}^{\check{e}bcd}-\frac{1}{2}\left(\frac{1}{2}+P_{b}^{a}\right)\sum_{em}\check{W}_{ie}^{ma}\check{t}_{jmkl}^{ebcd} \\
&+\frac{1}{4}\sum_{mn}\check{W}_{ij}^{mn}\check{t}_{mnkl}^{abcd}+\frac{1}{4}\sum_{ef}\check{W}_{ef}^{ab}\check{t}_{ijkl}^{efcd}+\frac{1}{8}\sum_{em}\tilde{\check{W}}_{\check{e}ij}^{\check{m}ab}\check{t}_{\check{m}kl}^{\check{e}cd} \\
&-\left(\frac{1}{2}+P_{c}^{a}\right)\sum_{em}\tilde{\check{W}}_{iej}^{mab}\check{t}_{kml}^{ecd}+\frac{1}{2}\sum_{mn}\tilde{\check{W}}_{ijk}^{amn}\check{t}_{mnl}^{bcd} \\
&-\frac{1}{2}\sum_{m}\tilde{\check{W}}_{ijk}^{abm}\check{t}_{ml}^{cd}+\frac{1}{2}\sum_{e}\tilde{\check{W}}_{ejk}^{abc}\check{t}_{il}^{ed}\Bigg\}
\end{aligned}
\tag{3.25}
$$

The intermediates used in the above equations are given by

$$\check{\tau}_{ij}^{ab} \;=\; \check{t}_{ij}^{ab}+\check{t}_{i}^{a}\check{t}_{j}^{b} \tag{3.26}$$

$$\check{F}_{i}^{m} \;=\; \left(1-\delta_{mi}\right)\check{f}_{i}^{m}+\sum_{e}\check{F}_{e}^{m}\check{t}_{i}^{e}+\sum_{efn}\check{v}_{\check{f}e}^{\check{n}m}\check{t}_{ni}^{fe}+\sum_{en}\check{v}_{\check{f}i}^{\check{n}m}\check{t}_{n}^{f} \tag{3.27}$$

$$\check{F}_{e}^{a} \;=\; \left(1-\delta_{ae}\right)\check{f}_{e}^{a}-\sum_{m}\check{F}_{e}^{m}\check{t}_{m}^{a}-\sum_{fmn}\check{v}_{\check{f}e}^{\check{n}m}\check{t}_{nm}^{fa}+\sum_{fm}\check{v}_{\check{f}e}^{\check{m}a}\check{t}_{m}^{f} \tag{3.28}$$

$$\check{F}_{e}^{m} \;=\; \check{f}_{e}^{m}+\sum_{fn}\check{v}_{\check{f}e}^{\check{n}m}\check{t}_{n}^{f} \tag{3.29}$$

$$\check{W}_{ej}^{mn} \;=\; \check{v}_{ej}^{mn}+\sum_{f}\check{v}_{ef}^{mn}\check{t}_{j}^{f} \tag{3.30}$$

$$\check{W}_{ef}^{am} \;=\; \check{v}_{ef}^{am}-\sum_{n}\check{v}_{ef}^{nm}\check{t}_{n}^{a} \tag{3.31}$$

$$\tilde{\check{W}}_{ij}^{am} \;=\; \check{v}_{ij}^{am}+\sum_{e}\check{v}_{ej}^{am}\check{t}_{i}^{e}+\sum_{e}\check{v}_{ie}^{am}\check{t}_{j}^{e}+\sum_{ef}\check{v}_{ef}^{am}\check{\tau}_{ij}^{ef} \tag{3.32}$$

$$\check{W}_{ij}^{am} \;=\; \tilde{\check{W}}_{ij}^{am}+\frac{1}{2}\sum_{en}\check{v}_{\check{e}j}^{\check{n}m}\check{t}_{\check{n}i}^{\check{e}a}-\left(\frac{1}{2}+P_{j}^{i}\right)\sum_{en}\check{v}_{je}^{nm}\check{t}_{in}^{ea}$$

$$
\begin{aligned}
& -\sum_{n} \check{W}_{ij}^{nm} \check{t}_{n}^{a} + \sum_{e} \check{F}_{e}^{m} \check{t}_{ij}^{ae} + \sum_{efn} \check{v}_{ef}^{mn} \check{t}_{\check{n}ij}^{\check{f}ae} && (3.33)\\
\tilde{\check{W}}_{ej}^{ab} &= \check{v}_{ej}^{ab} - \sum_{m} \tilde{\tilde{\check{W}}}_{ej}^{am} \check{t}_{m}^{b} - \sum_{m} \tilde{\tilde{\check{W}}}_{ej}^{mb} \check{t}_{m}^{a} + \sum_{mn} \check{W}_{ej}^{mn} \check{\tau}_{mn}^{ab} \\
&\quad + \sum_{f} \check{v}_{ef}^{ab} \check{t}_{j}^{f} + \frac{1}{2} \sum_{fm} \check{v}_{\check{f}e}^{\check{m}a} \left(\check{t}_{\check{m}j}^{\check{f}b} - \check{t}_{j}^{f} \check{t}_{m}^{b} \right) \\
&\quad - \left(\frac{1}{2} + P_{b}^{a} \right) \sum_{fm} \check{v}_{ef}^{ma} \check{\tau}_{jm}^{fb} - \sum_{fmn} \check{v}_{ef}^{mn} \check{t}_{\check{n}im}^{\check{f}ab} && (3.34)\\
\check{W}_{ej}^{ab} &= \tilde{\check{W}}_{ej}^{ab} - \sum_{m} \check{F}_{e}^{m} \check{t}_{mj}^{ab} && (3.35)\\
\tilde{\check{W}}_{ei}^{ma} &= \check{v}_{ei}^{ma} - \sum_{n} \check{W}_{ei}^{mn} \check{t}_{n}^{a} + \sum_{f} \check{v}_{ef}^{ma} \check{t}_{i}^{f} + \frac{1}{4} \sum_{fn} \check{v}_{\check{f}e}^{\check{n}m} \check{t}_{\check{n}i}^{\check{f}a} \\
&\quad -\frac{1}{4} \sum_{fn} \check{v}_{ef}^{nm} \check{t}_{in}^{fa} && (3.36)\\
\tilde{\check{W}}_{ie}^{ma} &= \check{v}_{ie}^{ma} - \sum_{n} \check{W}_{ie}^{mn} \check{t}_{n}^{a} + \sum_{f} \check{v}_{fe}^{ma} \check{t}_{i}^{f} - \frac{1}{2} \sum_{fn} \check{v}_{ef}^{nm} \check{t}_{in}^{fa} && (3.37)\\
\tilde{\tilde{\check{W}}}_{ei}^{ma} &= \check{v}_{ei}^{ma} + \frac{1}{2} \sum_{fn} \check{v}_{\check{f}e}^{\check{n}m} \check{t}_{\check{n}i}^{\check{f}a} - \frac{1}{2} \sum_{fn} \check{v}_{ef}^{nm} \check{t}_{in}^{fa} && (3.38)\\
\tilde{\tilde{\check{W}}}_{ie}^{ma} &= \check{v}_{ie}^{ma} - \sum_{fn} \check{v}_{ef}^{nm} \check{t}_{in}^{fa} && (3.39)\\
\check{W}_{ei}^{ma} &= \tilde{\check{W}}_{ei}^{ma} + \frac{1}{2} \tilde{\tilde{\check{W}}}_{ei}^{ma} - \frac{1}{2} \check{v}_{ei}^{ma} && (3.40)\\
\check{W}_{ie}^{ma} &= \tilde{\check{W}}_{ie}^{ma} + \frac{1}{2} \tilde{\tilde{\check{W}}}_{ie}^{ma} - \frac{1}{2} \check{v}_{ie}^{ma} && (3.41)\\
\check{W}_{ij}^{mn} &= \left(1 + P_{nj}^{mi}\right) \left\{ \frac{1}{2} \check{v}_{ij}^{mn} + \sum_{e} \check{v}_{ie}^{mn} \check{t}_{j}^{e} + \frac{1}{2} \sum_{ef} \check{v}_{ef}^{mn} \check{\tau}_{ij}^{ef} \right\} && (3.42)\\
\check{W}_{ef}^{ab} &= \left(1 + P_{fb}^{ea}\right) \left\{ \frac{1}{2} \check{v}_{ef}^{ab} + \sum_{m} \check{v}_{ef}^{am} \check{t}_{m}^{b} + \frac{1}{2} \sum_{mn} \check{v}_{ef}^{mn} \check{\tau}_{mn}^{ab} \right\} && (3.43)\\
\tilde{\check{W}}_{eij}^{mab} &= \left(1 + P_{bj}^{ai}\right) \left\{ \sum_{f} \check{W}_{ef}^{ma} \check{t}_{ji}^{bf} - \sum_{n} \check{W}_{ei}^{mn} \check{t}_{nj}^{ab} + \frac{1}{8} \sum_{fn} \check{v}_{\check{f}e}^{\check{n}m} \check{t}_{\check{n}ij}^{\check{f}ab} \right.
\end{aligned}
$$

$$-\frac{1}{4}\sum_{fn}\check{v}^{nm}_{ef}\check{t}^{fab}_{inj}\Bigg\} \tag{3.44}$$

$$\tilde{\check{W}}^{mab}_{iej} = \sum_{f}\check{W}^{ma}_{fe}\check{t}^{bf}_{ji} - \sum_{n}\check{W}^{mn}_{ie}\check{t}^{ab}_{nj} - \frac{1}{2}\sum_{fn}\check{v}^{nm}_{ef}\check{t}^{fab}_{inj} \tag{3.45}$$

$$\tilde{\check{W}}^{amn}_{ijk} = \left(1 + P^{mj}_{nk}\right)\Bigg\{\sum_{e}\check{W}^{mn}_{ek}\check{t}^{ae}_{ij} + \frac{1}{2}\sum_{ef}\check{v}^{mn}_{ef}\check{t}^{aef}_{ijk}\Bigg\} \tag{3.46}$$

$$\tilde{\check{W}}^{abm}_{ijk} = \left(1 + P^{ai}_{bj}\right)\Bigg\{\sum_{ef}\check{W}^{am}_{ef}\check{t}^{ebf}_{ijk} + \sum_{e}\check{W}^{ma}_{ei}\check{t}^{be}_{jk} + \sum_{e}\check{W}^{ma}_{ke}\check{t}^{be}_{ji}$$

$$-\frac{1}{2}\sum_{n}\check{W}^{mn}_{ki}\check{t}^{ab}_{nj} + \frac{1}{2}\sum_{efn}\check{v}^{mn}_{ef}\check{t}^{\check{f}abe}_{\check{n}ijk}\Bigg\} \tag{3.47}$$

$$\tilde{\check{W}}^{abc}_{ejk} = \left(1 + P^{bj}_{ck}\right)\Bigg\{\frac{1}{2}\sum_{f}\check{W}^{ab}_{ef}\check{t}^{fc}_{jk} - \frac{1}{2}\sum_{fmn}\check{v}^{mn}_{ef}\check{t}^{\check{f}abc}_{\check{n}mjk}\Bigg\} \tag{3.48}$$

3.3 CCSDT(Q)

The full CCSDTQ method, while it is generally extremely accurate, is also quite costly. The amplitudes are also quite large, scaling in size as $\mathscr{O}(n^8)$. Since it is an iterative method, the amplitudes must be stored and fully read through memory each iteration, possibly many times if there is not enough main memory to compute the $\mathbf{T}_4 \rightarrow \mathbf{Z}_4$ terms in one pass. However, the situation is similar to that in CCSDT when its computational cost and storage requirements are compared to CCSD. In that case, it is well-known that only an approximate treatment of the effect of $\hat{T}_3$ is required to gain a level of accuracy generally quite close to that of full CCSDT. By far the most commonly-used and successful approximation in this vein is the CCSD(T) approximation, which treats the effect of triples with an $\mathscr{O}(n^7)$ cost (compared to $\mathscr{O}(n^8)$ for full CCSDT), and is non-iterative such that the $\hat{T}_3$ amplitudes need not be stored on disk and can instead be computed in blocks as main memory permits.

The original derivation of non-iterative triples corrections to CCSD is based on an analysis of the CCSDT energy in terms of perturbation theory,[7,8] where the effects of $\hat{T}_3$ are included through fourth order. In this form of perturbation theory, the zeroth-order solution is taken as the self-consistent field (SCF) single-particle wavefunction, and $\hat{V}$ is used as the first-order perturbation. The Fock matrix $\hat{F}$ is kept as zero-order since it gives the SCF energy of the reference and excited single-particle states. The amplitudes $\hat{T}_k$ are then of order $k-1$ except for $\hat{T}_1$ which is generally treated as second-order since the SCF solution does not couple directly to single excitations. This method was termed CCSD+T(CCSD) (also called CCSD[T]), and obtained a reasonable level of accuracy compared to full CCSDT.[7] However, it was soon discovered that the addition of a particular fifth-order term improved the accuracy of the method substantially, and this modified method came to be known as CCSD(T).[8] A later derivation of CCSD(T) used perturbation theory based on the CCSD wavefunction as the starting point, rather than the SCF wavefunction.[67] From this approach, all of the terms in CCSD(T) arise together naturally in third order. Later work using this same method of perturbation theory extended the same type of approximation to CCSDT(Q),[57] CCSDTQ(P), and higher levels of coupled cluster.[58]

In this second type of perturbation theory, generally called Löwdin partitioning, the Hamiltonian and wavefunction are partitioned into "primary" (P), and "secondary" (Q) pieces. Schematically, the Schrödinger equation then becomes,

$$\left(\begin{array}{cc} \hat{H}_{PP} & \hat{H}_{PQ} \\ \hat{H}_{QP} & \hat{H}_{QQ} \end{array} \right) \left(\begin{array}{c} |\Psi_P\rangle \\ |\Psi_Q\rangle \end{array} \right) = E \left(\begin{array}{c} |\Psi_P\rangle \\ |\Psi_Q\rangle \end{array} \right) \tag{3.49}$$

As in equation (1.8), the coupled cluster energy and wavefunction can be represented as the solution of a non-Hermitian Schrödinger equation in a given space of single-particle functions (for example, the space of single, double, and triple excitations for CCSDT). However, the wavefunction in this case (which is simply the reference function $|\Phi_0\rangle$) in this picture is not an eigenfunction of $\bar{H}$ in the *un-truncated* space of single-particle functions. Rather, we can expand the exact eigenvector (of $\bar{H}$, not $\hat{H}$, although the exact energy is the same since a similarity transform preserves the spectrum) as $|\Psi_{P,Q}\rangle = \hat{R}_{P,Q}|\Phi_0\rangle$, where the additional operator $\hat{R}$ corrects for the solution of the cluster amplitudes in the truncated space (and the truncation of the cluster operator itself). Since the wavefunction in the truncated problem is the reference function, then for the truncated space P we can write this as $\hat{R}_P = \mathbf{1} + \Delta\hat{R}_P$. Then, we can obtain the partitioned equation (where E is the *exact* energy)

$$\left(\begin{array}{cc} \bar{H}_{PP} & \bar{H}_{PQ} \\ \bar{H}_{QP} & \bar{H}_{QQ} \end{array} \right) \left(\begin{array}{c} \hat{R}_P|\Phi_0\rangle \\ \hat{R}_Q|\Phi_0\rangle \end{array} \right) = E \left(\begin{array}{c} \hat{R}_P|\Phi_0\rangle \\ \hat{R}_Q|\Phi_0\rangle \end{array} \right) \tag{3.50}$$

Since we wish to obtain an approximation to CCSDTQ, the CCSDT wavefunction should be used as the starting point, so that P spans the reference state plus all single, double, and triple excitations (i.e. $P = 0 + S + D + T$), and so that Q contains all higher excitations. Multiplying through, we obtain,

$$\bar{H}_{PP}\hat{R}_P|\Phi_0\rangle + \bar{H}_{PQ}\hat{R}_Q|\Phi_0\rangle = E\hat{R}_P|\Phi_0\rangle \tag{3.51}$$

$$\bar{H}_{QP}\hat{R}_P|\Phi_0\rangle + \bar{H}_{QQ}\hat{R}_Q|\Phi_0\rangle = E\hat{R}_Q|\Phi_0\rangle \tag{3.52}$$

The second equation can be re-arranged to solve for $\hat{R}_Q|\Phi_0\rangle$,

$$\hat{R}_Q|\Phi_0\rangle = (E - \bar{H}_{QQ})^{-1}\bar{H}_{QP}\hat{R}_P|\Phi_0\rangle \tag{3.53}$$

Substituting this back into the first equation gives a single (albeit recursively-defined) equation for the energy,

$$\left[\bar{H}_{PP} + \bar{H}_{PQ}(E - \bar{H}_{QQ})^{-1}\bar{H}_{QP}\right]\hat{R}_P|\Phi_0\rangle = E\hat{R}_P|\Phi_0\rangle \tag{3.54}$$

This can be multiplied on the left by a suitable exact left-hand wavefunction, projected onto the P space, $\langle\Phi_0|\hat{L}_P$. The left- and right-hand wavefunctions are not the same, since the transformed Hamiltonian is not Hermitian. The left-hand wavefunction has a non-trivial structure even for the original truncated coupled cluster problem. Thus, we have for the truncated space P, $\hat{L}_P = \mathbf{1} + \hat{\Lambda} + \Delta\hat{L}_P$, where $\mathbf{1} + \hat{\Lambda}$ is the left-hand wavefunction of the truncated problem. The $\hat{\Lambda}$ vector will be discussed in more detail in the next section. After left-multiplication, the equation becomes

$$\langle\Phi_0|(\mathbf{1} + \hat{\Lambda} + \Delta\hat{L}_P)\left[\bar{H}_{PP} + \bar{H}_{PQ}(E - \bar{H}_{QQ})^{-1}\bar{H}_{QP}\right](\mathbf{1} + \Delta\hat{R}_P)|\Phi_0\rangle = E \tag{3.55}$$

Lastly, since $\bar{H}_{PP}$ is already block-diagonal due to the solution of the coupled cluster equations (with the coupled cluster energy as $\langle\Phi_0|\bar{H}_{PP}|\Phi_0\rangle$), then this rearranges slightly to,

$$\begin{aligned}\langle\Phi_0|(\mathbf{1}+\hat{\Lambda}+\Delta\hat{L}_P)\bar{H}_{PQ}(E-\bar{H}_{QQ})^{-1}\bar{H}_{QP}(\mathbf{1}+\Delta\hat{R}_P)|\Phi_0\rangle \\ = E - E_{CCSDT}\end{aligned} \qquad (3.56)$$

So far, the treatment has been formally exact, with the difficulty being that the energy appears on both sides of the equation (so that an iterative approach would be needed to solve it directly), and that the inverse of the transformed Hamiltonian $\bar{H}_{QQ}$ is needed. Thus, we must solve this approximately, expanding the transformed Hamiltonian, energy, and left- and right-hand wavefunctions in a perturbation series,

$$\bar{H} = \bar{H}^{[0]} + \bar{H}^{[1]} + \bar{H}^{[2]} + \ldots \qquad (3.57)$$

$$E = E^{[0]} + E^{[1]} + E^{[2]} + \ldots \qquad (3.58)$$

$$\Delta\hat{L}_P = \Delta\hat{L}_P^{[2]} + \Delta\hat{L}_P^{[3]} + \ldots \qquad (3.59)$$

$$\Delta\hat{R}_P = \Delta\hat{R}_P^{[4]} + \Delta\hat{R}_P^{[5]} + \ldots \qquad (3.60)$$

Since CCSDT is the starting point, we take $\hat{\Lambda}$ as zeroth-order and set $E^{[0]} = E_{CCSDT}$. The order of a given element of the transformed Hamiltonian is determined by adding up the order of each piece which contributes to it, with the original Hamiltonian being first order and the order of the amplitudes as defined above. The corrections to the wavefunctions do not start at first order since several elements of $\hat{\Lambda}$, $\hat{T}$, and $\hat{H}$ must be combined to first reach the Q space and then return to the P space. Inserting these into equation (3.56) gives a non-zero contribution first at third and fourth order

$$\langle\Phi_0|(\mathbf{1}+\hat{\Lambda})(\bar{H}^{[0]}_{PQ}+\bar{H}^{[1]}_{PQ})(E_{CCSDT}-\bar{H}^{[0]}_{QQ})^{-1}\bar{H}^{[3]}_{QP}|\Phi_0\rangle \\ = E - E_{CCSDT} \tag{3.61}$$

$\bar{H}^{[3]}_{QP}$ contains contributions of the type $\mathbf{VT_3}$ and $\frac{1}{2}\mathbf{VT_2^2}$, while $(\mathbf{1}+\hat{\Lambda})(\bar{H}^{[0]}_{PQ}+\bar{H}^{[1]}_{PQ})$ contains terms of the type $\mathbf{L}_2\mathbf{V}$, $\mathbf{L}_3\mathbf{F}$, and $\mathbf{L}_3\mathbf{V}$, where $\mathbf{L}$ does not need to be contracted with the Hamiltonian. The zero-order part of the transformed Hamiltonian is simply the Fock matrix $\hat{F}$ plus the coupled cluster energy on the diagonal. However, if the Fock matrix is not diagonal, then it is again a very difficult proposition to invert $\bar{H}^{[0]}_{QQ}$. Thus, it is customary to enforce this condition, which can always be obtained by diagonalizing the Fock matrix (separately for occupied and virtual orbitals so that the SCF and coupled cluster energy is unchanged), and then rotating the orbitals accordingly. Then, $(E_{CCSDT}-\bar{H}^{[0]}_{QQ})^{-1}$ is equal to the same inverse energy denominators $-\mathbf{D}^{-1}$ as used in the coupled cluster equations.

The solution of the $\hat{\Lambda}$ equations is approximately the same cost as solving the amplitude equations, meaning that the iterative cost would be doubled to require these elements. Instead, as is done for CCSD(T), the transpose of the cluster operator $\hat{T}^{\dagger}$ can be used instead, as it and the $\hat{\Lambda}$ operator have the same solution through the lowest non-zero order. The CCSDT(Q) correction is then obtained in schematic form as,

$$\begin{aligned} E_{(Q)} &= -(\mathbf{T}_2^\dagger \mathbf{V} + \mathbf{T}_3^\dagger \mathbf{F} + \mathbf{T}_3^\dagger \mathbf{V})\mathbf{D}_4^{-1}(\mathbf{V}\mathbf{T}_3 + \frac{1}{2}\mathbf{V}\mathbf{T}_2^2)_c \\ &= -\mathbf{Z}_4(d)\mathbf{D}_4^{-1}\mathbf{Z}_4(c) \\ &= \mathbf{Z}_4(d)\mathbf{T}_4(c) \end{aligned} \tag{3.62}$$

Efficient non-orthogonally spin-adapted equations can be obtained using the same factorization philosophy and the new diagrammatic technique, giving

$$E_{(Q)} = \frac{1}{12}\sum_{abcdijkl} \check{z}_{ijkl}^{abcd}(d)\check{t}_{\check{i}\check{j}\check{k}l}^{\check{a}\check{b}\check{c}d}(c) \tag{3.63}$$

$$\begin{aligned} \check{z}_{ijkl}^{abcd}(d) &= \check{z}_{ijkl}^{abcd}(e) + \left(1 + P_{dl}^{ai} + P_{dl}^{bj} + P_{dl}^{ck}\right)\left(1 + P_{ck}^{ai} + P_{ck}^{bj}\right) \times \\ & \left(1 + P_{bj}^{ai}\right)\left\{\frac{1}{4}\check{v}_{ij}^{ab}\check{t}_{kl}^{cd} + \frac{1}{6}\check{f}_i^a\check{t}_{jkl}^{bcd}\right\} \end{aligned} \tag{3.64}$$

$$\begin{aligned} \check{z}_{ijkl}^{abcd}(c) &= \check{z}_{ijkl}^{abcd}(e) + \left(1 + P_{dl}^{ai} + P_{dl}^{bj} + P_{dl}^{ck}\right)\left(1 + P_{ck}^{ai} + P_{ck}^{bj}\right) \times \\ & \left(1 + P_{bj}^{ai}\right)\left\{\frac{1}{2}\sum_e \tilde{\tilde{\check{W}}}_{ije}^{abc}\check{t}_{kl}^{ed} - \frac{1}{2}\sum_m \tilde{\tilde{\check{W}}}_{ijk}^{abm}\check{t}_{ml}^{cd}\right\} \end{aligned} \tag{3.65}$$

$$\begin{aligned} \check{z}_{ijkl}^{abcd}(e) &= \left(1 + P_{dl}^{ai} + P_{dl}^{bj} + P_{dl}^{ck}\right)\left(1 + P_{ck}^{ai} + P_{ck}^{bj}\right)\left(1 + P_{bj}^{ai}\right) \times \\ & \left\{\frac{1}{2}\sum_e \check{v}_{ie}^{ab}\check{t}_{jkl}^{ecd} - \frac{1}{2}\sum_m \check{v}_{ij}^{am}\check{t}_{mkl}^{bcd}\right\} \end{aligned} \tag{3.66}$$

using the intermediates

$$\tilde{\tilde{\check{W}}}_{ije}^{abc} = \sum_f \check{v}_{fe}^{bc}\check{t}_{ij}^{af} \tag{3.67}$$

$$\tilde{\tilde{\check{W}}}_{ijk}^{abm} = -\sum_n \check{v}_{jk}^{nm}\check{t}_{in}^{ab} + \sum_e \check{v}_{je}^{bm}\check{t}_{ik}^{ae} + \sum_e \check{v}_{ek}^{bm}\check{t}_{ij}^{ae} \tag{3.68}$$

The need for intermediates is a major difference between CCSD(T) and CCSDT(Q), especially as the necessity of the $\tilde{\tilde{\check{W}}}_{ije}^{abc}$ intermediate which is larger even than the $\hat{T}_3$ amplitudes complicates the implementation of the method when it does not fit in memory and when using distributed parallelism.

3.4 Beyond Single-point Energies

The equations given in the previous sections are sufficient to determine the energy of the ground state of the system. However, it is often desirable to determine additional properties of the system such as molecular geometry, dipole moment, polarizability, magnetic properties, etc. Determination of the equilibrium molecular geometry, that is the geometry at which the energy of the system (in the Born-Oppenheimer approximation) is minimized, generally requires knowledge of the energy gradient with respect to displacements of the positions of the atoms (point-based methods such as simplex optimization don't necessarily require this, but are rarely used).[68–70] Molecular properties, such as the dipole moment, require the wavefunction for their computation[*]. But, since coupled cluster is a non-Hermitian theory, this in reality means both the right- and left-hand wavefunctions.[6,71] The determination of this left-hand wavefunction is also closely related to the theory of coupled cluster gradients and to the calculation of excited states. Therefore, derivation of equations for the energy gradient represents a valuable theoretical goal.

The basic theory of coupled cluster gradients begins with a straightforward partial differentiation of the coupled cluster energy expression as given

[*] The wavefunction is required for exact (analytic) calculation, although some properties can be computed for example by finite differences with respect to an applied perturbation.

in equation (1.5). The derivative is taken with respect to some perturbation χ, which is often the x, y, or z coordinate of one the atoms. Additionally, partial derivatives of some quantity A are written in this work using the shorthand $A^\chi = \frac{\partial A}{\partial \chi}$. The differentiated expression is then,

$$\begin{aligned}
E_{CC}^\chi &= \langle \Phi_0 | \bar{H} | \Phi_0 \rangle^\chi \\
&= \langle \Phi_0^\chi | \bar{H} | \Phi_0 \rangle - \langle \Phi_0 | \hat{T}^\chi \bar{H} | \Phi_0 \rangle + \langle \Phi_0 | \bar{H}^\chi | \Phi_0 \rangle + \langle \Phi_0 | \bar{H} \hat{T}^\chi | \Phi_0 \rangle \\
&\quad + \langle \Phi_0 | \bar{H} | \Phi_0^\chi \rangle \\
&= \langle \Phi_0 | \bar{H}^\chi | \Phi_0 \rangle + \langle \Phi_0 | \bar{H} \hat{T}^\chi | \Phi_0 \rangle \qquad (3.69)
\end{aligned}$$

where the definition $\bar{H} = e^{-\hat{T}} \hat{H} e^{\hat{T}}$ is used along with the definition $\bar{H}^\chi = e^{-\hat{T}} \hat{H}^\chi e^{\hat{T}}$. Additionally, the derivatives of the SCF wavefunction $|\Phi_0^\chi\rangle$ may be neglected since this wavefunction is variationally determined,

$$\begin{aligned}
\langle \Phi_0^\chi | \bar{H} | \Phi_0 \rangle + \langle \Phi_0 | \bar{H} | \Phi_0^\chi \rangle &= E_{CC} \langle \Phi_0^\chi | \Phi_0 \rangle + E_{CC} \langle \Phi_0 | \Phi_0^\chi \rangle \\
&= E_{CC} \langle \Phi_0 | \Phi_0 \rangle^\chi \\
&= 0 \qquad (3.70)
\end{aligned}$$

The term $\langle \Phi_0 | \hat{T}^\chi \bar{H} | \Phi_0 \rangle$ is zero since the differentiated $\hat{T}$ operator must excite at least one electron, while it is multiplied on the left by the reference function $\langle \Phi_0 |$ which has no electrons excited. The term $\langle \Phi_0 | \bar{H}^\chi | \Phi_0 \rangle$ gives the contribution using the differentiated Hamiltonian transformed by the usual exponential coupled cluster operator.

The other non-zero term $\langle \Phi_0 | \bar{H} \hat{T}^\chi | \Phi_0 \rangle$, when not neglected, ostensibly requires the solution of the derivative of the cluster amplitudes. The equation determining these perturbed amplitudes is, not surprisingly, the derivative of the usual coupled cluster amplitude equations,

$$\begin{aligned}
0^{\chi} &= \langle\Phi_{i_1\ldots i_k}^{a_1\ldots a_k}|\bar{H}|\Phi_0\rangle^{\chi} \\
&= \langle\Phi_{i_1\ldots i_k}^{a_1\ldots a_k\chi}|\bar{H}|\Phi_0\rangle - \langle\Phi_{i_1\ldots i_k}^{a_1\ldots a_k}|\hat{T}^{\chi}\bar{H}|\Phi_0\rangle + \langle\Phi_{i_1\ldots i_k}^{a_1\ldots a_k}|\bar{H}^{\chi}|\Phi_0\rangle \\
&\quad + \langle\Phi_{i_1\ldots i_k}^{a_1\ldots a_k}|\bar{H}\hat{T}^{\chi}|\Phi_0\rangle + \langle\Phi_{i_1\ldots i_k}^{a_1\ldots a_k}|\bar{H}|\Phi_0^{\chi}\rangle \\
&= -E_{CC}\langle\Phi_{i_1\ldots i_k}^{a_1\ldots a_k}|\hat{T}^{\chi}|\Phi_0\rangle + \langle\Phi_{i_1\ldots i_k}^{a_1\ldots a_k}|\bar{H}^{\chi}|\Phi_0\rangle + \langle\Phi_{i_1\ldots i_k}^{a_1\ldots a_k}|\bar{H}\hat{T}^{\chi}|\Phi_0\rangle \quad (3.71)
\end{aligned}$$

where now the derivatives of the single-particle states disappear due to the structure of $\bar{H}$. The term arising from the differentiation of $e^{-\hat{T}}$ is no longer zero, but can be simplified using equation (1.8). Rearranging this into a solution for the derivative amplitudes gives,

$$\langle\Phi_{i_1\ldots i_k}^{a_1\ldots a_k}|\hat{T}^{\chi}|\Phi_0\rangle = \langle\Phi_{i_1\ldots i_k}^{a_1\ldots a_k}|(E_{CC}-\bar{H})^{-1}\bar{H}^{\chi}|\Phi_0\rangle \quad (3.72)$$

However, instead of obtaining the solution to this equation iteratively for each perturbation χ, we can insert this entire expression back into equation (3.69), giving,

$$\begin{aligned}
E_{CC}^{\chi} &= \langle\Phi_0|\left[\mathbf{1}+\bar{H}(E_{CC}-\bar{H})^{-1}\right]\bar{H}^{\chi}|\Phi_0\rangle \\
&= \langle\Phi_0|(\mathbf{1}+\hat{\Lambda})\bar{H}^{\chi}|\Phi_0\rangle \quad (3.73)
\end{aligned}$$

In terms of second-quantized operators, $\hat{\Lambda}$ is defined very similarly to $\hat{T}$,

$$
\begin{aligned}
\hat{\Lambda} &= \sum_{k=1}^{N} \hat{\Lambda}_k && (3.74)\\
\hat{\Lambda}_k &= \frac{1}{(k!)^2} \sum_{a_1 \ldots a_k i_1 \ldots i_k} \lambda^{i_1 \ldots i_k}_{a_1 \ldots a_k} a^{\dagger}_{i_1} \ldots a^{\dagger}_{i_k} a_{a_k} \ldots a_{a_1} && (3.75)
\end{aligned}
$$

This new de-excitation operator can be obtained by iteratively solving the equation,

$$
\langle \Phi_0 | \hat{\Lambda} (\bar{H} - E_{CC}) | \Phi^{a_1 \ldots a_k}_{i_1 \ldots i_k} \rangle + \langle \Phi_0 | \bar{H} | \Phi^{a_1 \ldots a_k}_{i_1 \ldots i_k} \rangle = 0 \qquad (3.76)
$$

But, since this equation does not depend on the perturbation χ, it must only be done once, no matter how many perturbations are present. Also, applying the Hellman-Feynman theorem in reverse shows that $\langle \Phi_0 | (\mathbf{1} + \hat{\Lambda})$ can be viewed as the left-hand wavefunction of $\bar{H}$,

$$
\langle \Phi_0 | (\mathbf{1} + \hat{\Lambda}) \bar{H} = \langle \Phi_0 | (\mathbf{1} + \hat{\Lambda}) E_{CC} \qquad (3.77)
$$

Furthermore, separation of the exponential terms from $\bar{H}$ shows that we can also represent the left- and right-hand coupled cluster wavefunctions as degenerate wavefunctions (although not technically eigenfunctions) of $\hat{H}$,

$$
\begin{aligned}
\hat{H} e^{\hat{T}} | \Phi_0 \rangle &= E_{CC} e^{\hat{T}} | \Phi_0 \rangle && (3.78)\\
\langle \Phi_0 | (\mathbf{1} + \hat{\Lambda}) e^{-\hat{T}} \hat{H} &= \langle \Phi_0 | (\mathbf{1} + \hat{\Lambda}) e^{-\hat{T}} E_{CC} && (3.79)
\end{aligned}
$$

This allows coupled cluster to be cast as an eigenvalue problem, and to calculate arbitrary molecular properties as an expectation value, for example the electronic dipole moment,

$$
\begin{aligned}
(\mu^e_{CC})^2 &= \sum_{\alpha=xyz} \left| \langle \Phi_0 | (\mathbf{1} + \hat{\Lambda}) e^{-\hat{T}} \mu_\alpha e^{\hat{T}} | \Phi_0 \rangle \right|^2 \\
&= \sum_{\alpha=xyz} \left| \langle \Phi_0 | (\mathbf{1} + \hat{\Lambda}) \bar{\mu}_\alpha | \Phi_0 \rangle \right|^2 \qquad (3.80)
\end{aligned}
$$

To aid in the calculation of gradients and other molecular properties using the above form, it is advantageous to rewrite the matrix element for the expectation value as a contraction with a density matrix,

$$
\begin{aligned}
E^\chi_{CC} &= \sum_{pq} \left(f^p_q\right)^\chi D^q_p + \frac{1}{4} \sum_{pqrs} (v^{pq}_{rs})^\chi \, \Gamma^{rs}_{pq} \qquad (3.81) \\
\eta_{CC} &= \sum_{pq} \eta^p_q D^q_p + \frac{1}{4} \sum_{pqrs} \eta^{pq}_{rs} \Gamma^{rs}_{pq} \qquad (3.82)
\end{aligned}
$$

where η is an arbitrary molecular property in normal-ordered form (this may often have only a one-electron component). Since the labels here run over both occupied and virtual orbitals, the density has several distinct pieces defined by the occupation state of each index, just as the Hamiltonian does. These density matrix elements can be determined diagrammatically by taking each (closed) diagram in the representation of equation (3.73) and removing the Hamiltonian vertex. The lines to which this vertex was connected now become the external vertices corresponding to the labels of D^p_q or Γ^{pq}_{rs}.

The $\hat{\Lambda}$ equations, after rearranging to schematic form very similar to that of the amplitude equations,

$$
\mathbf{Z} = -\mathbf{DL} = \bar{\mathbf{F}} + \mathbf{W} + \mathbf{L}(\bar{\mathbf{F}} - \mathbf{D}) + \mathbf{LW} \qquad (3.83)
$$

where $\bar{\mathbf{H}} = \bar{\mathbf{F}} + \mathbf{W}$ and there is no requirement that the terms be contracted, can also be evaluated diagrammatically. Non-orthogonally spin-adapted equations for $\hat{\Lambda}$, D^p_q, and Γ^{pq}_{rs} arising from CCSDTQ are given in appendix B.

3.5 Summary

The results from the previous chapter have been applied here to the specific cases of CCSDTQ, CCSDT(Q), and the CCSDTQ $\hat{\Lambda}$ and density matrix equations. For these cases, some simplifications of the full non-orthogonally spin-adapted rules and spin-summation operators are possible, and the resulting equations are shown to be very compact but still relatively simple and easy to understand. The CCSDT(Q) equations are considerably simpler than the full CCSDTQ method, and due to the lower cost ($\mathscr{O}(n^9)$ vs. $\mathscr{O}(n^{10})$) and non-iterative nature of CCSDT(Q), it promises to be a useful proxy for the very high accuracy attainable by CCSDTQ.

The $\hat{\Lambda}$ and density equations presented in this chapter are useful for calculating a range of molecular properties, and for computing the energy gradient which is used for finding the minimum (or minima – or saddle points) of the potential energy surface. Efficient implementations of these open up CCSDTQ to a wider range of chemical applications.

Chapter 4

Efficient Implementation of CCSDTQ

This chapter details the data structures, algorithms, and optimizations necessary to turn the non-orthogonally spin-adapted equations of the previous chapter into an efficient computer program. The structure of the orbital amplitudes will be exploited to reduce the amount of data storage needed while simultaneously allowing the use of optimized matrix-multiplication operations. The amplitudes must sometimes be rearranged (permuted) so that this is possible, since restrictions on the ordering of the orbital labels are placed by concerns of spatial symmetry and mapping to matrix multiplication. Nevertheless, a technique to minimize the number of permutation steps is presented which removes much of the cost of this overhead.

The resulting algorithm for CCSDTQ, as implemented in the CFOUR program suite,[72] is then timed for calculations on a variety of systems, in comparison with the leading existing implementation. The CCSDT(Q) method as described in the previous chapter has also been implemented using the same optimizations as for CCSDTQ, and is timed on the same set of systems (with a larger basis set for some systems, so that the cost of the calculation stays relatively the same). The efficiency of the implementations are assessed by comparison to existing implementations and by examining the time spent in different areas of the program. Lastly, results for larger systems with the CCSDT(Q) method are given, as well as a preliminary analysis of the multithreaded performance of the program.

4.1 The Utility of Non-orthogonal Spin-adaptation

While the use of non-orthogonal spin-adaptation produces a relatively simple and compact set of equations, even for complicated ring-type diagrams, the efficiency of an actual implementation relies in no small part on the physical layout of the amplitudes and how they must be manipulated to perform the necessary contractions.[73] For the orbital amplitudes, the column symmetry of the indices implies that only $\sim 1/2$ of the amplitudes must be stored for $\check{t}^{ab}_{ij}$, $\sim 1/6$ for $\check{t}^{abc}_{ijk}$, and $\sim 1/24$ for $\check{t}^{abcd}_{ijkl}$ etc. Even though this is a significant reduction from the full "dense" storage, it is still possible to derive the coupled cluster equations with a smaller set of amplitudes. The orthogonal spin-adaptation technique for example achieves a lower bound, requiring only $\sim 5/6$ as many triple excitation amplitudes and $\sim 7/12$ as many quadruple excitation amplitudes.[74] However, the amplitudes in this case have complicated symmetries which makes efficient implementations difficult. The numerical issues associated with overdetermination and linear dependency of the amplitude equations (since some "redundant" amplitudes are kept in the orbital case) are also conveniently controlled by the spin-summation and de-spin-summation operations as detailed in the previous chapter, as the choice of a fixed de-spin-summation relation allows one to “re-canonicalize” the amplitudes by simply spin-summing and then de-spin-summing them.

To take advantage of the symmetry of the orbital amplitudes, one could for example store elements of $\check{t}^{abc}_{ijk}$ for which compound column indices are restricted as $(ai) \leqslant (bj) \leqslant (ck)$. In practice, however, and as was pointed out by Kucharski and Bartlett,[53] it is much more advantageous to store either the virtual or occupied indices without restrictions, and then store only amplitudes with $i \leqslant j \leqslant k \leqslant \ldots$ or $a \leqslant b \leqslant c \leqslant \ldots$ respectively. For the specific case of the $\hat{T}_3$ and $\hat{T}_4$ amplitudes, this gives the storage format,

$$\check{t}^{abc}_{ijk} \quad\rightarrow\quad \check{t}^{abc}_{i\leqslant j\leqslant k} \tag{4.1}$$

$$\check{t}^{abcd}_{ijkl} \quad\rightarrow\quad \check{t}^{abcd}_{i\leqslant j\leqslant k\leqslant l} \tag{4.2}$$

Additionally, amplitudes with $i = j = k$, or any three indices equal for higher-excitation amplitudes such as $\check{t}^{abcd}_{iii\leqslant j}$, can be omitted as they cannot contribute to the energy due to the Pauli exclusion principle. In terms of computer implementation, this allows for the use of fast, vectorized matrix multiplication routines, for example from the BLAS libraries,[75–77] to perform the parts of each contraction involving the unrestricted indices. This is especially beneficial for the expensive particle-particle ladder term if the virtual indices are unrestricted. If point group symmetry is considered as well, storing half of the indices unrestricted also allows for efficient symmetry packing, for example using the DPD scheme[78,79] to reduce both storage and computational cost. Of course, this layout is not optimal in terms of sparsity, as redundant amplitudes are stored for $i = j$ or $j = k$. However, the amount of overhead incurred scales as only $\mathcal{O}(n^5)$ for triples compared to $\mathcal{O}(n^6)$ for the total amplitudes and so on for higher orders.

This storage format is also especially advantageous because it allows spin-summation and de-spin-summation operations the be performed "locally" on a dense tensor. Since spin-summation involves permutations of only virtual or only occupied indices, then by choosing virtual indices it is not affected by the compressed structure of the occupied labels. This also means that spin-summation can be performed independently for each value of $ijk\ldots$, which is why it can be classified as a "local" operation unlike contraction which may require many $ijk\ldots$ combinations to be operated on. As the following sections will show, locality is an important quality in the context of minimizing I/O operations.

4.2 The Basic Algorithm

With the $\hat{T}_3$ and $\hat{T}_4$ amplitudes stored as in equation (4.1) and equation (4.2), the operations on these elements become split into explicit tensor contractions on "virtual blocks" $\check{t}^{abc}_{ijk} \rightarrow \check{t}^{abc}$, $\check{z}^{abcd}_{ijkl} \rightarrow \check{z}^{abcd}$ etc., and implicit operations on the occupied indices, which are now simply treated as labels on the virtual blocks. Keeping the $\hat{T}_1$ and $\hat{T}_2$ amplitudes and Hamiltonian elements stored with no index restrictions, an algorithm for solving the full CCSDTQ equations (equation (3.22) though equation (3.25)) can then be derived in terms of contractions over sets of virtual blocks. Such an algorithm for

CCSDT will first be presented and used to illustrate important optimizations, before moving to the full CCSDTQ algorithm.

One effect of storing only the unique portions of the tensors, however, is that each single contraction may need to be computed in several steps. For example, when summing over an occupied index such as $\sum_m \check{F}_i^m \check{t}_{mjk}^{abc}$, the form of $\hat{T}_3$ needed may actually be $\check{t}_{mjk}^{abc}$, $\check{t}_{jmk}^{bac}$, or $\check{t}_{jkm}^{bca}$ depending on the relative values of m, j, and k. Similarly, occupied indices involved in a contraction which originate on different vertices may not obey the ordering restrictions, necessitating a permutation of the result. Even without these cases, the symmetrization operator, instead of being an explicit operation on a fully dense result, is implicitly applied by splitting each contraction into several pieces. Ideally one would simply be able to operate on the data in-place with the necessary indices transposed in the specification of the particular tensor contraction and permutations. However, the (current) necessity of casting tensor contractions as matrix multiplication places restrictions on the contraction types possible, and requires physical transposition of the tensor data. So, in order to compute all of the necessary pieces of each contraction, it is in general necessary to perform all possible permutations (although not every permutation is required in each contraction) of both the input quantities and the results. Including these permutation steps explicitly, and keeping the one- and two-body quantities as dense tensors (only the $\check{v}_{cd}^{ab}$ integrals give significant savings from using column symmetry, and treating the cd indices as external $c \leqslant d$ labels may reduce the operation from matrix multiplication to less-efficient matrix-vector or vector-

vector operations), the basic structure of, for example, a non-orthogonally spin-adapted CCSDT program is given in figure 4.1.

Note that this structure is not unique. For example, the loops over permutations of $\check{z}^{abc}$ and blocks of $\hat{T}_3$ are independent and can be interchanged. Similarly, the loops over blocks of $\hat{T}_3$ and loops over $\hat{T}_3 \rightarrow \hat{Z}_3$ contractions can be interchanged. Some loop orderings may be more advantageous – for example if $\hat{T}_3$ must be read from disk, then the loop over its virtual blocks should be put outside the loop over contractions to reduce the number of disk accesses. Some loop orderings may at first seem disadvantageous – for example putting the loop over blocks of $\hat{T}_3$ outside the loop over permutations of $\check{z}^{abc}$, as it multiplies the number of permutation operations by the number of blocks – until further optimizations are made.

4.3 Improving Performance with a Data Hierarchy

Perhaps the most important optimization at this point is to break the loops over blocks into two loops: one over "hunks" of many blocks each, and the second over the individual blocks in each hunk. This way, only part of each loop can be reordered with the inner loops so that all operations (permutation, disk access, spin-summation) are minimized. Furthermore, each hunk can be further subdivided (and a third loop added) into several "chunks" when the molecule possesses point group symmetry. In this case, all of the blocks in a given chunk are restricted so that each value of i corresponds to an orbital which transforms as a fixed irreducible representation (irrep) γ_i, each j as γ_j,

```
perform all CCSD contractions

loop over virtual blocks in $\check{z}^{abc}_{ijk}$ for $i \leqslant j \leqslant k$
  loop over permutations of $\check{z}^{abc}$
    perform $T_2 \rightarrow Z_3$ contractions
    loop over contractions involving $T_3$
      loop over virtual blocks in $\check{t}^{a'b'c'}_{i'j'k'}$ for $i' \leqslant j' \leqslant k'$
        loop over permutations of $t^{a'b'c'}$
          spin-sum $\check{t}^{a'b'c'}$ if necessary
          if $ijk$ and $i'j'k'$ are conformable
            perform tensor contraction over virtual indices
          end if
          de-spin-sum $\check{t}^{a'b'c'}$ if necessary
        end loop
      end loop
    end loop
  end loop
  denominator weight $\check{z}^{abc}$ and compute residual
end loop
loop over virtual blocks in $\check{t}^{abc}_{ijk}$ for $i \leqslant j \leqslant k$
  loop over permutations of $\check{t}^{abc}$
    spin-sum to $\check{t}^{\breve{a}bc}$
    perform $T_3 \rightarrow Z_2$ contractions
    spin-sum to $\check{t}^{\breve{a}\check{b}c}$
    perform $T_3 \rightarrow Z_1$ contractions
    de-spin-sum to $\check{t}^{abc}$
  end loop
end loop
```

Figure 4.1: Basic structure of the program using virtual blocks.

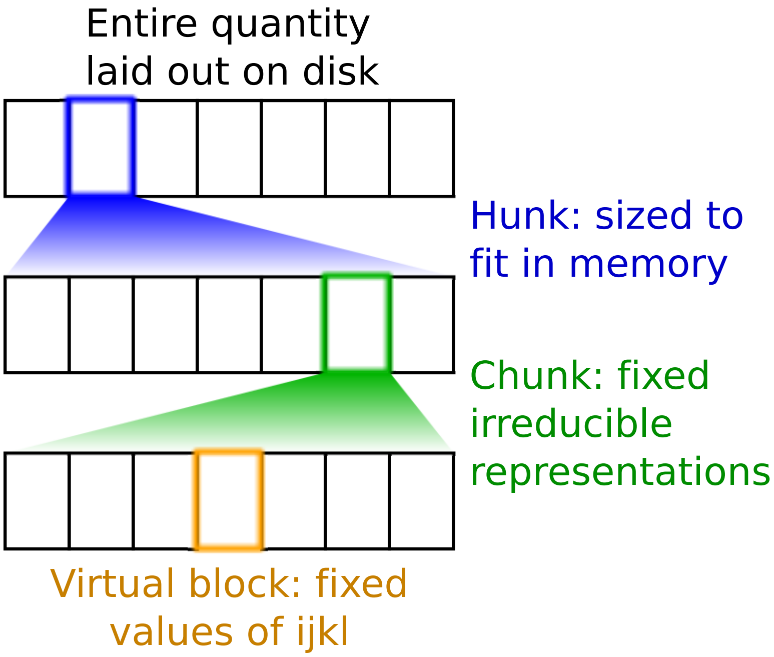
Entire quantity laid out on disk
Hunk: sized to fit in memory
Chunk: fixed irreducible representations
Virtual block: fixed values of ijkl

Figure 4.2: Data hierarchy for three- and four-body orbital quantities.

etc. Since the individual irreps must conform with the labeling of a given contraction, this extra layer of sorting allows many non-conformable blocks to be skipped easily. The relationship between the complete quantity and the component hunks, chunks, and blocks is illustrated in figure 4.2.

With the addition of this data hierarchy, the loops can be split and rearranged as in figure 4.3. The changes from figure 4.1 are highlighted, showing how the loops over blocks have been rearranged. The interchange of the loop over hunks of $\hat{T}_3$ with the loop over permutations of $\check{z}_{ijk}^{abc}$ does increase the number of permutations as before, but now the ratio is only the number of hunks and not the number of individual blocks. Since hunks are sized as large as possible to fit into main memory, this number is usually very small. This loop interchange also reduces the number of disk accesses on $\hat{T}_3$ by a factor of $\frac{n_{block} n_{perm}}{n_{hunk}}$ since the whole $\hat{T}_3$ does not need to be read through for each permutation (6 for CCSDT, but possibly more in general) of each $\hat{Z}_3$ block. Adding distributed parallelism is also straightforward with this structure as hunks can be distributed over the nodes, and the outside loops over hunks may be restricted to only the local hunk(s). The inner loop over T_3 hunks must still run over all hunks and so requires inter-node communication.

4.4 Reducing the Cost of Tensor Permutation: the Magic Cycle

Two issues still need to be addressed to ensure a highly efficient implementation. Both issues involve permutations – the use of dense virtual blocks allows the use of efficient matrix multiplication routines and no redundant computation is done, leaving memory operations such as permutation as the main source of overhead.

First, the nested loops of permutations of $\check{z}^{abc}_{ijk}$ and $\check{t}^{abc}_{ijk}$ requires 42 permutation steps (6 for the outer loop, $6 \times 6 = 36$ for the inner loop). However, not every combination of $\hat{T}_3$ and $\hat{Z}_3$ permutations is necessary to compute all of the necessary contraction pieces. For example, the contraction,

$$\left(1 + P^{ai}_{ck} + P^{bj}_{ck}\right)\left(1 + P^{ai}_{bj}\right)\frac{1}{2}\sum_e \check{F}^a_e \check{t}^{ebc}_{ijk} \tag{4.3}$$

expands in the case of restricted occupied indices into three partial contrac-

```
perform all CCSD contractions

loop over hunks in $\check{z}^{abc}_{ijk}$
  loop over hunks in $\check{t}^{a'b'c'}_{i'j'k'}$
    loop over permutations of $\check{z}^{abc}_{ijk}$
      loop over chunks in $\check{z}^{abc}_{ijk}$
        loop over blocks in $\check{z}^{abc}_{ijk}$
          perform $T_2 \rightarrow Z_3$ contractions
        end loop
      end loop
      loop over permutations of $t^{a'b'c'}_{i'j'k'}$
        loop over contractions involving $T_3$
          spin-sum $\check{t}^{a'b'c'}_{i'j'k'}$ if necessary
          loop over chunks in $\check{t}^{a'b'c'}_{i'j'k'}$
            if $\gamma_i \gamma_j \gamma_k$ are conformable
              loop over blocks in $\check{t}^{a'b'c'}_{i'j'k'}$
                if $ijk$ and $i'j'k'$ are conformable
                  perform tensor contraction over virtual indices
                end if
              end loop
            end if
          end loop
          de-spin-sum $\check{t}^{a'b'c'}_{i'j'k'}$ if necessary
        end loop
      end loop
    end loop
  end loop
  denominator weight $\check{z}^{abc}_{ijk}$ and compute residual
end loop
loop over hunks in $\check{t}^{abc}_{ijk}$
  loop over permutations of $\check{t}^{abc}$
    loop over chunks in $\check{t}^{abc}_{ijk}$
      loop over blocks in $\check{t}^{abc}_{ijk}$
        spin-sum to $\check{t}^{\breve{a}bc}$
        perform $T_3 \rightarrow Z_2$ contractions
        spin-sum to $\check{t}^{\breve{a}\check{b}c}$
        perform $T_3 \rightarrow Z_1$ contractions
        de-spin-sum to $\check{t}^{abc}$
      end loop
    end loop
  end loop
end loop
```

Figure 4.3: Program structure using hunk-chunk-block hierarchy. Changes from figure 4.1 are highlighted.

tions,

$$\sum_e \check{F}^a_e \check{t}^{ebc}_{i\leqslant j\leqslant k} + \sum_e \check{F}^b_e \check{t}^{aec}_{i\leqslant j\leqslant k} + \sum_e \check{F}^c_e \check{t}^{abe}_{i\leqslant j\leqslant k} \tag{4.4}$$

Supposing that the contraction can only be performed as a matrix multiplication when the e index is in the third position, the first term must have $\check{t}^{ebc}_{ijk}$ transposed to $\check{t}^{bce}_{jki}$ (a BCA permutation) or $\check{t}^{cbe}_{kji}$ (a CBA permutation) as well as the result tensor $\check{z}^{abc}_{ijk}$ transposed to $\check{z}^{bca}_{jki}$ (BCA) or $\check{z}^{cba}_{kji}$ (CBA) respectively. Similarly the second term requires $\hat{T}_3$ and $\hat{Z}_3$ transposed as ACB or BCA and the third term as ABC or BAC. Therefore, to fully compute this term we must visit three locations in the 6 × 6 "permutation space", with two possible choices for each location.

The restrictions on which contractions can be done as which permutation are governed by the types of tensor contractions which can be done efficiently using the DPD storage scheme. "Efficiently" in this context is taken to mean requiring g^2 or fewer individual matrix multiplications, where g is the number of irreducible representations. Contractions which, to be calculated using matrix multiplication primitives, require explicit iteration over virtual orbital indices are always considered inefficient. Considering the structure of DPD packing, a total of 18 "efficient" operations are possible with operands of 1-4 indices. These operations are summarized in figure 4.4.

Doing the analysis of possible efficient permutations for each contraction, a list of unique permutation restrictions can be built up. Plotting these restrictions (of which there are 12 for CCSDT) on the permutation space, a path can be chosen which visits each restriction at least once and which is

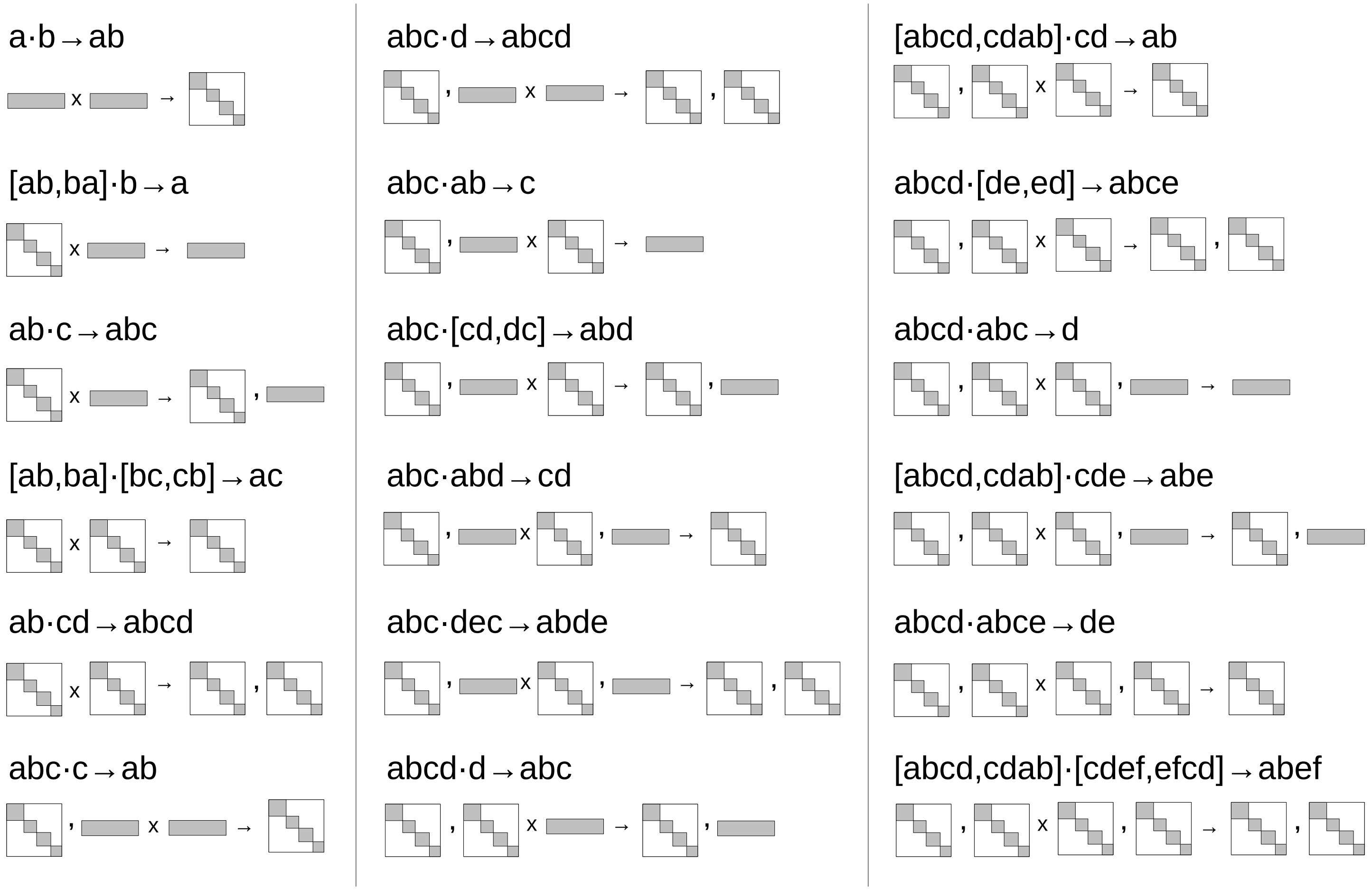

Figure 4.4: Efficient tensor contraction types possible with DPD packing and matrix multiplication.

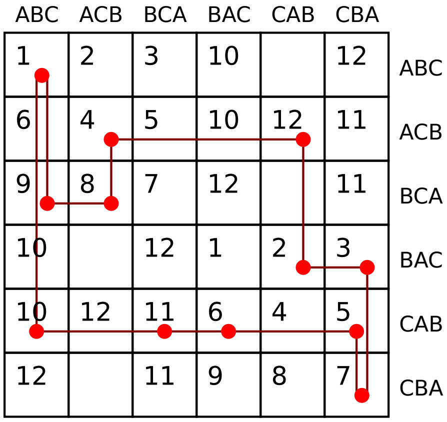

	ABC	ACB	BCA	BAC	CAB	CBA
ABC	1	2	3	10		12
ACB	6	4	5	10	12	11
BCA	9	8	7	12		11
BAC	10		12	1	2	3
CAB	10	12	11	6	4	5
CBA	12		11	9	8	7

Figure 4.5: The 12 unique permutation restrictions of CCSDT and an example "magic cycle", with the permutations of $\hat{T}_3$ on the horizontal and those of $\hat{Z}_3$ on the vertical.

of minimum length (the length being related to the number of permutations needed to traverse the path). Moving to a different location within the same column or row (i.e. which doesn't change either the $\hat{T}_3$ or $\hat{Z}_3$ permutation) incurs one permutation, while moving "diagonally" incurs two permutations. Since there are 12 unique restrictions, the minimum length is 12 permutations. A path with length equal to this lower bound and which visits each restriction, row, and column ($\hat{T}_3$ and $\hat{Z}_3$ permutation) at least once is called a "magic cycle", and prescribes a minimal sequence of permutations which allows all $\hat{T}_3$ and $\hat{Z}_3$ contractions to be fully computed. The 12 unique permutation restrictions and such a magic cycle for CCSDT are illustrated in figure 4.5.

Using this path, we can replace the double sum over permutations of $\hat{T}_3$ and $\hat{Z}_3$ by iteration over the magic cycle, reducing the number of permutations from 42 to 12 and also reducing the number of spin-summation steps since they must be done inside the loop over permutations (the partially spin-summed amplitudes do not have the full symmetry of the orbital quantity).

The second issue with permutations is the fact that, when memory limitations or considerations of distributed parallelism require the amplitudes to be split into more than one hunk, permutations of the hunk in the inner loop ($\hat{T}_3$ in figure 4.3) will be repeated for each hunk in the outer loop. In the distributed case especially this represents a possibility for a large amount of overhead. However, another consequence of having multiple hunks is that the number of blocks that are conformable for a given contraction per hunk is reduced, since some blocks which would match are now in a different hunk. Thus, if care is taken to only permute blocks from the inner hunk which will be needed for contraction with the blocks in the current outer loop hunk, the total number of permutations needed can be kept within a constant factor (constant for a given molecular system) of the one-hunk case. The approach taken here is to make all permutations "lazy", in that the permutation operations in figure 4.3 only signal that a permutation is desired and do not actually touch the data. Then, whenever a block is accessed for a contraction, its actual permutational ordering is checked against what is desired, and it is transposed if necessary. The same approach can also be applied to spin-summation operations and even to allocation of individual blocks (so that a block which is never touched for a given outer loop hunk is never even allocated).

A final issue which must be addressed is corner cases where occupied indices become equal. When this happens, some partial contractions may become equivalent or related by a permutation of virtual indices. For example, the first two partial contractions of,

$$\sum_m \check{F}_i^m \check{t}^{abc}_{m\leqslant j\leqslant k} + \sum_m \check{F}_i^m \check{t}^{bac}_{j\leqslant m\leqslant k} + \sum_m \check{F}_i^m \check{t}^{bca}_{j\leqslant k\leqslant m} \tag{4.5}$$

are identical when $m = j$. In this case only one should be included since the purpose of the multiple partial contractions is to enumerate all *unique* values of m. Another way in which equal occupied orbitals can affect the implementation is exemplified by the first two partial contractions of the above example,

$$\sum_e \check{F}_e^a \check{t}^{ebc}_{i\leqslant j\leqslant k} + \sum_e \check{F}_e^b \check{t}^{aec}_{i\leqslant j\leqslant k} + \sum_e \check{F}_e^c \check{t}^{abe}_{i\leqslant j\leqslant k} \tag{4.6}$$

when $i = j$. Since the multiple partial contractions here are produced by the symmetrization operator, the case of $i = j$ reduces the desired symmetry from $ai \leftrightarrow bj$ to simply $a \leftrightarrow b$. Then, it is possible to produce the desired symmetry by explicitly symmetrizing the result after the contractions have been completed. Thus, only one of the two partial contractions need be computed, albeit with an additional factor of 2. Both of these issues can be handled by constructing an "equality mask", where different pre-factors are stored for the general case ($i \neq j \neq k$), the case of $i = j$, the case of $j = k$, and (because the occupied indices may be permuted) the case of $i = k$. Then, each block may be checked during the contraction to determine which pre-factor to apply (and skip the block contraction if it is zero). Setting the pre-factors is dependent on the contraction and on the current permutations of $\hat{T}_3$ and $\hat{Z}_3$.

```
perform all CCSD contractions
loop over hunks in $\check{z}^{abc}_{ijk}$
  loop over hunks in $\check{t}^{a'b'c'}_{i'j'k'}$
    lazily loop over the CCSDT magic cycle
      perform $T_2 \rightarrow Z_3$ contractions over all blocks *
      perform non-spin-summed $T_3 \rightarrow Z_3$ contractions over all blocks *
      lazily spin-sum to $\check{t}^{\breve{a}'b'c'}_{\check{i}'j'k'}$
      if first hunk of $\check{z}^{abc}_{ijk}$
        perform $T_3 \rightarrow Z_2$ contractions over all blocks *
        perform $T_3 \rightarrow W$ contractions over all blocks *
      end if
      perform spin-summed $T_3 \rightarrow Z_3$ contractions over all blocks *
      lazily spin-sum to $\check{t}^{\breve{a}'\breve{b}'c'}_{\check{i}'\check{j}'k'}$
      if first hunk of $\check{z}^{abc}_{ijk}$
        perform $T_3 \rightarrow Z_1$ contractions over all blocks *
      end if
      lazily de-spin-sum to $\check{t}^{a'b'c'}_{i'j'k'}$
    end loop
  end loop
  symmetrize $\check{z}^{abc}_{ijk}$ for $i = j$ and $j = k$
  denominator weight $\check{z}^{abc}_{ijk}$ and compute residual
end loop

* perform contraction X over all blocks:

check permutations of $\check{z}^{abc}_{ijk}$ and $\check{t}^{a'b'c'}_{i'j'k'}$, skipping unnecessary combinations
loop over chunks in $\check{z}^{abc}_{ijk}$ and/or $\check{t}^{a'b'c'}_{i'j'k'}$
  set up equality masks for $\check{z}^{abc}_{ijk}$ and/or $\check{t}^{a'b'c'}_{i'j'k'}$
  if $\gamma_i\gamma_j\gamma_k$, $\gamma_{i'}\gamma_{j'}\gamma_{k'}$ are conformable
    loop over blocks in $\check{z}^{abc}_{ijk}$ and/or $\check{t}^{a'b'c'}_{i'j'k'}$
      determine prefactor from equality masks
      transpose and spin-sum blocks if necessary
      perform contraction X on blocks
    end loop
  end if
end loop
```

Figure 4.6: Final program structure for CCSDT.

The program structure taking all of these additional considerations into account is given in figure 4.6. The use of the magic cycle and explicit checking of the permutations of $\hat{T}_3$ and $\hat{Z}_3$ (and for $\hat{T}_3 \rightarrow \hat{T}_1$, W, and $\hat{T}_2$, the hunk of $\hat{Z}_3$ to prevent over-counting) allows all of the contractions to be fit into a unified loop structure. Each contraction now also has the same internal structure, involving looping over chunks and blocks and handling details such as occupied orbital equality and lazy transposition.

4.5 CCSDTQ and CCSDT(Q)

The application of this algorithm and the optimizations detailed in the previous three sections to CCSDTQ and CCSDT(Q) is rather straightforward. The main difference is that, while in the CCSDT algorithm only $\hat{T}_3$ and $\hat{Z}_3$ are stored using the hunk/chunk/block hierarchy, there are many quantities stored this way in CCSDTQ (and to a somewhat lesser degree in CCSDT(Q)). For example, in CCSDTQ, we must iterate over hunks for $\hat{T}_3$, $\hat{Z}_3$, $\hat{T}_4$, $\hat{Z}_4$, $\tilde{W}^{abc}_{ije}$, $\tilde{W}^{abm}_{ijk}$, $\tilde{W}^{amn}_{ijk}$, $\tilde{W}^{abm}_{ije}$, and $\tilde{W}^{abm}_{iej}$.

As with CCSDT, the relative permutations of $\hat{T}_4$ and $\hat{Z}_4$ can be optimized by using a magic cycle, although now it is necessary to satisfy 41 constraints in a 12×12 permutation space (the full 24×24 space is actually redundant). An illustration of the constraints and a CCSDTQ magic cycle is given in figure 4.7. The CCSDTQ magic cycle offers a drastic reduction in the number of necessary permutations. Looping over all permutations for both $\hat{T}_4$ and $\hat{Z}_4$ would require $24 + 24 \times 24 = 576$ permutations, while the

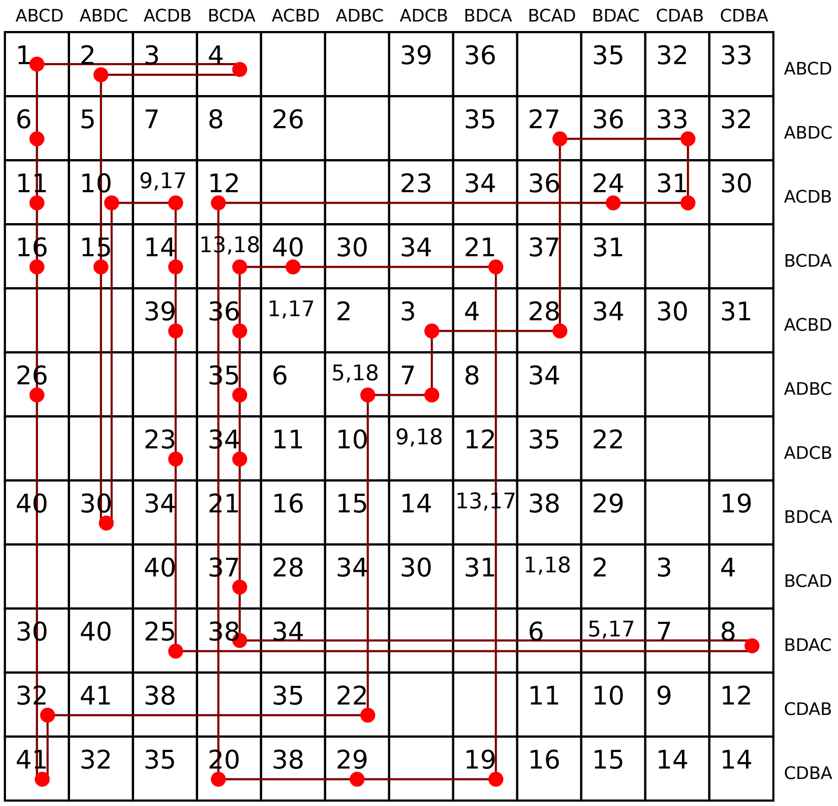

ABCD	ABDC	ACDB	BCDA	ACBD	ADBC	ADCB	BDCA	BCAD	BDAC	CDAB	CDBA	
1	2	3	4			39	36		35	32	33	ABCD
6	5	7	8	26			35	27	36	33	32	ABDC
11	10	9,17	12			23	34	36	24	31	30	ACDB
16	15	14	13,18	40	30	34	21	37	31			BCDA
		39	36	1,17	2	3	4	28	34	30	31	ACBD
26			35	6	5,18	7	8	34				ADBC
		23	34	11	10	9,18	12	35	22			ADCB
40	30	34	21	16	15	14	13,17	38	29		19	BDCA
		40	37	28	34	30	31	1,18	2	3	4	BCAD
30	40	25	38	34				6	5,17	7	8	BDAC
32	41	38		35	22			11	10	9	12	CDAB
41	32	35	20	38	29		19	16	15	14	14	CDBA

Figure 4.7: The 41 unique permutation restrictions of CCSDTQ and an example "magic cycle", with the permutations of $\hat{T}_4$ on the horizontal and those of $\hat{T}_3$ on the vertical. Since some restrictions are partially overlapping, the length of cycle is actually only 39.

magic cycle requires only 39. However, as significant as this reduction is, the necessity to perform contractions in certain relative permutations can increase the amount of transposition and spin-summation operations when combined with the need to split the amplitudes into multiple hunks. The development of new DPD-aware tensor contraction kernels (discussed in a later section) could relax some of the permutation restrictions and further reduce the overhead of tensor transposition.

The final algorithm for CCSDTQ, including all relevant optimizations from the previous sections is given in figure 4.8 and figure 4.9. The algorithm is somewhat lengthier than for CCSDT due to the need to handle the hierarchical structure of many different tensors, but the basic structure is identical. Furthermore, the optimizations which allow I/O and tensor transposition to be minimized for the $\hat{T}_3 \to \hat{Z}_3$ contractions in CCSDT extend seamlessly to the "three-level" contractions $\hat{T}_3 \times \tilde{W}_3 \to \hat{Z}_4$.

CCSDT(Q) requires a subset of the contractions in CCSDTQ, and the addition of the disconnected terms $\hat{T}_2 \times W \to \hat{Z}_4$ and $\hat{T}_3 \times F \to \hat{Z}_4$. Some additional rearrangement is also required for the shared terms since the contributions must go to $\hat{Z}_4(c)$ only, $\hat{Z}_4(d)$ only, or both. Finally, while both connected (c) and disconnected (d) parts must be symmetrized, only one should be denominator-weighted. The (Q) correction is then computed by a sum of the dot product of these parts over all of the hunks. The $\tilde{W}^{abc}_{ije}$ and $\tilde{W}^{abm}_{ijk}$ intermediates are still computed all at once before the loop over hunks in $\hat{Z}_4$, just as in CCSDTQ. This is now a complication, however, since if these intermediates

```
loop over hunks in $\tilde{\check{W}}^{abc}_{ije}$, $\tilde{\check{W}}^{abm}_{ijk}$, $\tilde{\check{W}}^{amn}_{ijk}$, $\tilde{\check{W}}^{abe}_{ijm}$, and $\tilde{\check{W}}^{abe}_{imj}$
  lazily loop over permutations of $\tilde{\check{W}}^{abc}_{ije}$, $\tilde{\check{W}}^{abm}_{ijk}$, $\tilde{\check{W}}^{amn}_{ijk}$, and $\tilde{\check{W}}^{abe}_{ijm}$
    perform $T_2 \rightarrow \tilde{\check{W}}^{abc}_{ije}$ contractions over all blocks
    perform $T_2 \rightarrow \tilde{\check{W}}^{abm}_{ijk}$ contractions over all blocks
    perform $T_2 \rightarrow \tilde{\check{W}}^{amn}_{ijk}$ contractions over all blocks
    perform $T_2 \rightarrow \tilde{\check{W}}^{abm}_{ije}$ contractions over all blocks
  end loop
  perform $T_2 \rightarrow \tilde{\check{W}}^{abe}_{imj}$ contractions over all blocks
  loop over hunks in $\check{t}^{a'b'c'}_{i'j'k'}$
    lazily loop over permutations of $\check{t}^{a'b'c'}_{i'j'k'}$
      perform $T_3 \rightarrow \tilde{\check{W}}^{abe}_{imj}$ contractions over all blocks
      perform $T_3 \rightarrow \tilde{\check{W}}^{abm}_{ijk}$ contractions over all blocks
      perform $T_3 \rightarrow \tilde{\check{W}}^{amn}_{ijk}$ contractions over all blocks
      lazily spin-sum to $\check{t}^{\breve{a}'b'c'}_{\breve{i}'j'k'}$
      perform $T_3 \rightarrow \tilde{\check{W}}^{abe}_{ijm}$ contractions over all blocks
      lazily de-spin-sum to $\check{t}^{a'b'c'}_{i'j'k'}$
    end loop
  end loop
  loop over hunks in $\check{t}^{a'b'c'd'}_{i'j'k'l'}$
    lazily loop over permutations of $\check{t}^{a'b'c'd'}_{i'j'k'l'}$
      lazily spin-sum to $\check{t}^{\breve{a}'b'c'd'}_{\breve{i}'j'k'l'}$
      perform $T_4 \rightarrow \tilde{\check{W}}^{abc}_{ije}$ contractions over all blocks
      perform $T_4 \rightarrow \tilde{\check{W}}^{abm}_{ijk}$ contractions over all blocks
      lazily de-spin-sum to $\check{t}^{a'b'c'd'}_{i'j'k'l'}$
    end loop
  end loop
end loop
```

Figure 4.8: Algorithm for forming three-body intermediates in CCSDTQ.

```
perform all CCSDT contractions and form three-body intermediates

loop over hunks in $\check{z}^{abc}_{ijk}$ and $\check{z}^{abcd}_{ijkl}$
  loop over hunks in $\check{t}^{a'b'c'}_{i'j'k'}$, $\tilde{\check{W}}^{a'b'c'}_{i'j'e'}$, and $\tilde{\check{W}}^{a'b'm'}_{i'j'k'}$
    lazily loop over permutations of $\check{z}^{abcd}_{ijkl}$
      lazily loop over permutations of $\check{t}^{a'b'c'}_{i'j'k'}$
        perform $T_3 \rightarrow Z_4$ contractions over all blocks
      end loop
      lazily loop over permutations of $\tilde{\check{W}}^{abc}_{ije}$, $\tilde{\check{W}}^{abm}_{ijk}$, $\tilde{\check{W}}^{amn}_{ijk}$, and $\tilde{\check{W}}^{abe}_{ijm}$
        perform $\tilde{\check{W}}^{abc}_{ije} \rightarrow Z_4$ contractions over all blocks
        perform $\tilde{\check{W}}^{abm}_{ijk} \rightarrow Z_4$ contractions over all blocks
      end loop
    end loop
    loop over hunks in $\tilde{\check{W}}^{a'm'n'}_{i'j'k'}$, $\tilde{\check{W}}^{a'b'e'}_{i'j'm'}$, and $\tilde{\check{W}}^{a'b'e'}_{i'm'j'}$
      lazily loop over permutations of $\check{t}^{a'b'c'}_{i'j'k'}$
        lazily loop over permutations of $\tilde{\check{W}}^{amn}_{ijk}$ and $\tilde{\check{W}}^{abe}_{ijm}$
          perform $\tilde{\check{W}}^{amn}_{ijk} \times T_3 \rightarrow Z_4$ contractions over all blocks
          lazily spin-sum to $\check{t}^{\breve{a}'b'c'}_{\breve{i}'j'k'}$
          perform $\tilde{\check{W}}^{abm}_{ije} \times T_3 \rightarrow Z_4$ contractions over all blocks
          lazily de-spin-sum to $\check{t}^{a'b'c'}_{i'j'k'}$
        end loop
        perform $\tilde{\check{W}}^{abm}_{iej} \times T_3 \rightarrow Z_4$ contractions over all blocks
      end loop
    end loop
  end loop
  loop over hunks in $\check{t}^{a'b'c'd'}_{i'j'k'l'}$
    lazily loop over the CCSDTQ magic cycle
      perform non-spin-summed $T_4 \rightarrow Z_4$ contractions over all blocks
      lazily spin-sum to $\check{t}^{\breve{a}'b'c'd'}_{\breve{i}'j'k'l'}$
      lazily loop over permutations of $\check{z}^{abc}_{ijk}$
        perform $T_4 \rightarrow Z_3$ contractions over all blocks
      end loop
      perform spin-summed $T_4 \rightarrow Z_4$ contractions over all blocks
      lazily spin-sum to $\check{t}^{\breve{a}'\breve{b}'c'd'}_{\breve{i}'\breve{j}'k'l'}$
      if first hunk of $\check{z}^{abcd}_{ijkl}$
        perform $T_4 \rightarrow Z_2$ contractions over all blocks
      end if
      lazily de-spin-sum to $\check{t}^{a'b'c'd'}_{i'j'k'l'}$
    end loop
  end loop
  symmetrize $\check{z}^{abcd}_{ijkl}$ for $i = j$, $j = k$, and $k = l$
  denominator weight $\check{z}^{abcd}_{ijkl}$ and compute residual
end loop
```

Figure 4.9: Final program structure for CCSDTQ.

must be split into multiple hunks, they have to be computed, written out to disk, and then read in fully for each $\hat{Z}_4$ hunk. This I/O cost is relatively much more expensive for CCSDT(Q) than for CCSDTQ. Redundantly computing the intermediates on the fly is not much of an improvement even though this is only an $\mathscr{O}(n^7)$ cost compared to $\mathscr{O}(n^9)$ for the contraction into $\hat{Z}_4$, since the cost of computing the intermediate is similar to the cost of reading it from disk (although this depends on the amount of I/O bandwidth available). A selected computation of only those blocks which are needed for the current $\hat{Z}_4$ hunk could reduce the cost of redundant computation (and more importantly limit the amount of redundancy to a constant factor), and such an optimization is planned for future work.

4.6 Numerical Results

The efficiency of the new CCSDT, CCSDT(Q), and CCSDTQ implementations in the CFOUR program suite have been tested on a variety of molecular systems. The results listed in table 4.1 and table 4.2 give per-iteration (for CCSDT and CCSDTQ) and per-correction (for the (Q) correction in CCSDT(Q)) timings on five molecular systems, as obtained by running on a single core of an Intel Xeon E5620 processor. These systems were chosen to span a wide range of molecular symmetries (C_1, C_s, C_{2v}, and D_{2h}) and ratio of number of virtual orbitals (n_v) to number of occupied orbitals (n_o). This ensures that a full profile of the performance characteristics are captured, as these variables greatly affect the size and number distributions of elementary matrix multiplication operations required for a similar total computational cost. The running time of the current implementations are compared to the MRCC program by Kállay,[80,81] which is currently used for the vast majority of production CCSDT(Q) and CCSDTQ calculations.

As can be seen from these results, it is already feasible to perform full CCSDTQ calculations of four heavy atoms with a double-ζ quality basis set (and even on a single core). Additionally, while the CCSDTQ calculations on O_3 and FO_3^- were performed using an out-of-core algorithm (i.e. the $\hat{T}_4$ amplitudes were split into multiple hunks and only one hunk read from disk at a time), these runs obtained the same high level of efficiency as the in-core cases (for example, in going from butatriene to ozone the CCSDTQ timing only increases by a factor of 2.8 which is in-line with the increase in the in-core CCSDT timings). Of course, it should be noted that these tests we also performed on a system with six hard disks in a RAID0 configuration, providing very high sequential I/O throughput. On systems with less capable I/O configurations, a larger increase in time is expected. Nevertheless, the results show that the algorithm is capable of putting the given computational resources to full use.

The CCSDT(Q) results (with an increase in basis set size for the first three systems) again show a high level of efficiency. For example, the (Q) correction for water with a quadruple-ζ basis set ($>$ 100 orbitals) can be computed in a matter of minutes. The most expensive calculation in this table (HSOH with a triple-ζ basis, no molecular symmetry) requires less than

Molecule/ Basis Set	n_o/n_v	CCSDT Iteration (s)			CCSDTQ Iteration (s)		
		Current	MRCC	r	Current	MRCC	r
HSOH/ cc-pVDZ	7/29	3.73	28.5	7.6	559^a	3467^a	6.2
H_2O/ aug-cc-pVTZ	4/87	7.3	48.2	6.6	1179^a	5144^a	4.4
H_2CCCCH_2/ DZ	10/34	8.65	68.1	7.9	2105^a	11028^b	5.2
O_3/ aug-cc-pVDZ	9/57	14.5	132	9.1	5973^b	36994^b	6.2
FO_3^-/ cc-pVDZ	13/39	32.2	170	5.3	14476^b	71030^b	4.9

Table 4.1: Average per-iteration timings for CCSDT and CCSDTQ calculations on a variety of molecular systems. The improvement of the new implementation is given by $r = t(current)/t(MRCC)$. All calculations use frozen core orbitals.
a) In-core
b) Out-of-core, 12GB memory limit

two hours for 86 correlated orbitals. In fact, the limit on the size of the calculations performed in this table is the time to run the MRCC comparison. Overall, the CCSDT and CCSDTQ timings for the current implementations are $\sim$ 5 times faster than previously possible, and the (Q) correction can be obtained 20-100 times faster. The difference between the CCSDTQ and CCSDT(Q) improvements highlights the effect of tensor transposition and other data movement on the computation efficiency, as these operations are relatively more important for CCSDT(Q) (which has only an $\mathscr{O}(n^9)$ floating-point cost compared to an $\mathscr{O}(n^8)$ data cost vs. $\mathscr{O}(n^{10})$ to $\mathscr{O}(n^8)$ for CCSDTQ).

More expensive CCSDT(Q) calculations have also been carried out, at a

Molecule/ Basis Set	n_o/n_v	CCSDT Iteration (s)			(Q) correction (s)		
		Current	MRCC	r	Current	MRCC	r
HSOH/ cc-pVTZ	7/79	222	1791	8.1	5131	169889	33.1
H_2O/ cc-pVQZ	4/110	18.1	123	6.8	351	36002	102.6
H_2CCCCH_2/ cc-pVDZ	10/62	75.2	694	9.2	2632	47912	18.2
O_3/ aug-cc-pVDZ	9/57	14.5	132	9.1	447	12840	28.7
FO_3^-/ cc-pVDZ	13/39	32.2	170	5.3	739	12720	17.2

Table 4.2: Average per-iteration CCSDT and (Q) correction timings on a variety of molecular systems. The improvement of the new implementation is given by $r = t(current)/t(MRCC)$. All calculation use frozen core orbitals and are out-of-core with a memory limit of 22GB.

scale for which it is not feasible to compare to existing codes. Several example results are given in table 4.3. The benzene dimer calculations were performed using all 12 cores of a dual Xeon X5670 system with five disks in a RAID0 configuration. The other calculations were performed using 4 cores on a Xeon E5-1620 system with only a single hard drive. The latter calculations, owing to the less-performant I/O system, spent more than 50% of the calculation time performing I/O operations. However, even with the modest computational resources allocated, a CCSDT(Q) calculation on a system with more than 150 orbitals can be completed in only a few days.

All of the methods implemented are multithreaded explicitly using the OpenMP interface, and implicitly through the ability to use a multithreaded BLAS library for elementary matrix operations. The choice of explicit or

Molecule/Basis Set	n_o/n_v	CCSDT Iteration (s)	(Q) correction (s)
Bz$_2$ (C_1)/6-31G	14/90	523	55111
Bz$_2$ (C_s)/6-31G	14/90	147	23032
(C$_2$H$_4$)$_2$ (D_{2d})/ aug-cc-pVDZ	12/148	518	246666
C$_2$H$_4\cdots$HCCH (C_{2v})/ aug-cc-pVDZ	11/131	108	94034

Table 4.3: Timings for one iteration of CCSDT and for the (Q) correction for several large molecular systems. See text for a description of the computational details.

implicit threading for a given tensor contraction is determined dynamically by the available parallelism at each level. An example of the parallel speedup obtained through multithreading on a dual Xeon E5620 system is given in figure 4.10. The speedup obtained using all 8 cores is about 4x, giving a parallel efficiency of $\sim$ 50%. While this is not perfect, it is encouraging given the fact that the code makes no attempt to address issues such as NUMA memory accesses, thread locality, cache sharing, etc. Also, scheduling of work units (individual matrix multiplications in the explicit threading case) is determined statically, leaving the possibility for increased performance through dynamic scheduling. The parallel efficiency on one processor only (up to 4 cores), remains at least 75%.

A more in-depth analysis of the performance of the CCSDT(Q) and CCSDTQ implementations can be obtained by examining the breakdown of the running time into several categories. Example performance breakdowns are given in table 4.4 for the CCSDTQ calculation on HSOH and in table 4.5 for

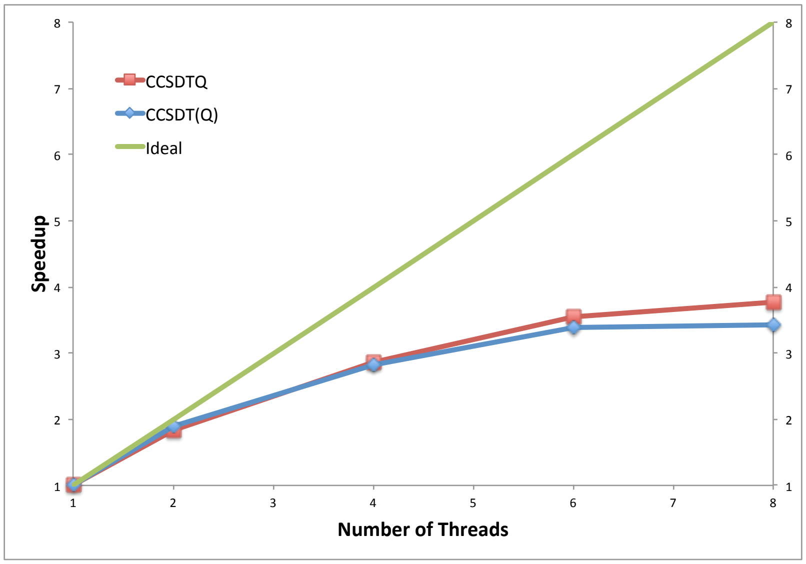

Figure 4.10: Parallel speedup obtained through explicit (OpenMP) and implicit multithreading.

the CCSDT(Q) calculation on the same system ((Q) correction only). These performance breakdowns are created by measuring the time spent in different classes of operations (various BLAS operations, disk I/O, etc.) at a low level and aggregating the timings, and also by measuring the time spent on a high level in different classes of coupled cluster diagrams.

For the CCSDTQ calculation, the low-level timings show that a majority (61.4%) of time is spent in level 3 BLAS (matrix multiplication). This is desirable since the matrix multiplication operations are generally very efficient, although the percentage time given does not give an indication as to how efficient each individual matrix operations was. Due to various factors, matrix multiplication on small matrices is less efficient than for large matrices. So, a handful of matrix multiplications which together take 10 seconds is much

Breakdown by Kernel		Breakdown by Diagram	
Level 1 BLAS	12.2%	All CCSD	$< 0.1\%$
Level 2 BLAS	0.4%	All CCSDT	0.8%
Level 3 BLAS	61.4%	$\tilde{W}_3$ intermediates	3.7%
Disk I/O	1.1%	$\hat{T}_2$ and $\hat{T}_3 \rightarrow \hat{Z}_4$	31.6%
Spin-summation	10.4%	$\hat{T}_4 \times F \rightarrow \hat{Z}_4$	2.8%
Transpose	14.3%	$\hat{T}_4 \times W^{ab}_{ef} \rightarrow \hat{Z}_4$	15.7%
Other	0.2%	$\hat{T}_4 \times W^{am}_{ie} \rightarrow \hat{Z}_4$	26.0%
		$\hat{T}_4 \times W^{mn}_{ij} \rightarrow \hat{Z}_4$	7.9%
		$\hat{T}_4 \rightarrow \hat{Z}_2$ and $\hat{Z}_3$	8.7%

Table 4.4: Example performance breakdown of CCSDTQ timings.

Breakdown by Kernel		Breakdown by Diagram	
Level 1 BLAS	2.4%	$\hat{T}_2 \times W \rightarrow \tilde{W}^{abc}_{ije}$	6.8%
Level 2 BLAS	2.0%	$\hat{T}_2 \times W \rightarrow \tilde{W}^{abm}_{ijk}$	0.1%
Level 3 BLAS	47.9%	$\hat{T}_2 \times \tilde{W}^{abc}_{ije} \rightarrow \hat{Z}_4$	29.3%
Disk I/O	$< 0.1\%$	$\hat{T}_2 \times \tilde{W}^{abc}_{ije} \rightarrow \hat{Z}_4$	12.9%
Spin-summation	3.7%	$\hat{T}_2 \times v^{ab}_{ij} \rightarrow \hat{Z}_4$	6.8%
Transpose	41.1%	$\hat{T}_3 \times W^{ab}_{ie} \rightarrow \hat{Z}_4$	17.0%
Other	2.8%	$\hat{T}_3 \times W^{am}_{ij} \rightarrow \hat{Z}_4$	14.8%
		Weighting and Spin-summation	5.1%
		Energy	4.5%

Table 4.5: Example performance breakdown of (Q) correction timings.

better than 10,000 matrix multiplications taking the same amount of time (the second case will be doing less useful work in the same time). Additional profiling of the CCSDTQ and CCSDT(Q) code shows that there are often 10-100 million matrix multiplication calls in a single calculation, which shows that there is room for improvement in the kinds of matrix multiplications done. Splitting the amplitudes into virtual blocks is responsible for some of this subdivision, as is the DPD packing scheme. Some possible methods to recombine these smaller operations are outlined in the next section. The spin-summation and transposition operations, while they take a non-trivial amount of time, are kept to a manageable level by the data hierarchy of the amplitudes.

The high-level breakdown of the CCSDTQ timings shows that the most expensive diagrams are $\hat{T}_3 \times \tilde{W}^{abe}_{ijm}$ and $\hat{T}_4 \times W^{am}_{ie}$ contributions to $\hat{Z}_4$, followed by $\hat{T}_4 \times W^{ab}_{ef}$. The first two contributions are the "ring" diagrams, which for CCSDTQ now have both a $\hat{T}_4$ and $\hat{T}_3$ part which are both $\mathscr{O}(n^{10})$ scaling. These are especially expensive because, unlike the ladder terms, multiple contractions and a tensor transposition are necessary in the non-orthogonally spin-adapted equations for each spin-orbital diagram. The particle-particle ladder term $\hat{T}_4 \times W^{ab}_{ef}$, although it scales with a larger number of virtual orbitals (and hence is more expensive for most basis sets), is fairly simple to cast as very large and efficient matrix multiplication operations. The relative efficiency of the diagrams is also very evident in the hole-hole ladder ($\hat{T}_4 \times W^{mn}_{ij}$) timings, which should "in theory" be insignificant compared to the other terms. But, profiling shows that this term takes half as long as the particle-particle ladder term. This is primarily because the matrix multiplication involves summing over only occupied indices which spreads the operation over many virtual blocks. The actual BLAS kernel which can be used is only the level 1 DAXPY operation (this is the cause of the 12.2% for level 1 BLAS in the table), which cannot take advantage of data reuse in the cache hierarchy. Also, taking data from possibly very distant (in memory location) virtual blocks causes a large number of page faults which are a serious performance penalty.

The CCSDT(Q) breakdown shows a large shift in time from level 3 BLAS to tensor transposition. This is because the size of the amplitudes (and hence the cost of transposition) remains the same but the number of floating point operations decreases from $\mathscr{O}(n^{10})$ to $\mathscr{O}(n^9)$. This highlights the importance of reducing the number and cost of data movement operations. The breakdown by diagram shows that now the most expensive operation by far is the $\hat{T}_2 \times \tilde{W}^{abc}_{ije}$ contraction. This is expected to be an expensive operation, but one factor that contributes to its large cost is the fact that the summation index e is treated as a label on the $\tilde{W}^{abc}$ virtual blocks along with the occupied indices. This reduces the type of BLAS kernel from level 3 (matrix multiplication) to level 2 (outer product). The level 2 operations are inherently less efficient that the level 3 ones, leading to an inflated cost for this term. In this example, the $\tilde{W}^{abc}_{ije}$ intermediate was stored in memory for the entire computation, so that there was only an insignificant amount of disk access ($< 0.1\%$). When this is not possible however, such as for the calculation on $(C_2H_4)_2$/aug-cc-pVDZ, the disk usage increases dramatically, reaching as much as 50% on a computer system with only one disk drive. Recomputation of the intermediate is also expensive as computing it only once is already 6.8% of the total time.

4.7 Summary

The special structure of the orbital amplitudes was shown to lead to an efficient storage scheme which allows the use of optimized matrix multiplication functions, while also retaining the sparsity due to column symmetry. Splitting up the resulting virtual blocks in a hierarchical manner leads to a reduction in the cost of disk I/O, permutations, and spin-summations, while grouping blocks by their labels' irreducible representations allows nonconformant contributions to be easily skipped.

The restrictions of the DPD packing scheme for point group symmetry and the need to use matrix multiplication for high efficiency requires permutations of the tensors. However, it was shown that careful analysis of the required relative permutations of input ($\mathbf{T}_3$, $\mathbf{T}_4$) and output ($\mathbf{Z}_3$, $\mathbf{Z}_4$) tensors reveals that only 12 permutations for CCSDT and 39 permutations for CCSDTQ are required to fulfill all of the permutation requirements. Additionally, the use of lazy evaluation of permutation and spin-summation operations reduces the overhead when the tensor are split into multiple hunks, since blocks which have no contribution from the current hunk need not be manipulated.

The efficiency of the resulting algorithms as implemented in CFOUR was compared to the current leading implementation, MRCC. CFOUR shows a ˜5x improvement over MRCC for CCSDTQ and a 20-100x improvement for CCSDT(Q). Additionally, looking at the breakdown of the timings into time spent in various operations (matrix multiplication, permutation, spin-summation, etc.), shows that 50-60% of time is spent in matrix multiplication (100% is optimal, but not achievable due to permutations), while only ˜15% is spent in permutation for CCSDTQ. Up to 40-50% of time is spent doing permutations for CCSDT(Q), but the improvement of the existing implementation shows that this is already a vast improvement. Lastly, the speedup of the program from using multiple threads shows that a ˜50% parallel efficiency is possible at 8 cores, without taking into consideration NUMA memory access and data or thread locality, and ˜75% efficiency is possible up to 4 cores (i.e. using a single physical processor chip).

Chapter 5

Conclusions and Future Work

5.1 Conclusions

The main contributions of this work are 1) a new diagrammatic interpretation for coupled cluster diagrams, and those from related methods, which yields compact, factorized equations for closed shell systems using the orbital (non-orthogonally spin-adapted) representation of the Hamiltonian and wavefunction parameters ($\hat{T}$ for coupled cluster), and 2) an efficient implementation of the CCSDTQ and CCSDT(Q) methods in terms of these equations.

The new diagrammatic interpretation using the orbital representation is derived directly from the usual spin-orbital interpretation of the Brandow diagrams. Using an algebraic representation of the Brandow rules, permutation operators can be manipulated to reveal an algebraic equation for the orbital case. Furthermore, the remaining permutation operators can be conveniently factorized, and the result summarized again as a set of diagrammatic interpretation rules. The main advantages of this approach are that the tedious and error-prone methods of either converting the spin-orbital equations into the orbital ones, or obtaining them directly using Goldstone diagrams is avoided. In the case of using the spin-orbital equations, the difficulties of dealing with removal of antisymmetry and symmetrization operations is avoided, which can multiply the number of terms which must be manipulated by as much as a factor of 96 for CCSDTQ. Compared to the Goldstone approach, the need to enumerate all unique Goldstone diagrams is removed, and the extension of the Goldstone diagrams to higher-order coupled cluster (which is not clearly laid out) is avoided. Lastly, the equations are produced in already-factored form, since factorization occurs at the level of the algebraic permutation operators. The resulting factorized operators, called spin-summation operators, can also be conveniently indicated in the final equations using a simple shorthand.

Using this diagrammatic interpretation, equations for the CCSDTQ amplitude equations, as well as the CCSDT(Q) energy, the CCSDTQ $\hat{\Lambda}$ equations, and the CCSDTQ density equations were derived. The equations obtained are clear and concise, and are immediately suitable for implementation in a computer program.

The column-symmetry of the orbital quantities was shown to lead to an efficient way to store the elements in a way which enables the use of optimized matrix multiplication routines while also preserving the sparsity induced by this symmetry. The resulting data format was also used to construct a hierarchical data structure for storing the $\mathbf{T}_3$ and $\mathbf{T}_4$ tensor elements. The hierarchical nature of the structure allows for reduction in the cost of disk I/O and of operations like permutation and spin-summation which must be repeated as data is moved in and out of main memory. It was shown that permutations, which are necessary due to the restrictions of casting the operations as matrix multiplication and to the structure of the DPD symmetry packing, can be minimized by analyzing the necessary relative permutations for each of the terms in the equations. By plotting a minimum-length path (in the space of relative permutations) through each of these restrictions, the number of permutations is reduced to 12 for CCSDT and 39 for CCSDTQ.

By putting all of these results together, an efficient implementation of CCSDTQ and CCSDT(Q) was written in the CFOUR program suite. Comparison of these implementations to the leading existing implementation shows a ˜5x improvement for CCSDTQ and a 20-100x improvement for CCSDT(Q). Analysis of the timings shows a relatively low degree of overhead due to operations like permutation, although some improvement may be possible especially for CCSDT(Q). The performance of the program using multiple threads shows a ˜50% efficiency at 8 cores and ˜75% efficiency at 4 cores, without consideration of issues such as NUMA memory access, data and thread locality, and improved work scheduling.

In total, this work shows that the non-othogonally spin-adapted representation of coupled cluster for closed shell molecules leads to efficient calculations, even for expensive and complicated methods such as CCSDTQ and CCSDT(Q).

5.2 Future Work

While the efficiency of the CCSDTQ and CCSDT(Q) implementations, both through comparison to existing codes and from the analysis of the timing breakdowns is good, there is still a lot of room for improvement. A major factor in the loss of efficiency in the current implementation in that the data hierarchy of the amplitudes causes large matrix multiplications to be split into many smaller (and less efficient) ones, and sometimes to be reduced into inherently less efficient matrix-vector or vector-vector operations. The structure of the DPD packing also creates restrictions on which permutations of the amplitudes are required to compute certain terms, which necessitates additional tensor transpositions.

A solution to this is to go beyond matrix multiplication as the primitive kernel of the program and create new, tensor- and DPD-aware kernels which can obtain a higher level of efficiency and reduce the amount of overhead in the program as a whole. To do this in the general case is a difficult proposition, as there are exponentially more types of tensor operations than matrix ones (which only need to deal with transposition of the input matrices). Requiring DPD packing further complicates the algorithms, and since this structure is essentially unique to quantum chemistry, is unlikely to be implemented independently by other scientific communities. A better solution, then, is to take existing efficient matrix multiplication kernels and modify them to take advantage of (a possibly limited set of) tensor and DPD structure.

For many operations needed in CCSDTQ, a full 8-dimensional tensor kernel is not really required to regain much of the lost efficiency. Often, just extending matrix multiplication ($2 \times 2 \rightarrow 2$) by one dimension to a $3 \times 2 \rightarrow 3$ or $3 \times 3 \rightarrow 2$ tensor operation would suffice. Additionally, keeping within the realm of matrix multiplication but loosening the storage structure of the matrices would help greatly, for example in the hole-hole ladder term where the entire contraction could be written as a matrix multiplication if the memory locations of rows of the matrices could be specified independently. Current high-performance matrix multiplication implementations such as OpenBLAS, ATLAS, and Intel MKL are either closed source, largely written in assembly language, or highly specialized to the task of matrix multiplication (understandably). However, the new BLIS framework being developed at UT Austin[82–84] has a very flexible and modular structure with specialized, high-performance code isolated to a single "micro-kernel", while maintaining very high efficiency. In particular, matrices are "packed" into local storage during the operation in a standard way. The packing step gives the opportunity to simply replace the matrix→matrix function with a somewhat more complicated tensor→matrix function so that the rest of the framework can use the data seamlessly and with the same high efficiency. Work on implementing such "hybrid" tensor-matrix operations in collaboration with the van de Geijn group is planned.

Additionally, implementations of the CCSDTQ $\hat{\Lambda}$ and density equations in CFOUR are underway, using the equations derived in B. These implementations will allow for the gradient of the CCSDTQ energy and CCSDTQ properties to be computed analytically (which means better numerical precision and lower cost) than by energy-only methods. The program has been structured into several "layers", so that as much code as possible can be reused for example from the CCSDTQ amplitudes to the $\hat{\Lambda}$ equations, which should make the implementation much easier. Furthermore, the calculation of excited states using equation-of-motion coupled cluster (EOM-CCSDTQ) will be implemented in CFOUR, again reusing much of the existing code, which will speed the implementation and prevent errors.

Lastly, distributed parallelism is being explored for all of the implemented methods. The hierarchical data structure for the amplitudes facilitates distributed operation as processors can be assigned ownership of individual “hunks” of amplitudes and these can then be communicated through the network to the other processors in a synchronized fashion to ensure that all contributions are calculated. Initial results for CCSDT are promising.

Appendices

Appendix A

Proofs

Lemma. *Elements of $\tilde{P}^k$ are unique.*

Proof. The proof is trivial for $k = 0$ and $k = 1$. For $k = 2$, note that there are three distinct types of products: $P(ab)P(cd)$, $P(ab)P(bc)$, and $P(ac)P(bc)$. The permutations in the first case, since they share no common labels, commute, and so the product is equivalent only to itself and hence unique. The second type is equivalent by inspection to $P(bc)P(ac)$ and $P(ac)P(ab)$. However, since $a < b$ neither of these is a permissible element of $\tilde{P}^2$ and so products of this type are unique. Similarly for the third type, $P(ac)P(bc)$ is equivalent to $P(bc)P(ab)$ and $P(ab)P(ac)$ and so these too are unique. For $k > 2$ we can proceed inductively, assuming that elements of $\tilde{P}^{k-1}$ are unique. From the relations for $\tilde{P}^2$, it can be seen that when going to any different related permutation, the set of "from" labels can never contain any labels which are not "from" labels in the original $\tilde{P}^k$ element (although one can exchange a larger "from" label for two of a smaller one). So, to relate this permutation to one in $\tilde{P}^k$ where the "from" labels must be strictly ordered, the last and largest "from" element must always be the same. Additionally, it can be seen from the analysis of $\tilde{P}^2$ that the "to" label associated with the larger "from" label always remains in the correct position such that when eventually the permutation is related to one with the maximal "from" label in the last position, the "to" label will also be the same as in the original permutation. Thus, any $\tilde{P}^k$ element related to the original is built from a $\tilde{P}^{k-1}$ element in conjunction with the same final simple permutation. However, since elements of $\tilde{P}^{k-1}$ are unique, any related $\tilde{P}^k$ element is in fact the original one and so it is also unique. Starting the induction with $\tilde{P}^2$ completes the proof. □

Lemma. *$\tilde{P}^k \cap \tilde{P}^l = \varnothing \, \forall \, k \neq l$.*

Proof. Assume for simplicity that $k < l$ and that the converse is true. For $\tilde{P}^k$ and $\tilde{P}^l$ to share any elements, some elements from $\tilde{P}^l$ would need to be removed due to the product of two permutations being the identity. Since two permutations only produce the identity when they are equal, then $\tilde{P}^l$, possibly in some equivalent form, would need to have two identical permutations next to each other. Taking this hypothetical permutation as $P(ab)$, we can use the observations from the proof of lemma A to see that another $P(ab)$ would have to be produced from $P(ac)P(cb)$ or $P(ac)P(bc)$ for some c. Since this would require two permutations with the same "from" index and violate the ordering restriction for $\tilde{P}^l$, then these permutations would in turn have to be produced from yet more permutations. However, the label a remains as the "from" label in some permutation for any decomposition of the permutations, and so it is never possible to create the necessary pair of $P(ab)$ permutations from a valid element of $\tilde{P}^l$. So, each permutation in $\tilde{P}^l$ cannot be equivalent to one with fewer individual permutations, in particular k of them. □

Lemma. *$\tilde{P}^k$ contains all k-fold permutations which are not reducible.*

Proof. For each successive pair of permutations in each k-fold permutation, the labels will be either 1) in an ordering consistent with $\tilde{P}^k$, 2) disjoint, such that the permutations commute, or 3) in one of three non-consistent orderings: $P(bc)P(ac)$, $P(bc)P(ab)$, or $P(ab)P(ac)$, where $a < b$ in all cases ($P(ab)P(ab)$ is not permissible since the total permutation is not reducible). However, the first is equivalent to $P(ab)P(bc)$ and the second and third to $P(ac)P(bc)$. Therefore, going from left to right, successive pairs or permutations can be placed into the proper order by 1) doing nothing, 2) interchanging the permutations if they are in the wrong order since they commute, or 3) switching to an equivalent pair of permutations which have the proper ordering restriction. In this way, any k-fold permutation can be related to an element of $\tilde{P}^k$. □

Theorem 1. *$\mathscr{A}_P = \{\tilde{P}^k\}_{k=0}^{n-1}$ contains all possible permutations of n labels exactly once.*

Proof. From the lemmas, we see that the elements of each $\tilde{P}^k$ are unique, and that the sets are also unique amongst each other. Since also each $\tilde{P}^k$ contains all unique products of k individual permutations, and $\tilde{P}^n$ and higher products are empty (since there are not enough labels to satisfy the ordering restriction), then the collection of all $\tilde{P}^k$, for which $0 \leqslant k < n$ are non-empty, gives all possible unique permutations of the n labels, denoted as $\mathscr{A}_P$. □

Theorem 2. *Given a set of n labels and their two-index permutations P, define on any disjoint partitioning (into partitions of size m and $n - m$) of* *the labels the sets of permutations P_1, P_2, and P_x which permute labels within in the first partition, within the second partition, and between the partitions, respectively. Define antisymmetrizers $\mathscr{A}_{P_1}$ and $\mathscr{A}_{P_2}$ for the sets of permutations P_1 and P_2 and the partial antisymmetrizer $\tilde{\mathscr{A}_x} = \{\tilde{\tilde{P}}_x^k\}_{k=0}^{min\{m,n-m\}}$. Then, the total antisymmetrizer $\mathscr{A}_P = \mathscr{A}_{P_1}\mathscr{A}_{P_2}\tilde{\mathscr{A}_x} = \tilde{\mathscr{A}_x}\mathscr{A}_{P_1}\mathscr{A}_{P_2}$ (and by extension $\mathscr{A}_{P_2}\mathscr{A}_{P_1}\tilde{\mathscr{A}_x}$ and $\tilde{\mathscr{A}_x}\mathscr{A}_{P_2}\mathscr{A}_{P_1}$ since $\mathscr{A}_{P_1}$ and $\mathscr{A}_{P_2}$ commute).*

Proof. From theorem 1 we know that $\mathscr{A}_{P_1}$ and $\mathscr{A}_{P_2}$ have $m!$ and $(n-m)!$ unique permutations respectively. For $\tilde{\mathscr{A}_x}$, the number of elements can be easily enumerated as the "from" and "to" labels come from distinct sets. The number of elements in $\tilde{\tilde{P}}_x^0$ is of course 1, the number in $\tilde{\tilde{P}}_x^1$ is $m(n-m)$, and in general the number in $\tilde{\tilde{P}}_x^k$ is $\binom{m}{k}\binom{n-m}{k}$ where $\binom{a}{b}$ are the binomial coefficients, since you must choose k unique labels from each set. Using a special case of Vandermonde's identity, the total number in $\tilde{\mathscr{A}_x}$ is then,

$$\begin{aligned} N(\tilde{\mathscr{A}_x}) &= \sum_{k=0}^{min\{m,n-m\}} \begin{pmatrix} m \\ k \end{pmatrix} \begin{pmatrix} n-m \\ k \end{pmatrix} \\ &= \begin{pmatrix} n \\ m \end{pmatrix} \\ &= \frac{n!}{m!(n-m)!} \end{aligned} \tag{A.1}$$

The products $\mathscr{A}_{P_1}\mathscr{A}_{P_2}\tilde{\mathscr{A}_x}$ and $\tilde{\mathscr{A}_x}\mathscr{A}_{P_1}\mathscr{A}_{P_2}$ then have at most (since some elements may be equivalent) $m!(n-m)!N(\tilde{\mathscr{A}_x}) = n!$ elements each.

By construction, one can also show that any total permutation can be represented as an element of both $\mathscr{A}_{P_1}\mathscr{A}_{P_2}\tilde{\mathscr{A}_x}$ and $\tilde{\mathscr{A}_x}\mathscr{A}_{P_1}\mathscr{A}_{P_2}$. In both cases, consider the positions of the labels from the two disjoint sets. After any permutation, some set of labels from set 1, which we will call set $1'$ of size k, have moved to positions formerly occupied by set 2, and a set of the same size from set 2, called set $2'$, are now in set 1 spots. For the first case ($\mathscr{A}_{P_1}\mathscr{A}_{P_2}\tilde{\mathscr{A}}_x$), the construction is as follows: 1) exchange the labels at the positions occupied in the final permutation by sets $1'$ and $2'$, which is an element of $\tilde{\mathscr{A}}_x$ (specifically $\tilde{\tilde{P}}_x^k$), 2) permute the labels of set 2 to the locations and order of the final permutation. Since the permutation from $\tilde{\mathscr{A}}_x$ puts *some* labels from set 2 (but not necessarily set $2'$) in the proper set 1 spots, this is accomplished by permuting only set 2 labels which is an element of $\mathscr{A}_{P_2}$. 3) Similarly permute the set 1 labels, which is an element of $\mathscr{A}_{P_1}$. For the second case, the construction is similar: 1) permute the labels of set 2, which is of course an element of $\mathscr{A}_{P_2}$, so that set $2'$ occupies the positions which will be taken by set $1'$ in the final permutation, with the set $2'$ labels in the order (based on magnitude) of the desired final set $1'$ labels. This is necessary since we wish to later apply an element of $\tilde{\mathscr{A}}_x$, which has ordering restrictions on both "from" and "to" labels. 2) Similarly permute the labels of set 1, an element of $\mathscr{A}_{P_1}$, and 3) exchange the labels in sets $1'$ and $2'$ in order of magnitude, an element of $\tilde{\mathscr{A}}_x$. Thus, any total permutation of n labels from $\mathscr{A}_P$ can be written in either of these ways. Since there are $n!$ unique permutations in $\mathscr{A}_P$ and at most $n!$ permutations in each of $\mathscr{A}_{P_1}\mathscr{A}_{P_2}\tilde{\mathscr{A}}_x$ and $\tilde{\mathscr{A}}_x\mathscr{A}_{P_1}\mathscr{A}_{P_2}$, there must be $n!$ unique elements in each set and they must then be equal to $\mathscr{A}_P$. □

Theorem 3. *Given a set of n labels partitioned into three disjoint sets a, b,* *and c, the following relationship holds,*

$$\mathscr{A}_{bc}\tilde{\mathscr{A}}_{ab-c} = \mathscr{A}_{bc} \sum_{k=0}^{min\{n_a,n_c\}} \tilde{\tilde{P}}^k_{a-c} \frac{(n_b+n_c)!k!}{(n_b+k)!n_c!} \tag{A.2}$$

where $\mathscr{A}_{bc}$ is the antisymmetrizer for $b \cup c$, $\tilde{\mathscr{A}}_{ab-c}$ is the special antisymmetrizer connecting $a \cup b$ and c, and finally $\tilde{\tilde{P}}^k_{a-c}$ are the k-fold doubly-ordered permutations connecting a and c.

Proof. Using the definition of the special antisymmetrizers, we can write,

$$\mathscr{A}_{bc}\tilde{\mathscr{A}}_{ab-c} = \mathscr{A}_{bc} \sum_{l=0}^{min\{n_a+n_b,n_c\}} \tilde{\tilde{P}}^l_{ab-c} \tag{A.3}$$

For each element of $\tilde{\tilde{P}}^l_{ab-c}$, we can classify it by the number m of "from" labels which belong to the set b. This also gives the number of two-index permutations which belong to P_{b-c}, so that each element of $\tilde{\tilde{P}}^l_{ab-c}$ can be written as a product of elements from $\tilde{\tilde{P}}^m_{b-c}$ and $\tilde{\tilde{P}}^{l-m}_{a-c}$. Since $\mathscr{A}_{bc}$ already contains all antisymmetrizers from $\tilde{\tilde{P}}^m_{b-c}$, these elements reduce to unity. Additionally, since $\mathscr{A}_{bc}$ contains $\mathscr{A}_c$, an element of $\tilde{\tilde{P}}^l_{ab-c}$ with one set of "to" labels in c may be related to any other set of "to" labels (although the specific "from" labels must be the same). Specifically, we may "redistribute" elements of $\tilde{\tilde{P}}^{l-m}_{a-c}$ (which may all be related this way) such that each one receives an equal numerical factor. The number of elements in $\tilde{\tilde{P}}^l_{ab-c}$ for a fixed set of a "from" labels is $\binom{n_c}{l}\binom{n_b}{m}$ since some l indices from c must be selected as "to" labels and m from b as "from" labels. After redistribution, we are dividing the result amongst $\binom{n_c}{l-m}$ elements of $\tilde{\tilde{P}}^{l-m}_{a-c}$ for the same fixed a labels, so that each one receives the same factor and the total set $\tilde{\tilde{P}}^{l}_{ab-c}$ can be written (with the implicit understanding that $\mathscr{A}_{bc}$ is to be applied later),

$$\tilde{\tilde{P}}^{l}_{ab-c} = \sum_{m=max\{0,l-n_a\}}^{min\{l,n_b\}} \tilde{\tilde{P}}^{l-m}_{a-c} \binom{n_c}{l} \binom{n_b}{m} \binom{n_c}{l-m}^{-1} \tag{A.4}$$

The original equation of interest can then be written and refactored as,

$$\begin{aligned}
\mathscr{A}_{bc}\tilde{\mathscr{A}}_{ab-c} &= \mathscr{A}_{bc} \sum_{l=0}^{min\{n_a+n_b,n_c\}} \sum_{m=max\{0,l-n_a\}}^{min\{l,n_b\}} \tilde{\tilde{P}}^{l-m}_{a-c} \times \\
&\quad \binom{n_c}{l} \binom{n_b}{m} \binom{n_c}{l-m}^{-1} \\
&= \mathscr{A}_{bc} \sum_{k=0}^{min\{n_a,n_c\}} \tilde{\tilde{P}}^{k}_{a-c} \sum_{m=0}^{min\{n_b,n_c-k\}} \times \\
&\quad \binom{n_c}{k+m} \binom{n_b}{m} \binom{n_c}{k}^{-1} \\
&= \mathscr{A}_{bc} \sum_{k=0}^{min\{n_a,n_c\}} \tilde{\tilde{P}}^{k}_{a-c} \sum_{m=0}^{min\{n_b,n_c-k\}} \times \\
&\quad \binom{n_c}{(n_c-k)-m} \binom{n_b}{m} \binom{n_c}{k}^{-1} \\
&= \mathscr{A}_{bc} \sum_{k=0}^{min\{n_a,n_c\}} \tilde{\tilde{P}}^{k}_{a-c} \binom{n_b+n_c}{n_c-k} \binom{n_c}{k}^{-1} \\
&= \mathscr{A}_{bc} \sum_{k=0}^{min\{n_a,n_c\}} \tilde{\tilde{P}}^{k}_{a-c} \frac{(n_b+n_c)!k!}{(n_b+k)!n_c!}
\end{aligned} \tag{A.5}$$

where $k = l - m$ and the fourth equality is obtained using Vandermonde's identity. □

Theorem 4. *Given a set of n out-labels partitioned into two sets a and j of size n_a and n_j, and n in-labels partitioned into two sets b and i of size*

n_b and n_i, and a bijective mapping $* : a \cup j \mapsto b \cup i$ (where the mapping is altered by permutations of the labels), assume that the symmetry $P(pq) = P(p^*q^*)\,\forall\, p, q \in a \cup j$ exists. For a certain mapping $*$, define $n_s = n_{a;s} + n_{j;s}$ where $n_{a;s} = |a^* \cap i|$ and $n_{j;s} = |j^* \cap b|$. Then, define $\mathscr{A}_a$ and $\mathscr{A}_j$ as the total antisymmetrizers of the a and j labels, and $\tilde{\mathscr{A}}_{ai-ji}$ and $\tilde{\mathscr{A}}_{jb-ab}$ as,

$$\tilde{\mathscr{A}}_{ai-ji} = \{\tilde{\tilde{P}}^k_{ai-ji}\}_{k=0}^{min(n_j-n_{j;x},n_{a;x})} \tag{A.6}$$

$$P_{ai-ji} = \{P(a_k j_l)\,|\,a^*_k, j^*_l \in i\}_{k,l=0}^{n_a,n_j} \tag{A.7}$$

$$\tilde{\mathscr{A}}_{jb-ab} = \{\tilde{\tilde{P}}^k_{jb-ab}\}_{k=0}^{min(n_a-n_{a;x},n_{j;x})} \tag{A.8}$$

$$P_{jb-ab} = \{P(j_k a_l)\,|\,j^*_k, a^*_l \in b\}_{k,l=0}^{n_j,n_a} \tag{A.9}$$

Lastly, define a set of permutations $P_s = \{P(a_k j_l)\,|\,a^*_k \in b \wedge j^*_l \in i\}_{k,l=0}^{n_a,n_j}$. Then, the antisymmetrizer of all in or by symmetry of all out labels, $\mathscr{A}$, relative to some permutation with a mapping $*$ with $n_s = |n_a - n_b|$ is equal to $\{\mathscr{A}_a\mathscr{A}_i\tilde{\mathscr{A}}_{ai-ji}\tilde{\mathscr{A}}_{jb-ab}(\tilde{\tilde{P}}^k_s)_0\}_{k=0}^{(n-|n_a-n_i|-|n_a-n_b|)/2}$, where e.g. $(S)_0$ is an arbitrary element from the set S.

Proof. All possible permutations of the *in* or *out* labels can be classified by their value of n_s. The minimum possible value is $|n_a - n_b|$, as at most $min\{n_a, n_b\}$ labels may be paired as $a \leftrightarrow b$ and $min\{n_i, n_j\}$ labels as $j \leftrightarrow i$, leaving $\frac{|n_a-n_b|+|n_i-n_j|}{2} = |n_a - n_b|$ pairs as $a \leftrightarrow i$ or $j \leftrightarrow b$. The maximum possible value is $n - |n_a - n_i|$, as similarly at most $min\{n_a, n_i\}$ labels may be paired as $a \leftrightarrow i$ and $min\{n_j, n_b\}$ labels as $j \leftrightarrow b$, leaving $\frac{|n_a-n_i|+|n_b-n_j|}{2} = |n_a - n_i|$ out of n pairs of labels as $a \leftrightarrow b$ or $j \leftrightarrow i$. Also, the value of n_s must vary between these values in steps of two since for example a permutation which results in $aj \leftrightarrow bi \rightarrow aj \leftrightarrow ib$ (i.e. an element of P_s) changes two pairs of labels at a time. Thus, n_s may have $\frac{n-|n_a-n_i|-|n_a-n_b|}{2}+1$ distinct values which are generated by applying successive distinct elements of P_s, namely the elements $(\tilde{\tilde{P}}_s^k)_0$. For each value of n_s, the number of permutations in $\mathscr{A}_a\mathscr{A}_i\tilde{\mathscr{A}}_{ai-ji}\tilde{\mathscr{A}}_{jb-ab}$ is equal to $n_a!n_i!\binom{n_i}{n_{a;s}}\binom{n_b}{n_{j;s}}$ from previous analysis. Defining $n_{a;s}$ and $n_{j;s}$ in terms of a more convenient variable $k=\frac{n_s-|n_a-n_b|}{2}$ as $n_{a;s}=max\{n_a-n_b,0\}+k$ and $n_{j;s}=max\{n_j-n_i,0\}+k$, we can write the total number of permutations as,

$$\begin{aligned}
N_{total} &= n_a!n_j! \sum_{k=0}^{(n-|n_a-n_i|-|n_a-n_b|)/2} \begin{pmatrix} n_i \\ max\{n_a-n_b,0\}+k \end{pmatrix} \times \\
&\quad \begin{pmatrix} n_b \\ max\{n_j-n_i,0\}+k \end{pmatrix} \\
&= \begin{cases} n_a!n_j! \sum_{k=0}^{(n-|n_a-n_i|-|n_a-n_b|)/2} \begin{pmatrix} n_i \\ n_j-k \end{pmatrix} \begin{pmatrix} n_b \\ k \end{pmatrix} \\ \qquad\qquad \text{if } n_a > n_b \text{ and } n_i > n_j \\ n_a!n_j! \sum_{k=0}^{(n-|n_a-n_i|-|n_a-n_b|)/2} \begin{pmatrix} n_i \\ k \end{pmatrix} \begin{pmatrix} n_b \\ n_a-k \end{pmatrix} \\ \qquad\qquad \text{if } n_b > n_a \text{ and } n_j > n_i \end{cases}
\end{aligned} \tag{A.10}$$

Using Vandermonde's identity again, these two cases are equal to $n_a!n_j!\binom{n}{n_j}$ and $n_a!n_j!\binom{n}{n_a}$ respectively which are both equal to $n!$ upon expansion of the binomial coefficient. To show that these permutations are unique and hence equal to $\mathscr{A}$, we can show that all possible permutations which conserve n_s are related to elements of $\mathscr{A}_a\mathscr{A}_i\tilde{\mathscr{A}}_{ai-ji}\tilde{\mathscr{A}}_{jb-ab}$. The permutations which conserve n_s can be written non-uniquely as

$$\mathscr{A}_{\delta n_s=0} = \mathscr{A}_a\mathscr{A}_j\mathscr{A}_b\mathscr{A}_i \tag{A.11}$$

since these are all permutations which involve either “in” out “out” labels of the same type. However, as shown in theorem 2, we can re-write this as,

$$\mathscr{A}_{\delta n_s=0} = \tilde{\mathscr{A}}_{ai-ab}\tilde{\mathscr{A}}_{jb-ji}\mathscr{A}_{ab}\mathscr{A}_{ji}\mathscr{A}_{ai}\mathscr{A}_{jb}\mathscr{A}_{ab}\mathscr{A}_{ji}\mathscr{A}_{ai}\mathscr{A}_{jb}\tilde{\mathscr{A}}_{ai-ji}\tilde{\mathscr{A}}_{jb-ab} \tag{A.12}$$

where $\mathscr{A}_{pq}$ is the antisymmetrizer for labels p which map as $p \leftrightarrow q$ etc., and $\tilde{\mathscr{A}}_{ai-ab}$ and $\tilde{\mathscr{A}}_{jb-ji}$ are defined with similar notation to $\tilde{\mathscr{A}}_{ai-ji}$ and $\tilde{\mathscr{A}}_{jb-ab}$. Since $\mathscr{A}_{pq}^2 = K\mathscr{A}_{pq}$ for some integer constant K and different $\mathscr{A}_{pq}$ commute, we can remove some antisymmetrizers, recombine the pieces of $\mathscr{A}_a$ and $\mathscr{A}_j$, and arrive at,

$$\mathscr{A}_{\delta n_s=0} = K\mathscr{A}_a\mathscr{A}_j\tilde{\mathscr{A}}_{ai-ji}\tilde{\mathscr{A}}_{jb-a} \tag{A.13}$$

for some K. Thus, any permutation for a fixed n_s is relatable to $\mathscr{A}_a\mathscr{A}_j\tilde{\mathscr{A}}_{ai-ji}\tilde{\mathscr{A}}_{jb-a}$. The elements are unique since the set of all unique $\mathscr{A}_{\delta n_s=0}$ for all n_s is the same size as the set of all $\mathscr{A}_a\mathscr{A}_j\tilde{\mathscr{A}}_{ai-ji}\tilde{\mathscr{A}}_{jb-a}$, and so we have $n!$ unique permutations which must be equal to the total antisymmetrizer $\mathscr{A}$. □

Appendix B

Non-orthogonally Spin-adapted $\hat{\Lambda}$ and Density Matrix Equations

The non-orthogonally spin-adapted equations for the CCSDTQ $\hat{\Lambda}$ equations have been derived using the diagrammatic techniques previously presented. The equations are,

$$
\begin{aligned}
\check{z}^{i}_{a} \;=\;& \check{F}^{i}_{a} + \sum_{e} \check{F}^{e}_{a}\check{\lambda}^{i}_{e} - \sum_{m} \check{F}^{i}_{m}\check{\lambda}^{m}_{a} + \sum_{em} \check{W}^{\check{e}i}_{\check{m}a}\check{\lambda}^{m}_{e} - \sum_{emn} \check{W}^{ei}_{mn}\check{\lambda}^{\check{m}n}_{\check{e}a} \\
&+ \sum_{efm} \check{W}^{ef}_{ma}\check{\lambda}^{\check{m}i}_{\check{e}f} + \sum_{em} \check{W}^{\check{m}i}_{\check{e}a}\tilde{\check{D}}^{e}_{m} + \sum_{efm} \check{W}^{\check{e}i}_{\check{m}f}\tilde{\check{\Gamma}}^{mf}_{ea} \\
&- \sum_{emn} \check{W}^{\check{e}n}_{\check{m}a}\tilde{\check{\Gamma}}^{mi}_{en} + \sum_{mno} \check{W}^{oi}_{mn}\tilde{\check{\Gamma}}^{\check{m}n}_{\check{o}a} - \sum_{efg} \check{W}^{ef}_{ga}\tilde{\check{\Gamma}}^{\check{g}i}_{\check{e}f} + \sum_{e} \check{F}^{i}_{e}\tilde{\tilde{\check{D}}}^{e}_{a} \\
&- \sum_{m} \check{F}^{m}_{a}\tilde{\tilde{\check{D}}}^{i}_{m} - \sum_{mn} \check{W}^{\check{n}i}_{\check{m}a}\tilde{\tilde{\check{D}}}^{m}_{n} - \sum_{ef} \check{W}^{\check{f}i}_{\check{e}a}\tilde{\tilde{\check{D}}}^{e}_{f} - \sum_{efg} \check{W}^{\tilde{g}i}_{\tilde{e}f}\tilde{\check{\Gamma}}^{ef}_{ga} \\
&+ \sum_{mno} \check{W}^{\check{m}n}_{\check{o}a}\tilde{\check{\Gamma}}^{oi}_{mn} - \sum_{emn} \check{W}^{mi}_{en}\tilde{\tilde{\check{\Gamma}}}^{\check{e}n}_{\check{m}a} + \sum_{efm} \check{W}^{mf}_{ea}\tilde{\tilde{\check{\Gamma}}}^{\check{e}i}_{\check{m}f} \\
&+ \sum_{efm} \check{W}^{\check{m}i}_{\check{e}f}\tilde{\check{\Gamma}}^{ef}_{ma} - \sum_{emn} \check{W}^{\check{m}n}_{\check{e}a}\tilde{\check{\Gamma}}^{ei}_{mn} \qquad \text{(B.1)}
\end{aligned}
$$

$$
\begin{aligned}
\check{z}^{ij}_{ab} \;=\;& \left(1 + P^{ai}_{bj}\right)\left\{\frac{1}{2}\check{W}^{mn}_{ef} + \check{F}\check{\lambda}^{j}_{b} - \sum_{m} \check{W}^{ij}_{mb}\check{\lambda}^{m}_{a} + \sum_{e} \check{W}^{ej}_{ab}\check{\lambda}^{i}_{e}\right. \\
&- \sum_{m} \check{F}^{i}_{m}\check{\lambda}^{mj}_{ab} + \sum_{e} \check{F}^{e}_{a}\check{\lambda}^{ij}_{eb} + \frac{1}{2}\sum_{em} \check{W}^{\check{e}j}_{\check{m}b}\check{\lambda}^{\check{m}i}_{\check{e}a} \\
&- \left(\frac{1}{2} + P^{i}_{j}\right)\sum_{em} \check{W}^{ej}_{bm}\check{\lambda}^{mi}_{ae} + \frac{1}{2}\sum_{mn} \check{W}^{ij}_{mn}\check{\lambda}^{mn}_{ab}
\end{aligned}
$$

$$
\begin{aligned}
&+\frac{1}{2}\sum_{ef}\check{W}^{ef}_{ab}\check{\lambda}^{ij}_{ef}+\sum_{e}\check{W}^{ij}_{eb}\check{\tilde{D}}^{e}_{a}-\sum_{m}\check{W}^{mj}_{ab}\check{\tilde{D}}^{i}_{m}\\
&-\sum_{emn}\check{W}^{ei}_{mn}\check{\lambda}^{\check{m}nj}_{\check{e}ab}+\sum_{e}\check{W}^{ef}_{ma}\check{\lambda}^{\check{m}ij}_{\check{e}fb}-\frac{1}{2}\sum_{mn}\check{W}^{\check{n}i}_{\check{m}a}\check{\tilde{\Gamma}}^{mj}_{nb}\\
&+\left(\frac{1}{2}+P^{i}_{j}\right)\sum_{mn}\check{W}^{ni}_{am}\check{\tilde{\Gamma}}^{mj}_{bn}+\frac{1}{2}\sum_{ef}\check{W}^{\check{e}i}_{\check{f}a}\check{\tilde{\Gamma}}^{\check{f}j}_{\check{e}b}\\
&-\left(\frac{1}{2}+P^{i}_{j}\right)\sum_{ef}\check{W}^{ei}_{af}\check{\tilde{\Gamma}}^{fj}_{be}+\frac{1}{2}\sum_{em}\check{W}^{\check{m}i}_{\check{e}a}\check{\tilde{\Gamma}}^{\check{e}j}_{\check{m}b}\\
&-\left(\frac{1}{2}+P^{i}_{j}\right)\sum_{em}\check{W}^{mi}_{ae}\check{\tilde{\Gamma}}^{ej}_{bm}-\sum_{em}\check{W}^{me}_{ab}\check{\tilde{\Gamma}}^{ij}_{me}-\sum_{em}\check{W}^{ij}_{em}\check{\tilde{\Gamma}}^{em}_{ab}\\
&+\frac{1}{2}\sum_{mn}\check{W}^{mn}_{ab}\check{\tilde{\Gamma}}^{ij}_{mn}+\frac{1}{2}\sum_{ef}\check{W}^{ef}_{ij}\check{\tilde{\Gamma}}^{ab}_{ef}-\frac{1}{2}\sum_{efmno}\check{W}^{efi}_{mno}\check{\lambda}^{\check{m}\check{n}oj}_{\check{e}\check{f}ab}\\
&+\frac{1}{2}\sum_{efgmn}\check{W}^{efg}_{mna}\check{\lambda}^{\check{m}\check{n}ij}_{\check{e}\check{f}gb}\Bigg\}
\end{aligned}
\tag{B.2}
$$

$$
\begin{aligned}
\check{z}^{ijk}_{abc} &= \left(1+P^{ai}_{ck}+P^{bj}_{ck}\right)\left(1+P^{ai}_{bj}\right)\Bigg\{\frac{1}{2}\check{W}^{ij}_{ab}\check{\lambda}^{k}_{c}+\frac{1}{2}\check{F}^{i}_{a}\check{\lambda}^{jk}_{bc}\\
&-\sum_{m}\check{W}^{jk}_{mc}\check{\lambda}^{im}_{ab}+\sum_{e}\check{W}^{ek}_{bc}\check{\lambda}^{ij}_{ae}-\frac{1}{2}\sum_{m}\check{F}^{i}_{m}\check{\lambda}^{mjk}_{abc}\\
&+\frac{1}{2}\sum_{e}\check{F}^{e}_{a}\check{\lambda}^{ijk}_{ebc}+\frac{1}{4}\sum_{em}\check{W}^{\check{e}a}_{\check{m}i}\check{\lambda}^{\check{m}jk}_{\check{e}bc}\\
&-\left(\frac{1}{2}+P^{i}_{j}\right)\sum_{em}\check{W}^{ea}_{im}\check{\lambda}^{mjk}_{bec}+\frac{1}{2}\sum_{mn}\check{W}^{ij}_{mn}\check{\lambda}^{mnk}_{abc}\\
&+\frac{1}{2}\sum_{ef}\check{W}^{ef}_{ab}\check{\lambda}^{ijk}_{efc}-\frac{1}{2}\sum_{emn}\check{W}^{ei}_{mn}\check{\lambda}^{\check{m}njk}_{\check{e}abc}+\frac{1}{2}\sum_{efm}\check{W}^{ef}_{ma}\check{\lambda}^{\check{m}ijk}_{\check{e}fbc}\\
&+\sum_{e}\check{W}^{ij}_{ae}\check{\tilde{\Gamma}}^{ek}_{bc}-\sum_{m}\check{W}^{im}_{ab}\check{\tilde{\Gamma}}^{jk}_{mc}+\frac{1}{8}\sum_{efmn}\check{W}^{\check{i}ef}_{\check{a}mn}\check{\lambda}^{\check{m}\check{n}jk}_{\check{e}\check{f}bc}\\
&-\left(\frac{1}{2}+P^{i}_{j}\right)\sum_{mnef}\check{W}^{ief}_{nma}\check{\lambda}^{\check{m}njk}_{\check{e}bfc}\Bigg\}
\end{aligned}
\tag{B.3}
$$

$$
\check{z}^{ijkl}_{abcd} = \left(1+P^{ai}_{dl}+P^{bj}_{dl}+P^{ck}_{dl}\right)\left(1+P^{ai}_{ck}+P^{bj}_{ck}\right)\left(1+P^{ai}_{bj}\right)\times
$$

$$\begin{aligned}&\left\{\frac{1}{4}\check{W}^{ij}_{ab}\check{\lambda}^{kl}_{cd}+\frac{1}{6}\check{F}^{i}_{a}\check{\lambda}^{jkl}_{bcd}-\frac{1}{2}\sum_{m}\check{W}^{ij}_{am}\check{\lambda}^{mkl}_{bcd}\right.\\&+\frac{1}{2}\sum_{e}\check{W}^{ie}_{ab}\check{\lambda}^{jkl}_{ecd}-\frac{1}{6}\sum_{m}\check{F}^{i}_{m}\check{\lambda}^{mjkl}_{abcd}+\frac{1}{6}\sum_{e}\check{F}^{e}_{a}\check{\lambda}^{ijkl}_{ebcd}\\&+\frac{1}{12}\sum_{em}\check{W}^{\check{e}i}_{\check{m}a}\check{\lambda}^{\check{m}jkl}_{\check{e}bcd}-\frac{1}{2}\left(\frac{1}{2}+P^{i}_{j}\right)\sum_{em}\check{W}^{ei}_{am}\check{\lambda}^{mjkl}_{becd}\\&+\frac{1}{4}\sum_{mn}\check{W}^{ij}_{mn}\check{\lambda}^{mnkl}_{abcd}+\frac{1}{4}\sum_{ef}\check{W}^{ef}_{ab}\check{\lambda}^{ijkl}_{efcd}\\&\left.+\frac{1}{2}\sum_{e}\check{W}^{ij}_{ae}\check{\tilde{\Gamma}}^{ekl}_{bcd}-\frac{1}{2}\sum_{m}\check{W}^{im}_{ab}\check{\tilde{\Gamma}}^{jkl}_{mcd}\right\}\end{aligned}\tag{B.4}$$

One major difference between these equations and the CCSDTQ amplitude equations is in the factorization. Where the amplitude equations rely as much as possible on intermediates which mirror elements of the transformed Hamiltonian $\bar{H}$, the terms in the $\hat{\Lambda}$ equations which call for an intermediate which contains a $\hat{\Lambda}$ element are more efficiently represented using intermediates which instead look like elements of the one- or two-particle density matrices, D^{p}_{q} and Γ^{pq}_{rs} . These intermediates, composed of contractions between $\hat{\Lambda}$ and $\hat{T}$, are then contracted with the transformed Hamiltonian to give a contribution to the new $\hat{\Lambda}$.

The density matrix contains all terms from the complete coupled cluster energy functional,

$$E_{CC}=\langle\Phi_0|(1+\hat{\Lambda})\bar{H}|\Phi_0\rangle\tag{B.5}$$

which, viewed diagrammatically, have the Hamiltonian vertices removed. The non-orthogonally spin-adapted equations for these quantities, along with the partial expressions used as intermediates in the $\hat{\Lambda}$ equations are,

$$\check{D}_{a}^{i} = \check{\lambda}_{a}^{i} \tag{B.6}$$

$$\tilde{\tilde{\check{D}}}_{b}^{a} = -\frac{1}{2}\sum_{efmno}\check{\lambda}_{\check{e}\check{f}b}^{\check{m}\check{n}o}\check{t}_{mno}^{efa} - \frac{1}{6}\sum_{efgmnop}\check{\lambda}_{\check{e}\check{f}\check{g}b}^{\check{m}\check{n}\check{o}p}\check{t}_{mnop}^{efga} \tag{B.7}$$

$$\tilde{\check{D}}_{b}^{a} = \tilde{\tilde{\check{D}}}_{b}^{a} - \sum_{emn}\check{\lambda}_{\check{e}b}^{\check{m}n}\check{t}_{mn}^{ea} \tag{B.8}$$

$$\check{D}_{b}^{a} = \tilde{\check{D}}_{b}^{a} - \sum_{m}\check{\lambda}_{b}^{m}\check{t}_{m}^{a} \tag{B.9}$$

$$\tilde{\tilde{\check{D}}}_{j}^{i} = \frac{1}{2}\sum_{efgmn}\check{\lambda}_{\check{e}\check{f}g}^{\check{m}\check{n}i}\check{t}_{mnj}^{efg} + \frac{1}{6}\sum_{efghmno}\check{\lambda}_{\check{e}\check{f}\check{g}h}^{\check{m}\check{n}\check{o}i}\check{t}_{mnoj}^{efgh} \tag{B.10}$$

$$\tilde{\check{D}}_{j}^{i} = \tilde{\tilde{\check{D}}}_{j}^{i} + \sum_{efm}\check{\lambda}_{\check{e}f}^{\check{m}i}\check{t}_{mj}^{ef} \tag{B.11}$$

$$\check{D}_{j}^{i} = \tilde{\check{D}}_{j}^{i} + \sum_{e}\check{\lambda}_{e}^{i}\check{t}_{j}^{e} \tag{B.12}$$

$$\begin{aligned} \tilde{\check{D}}_{i}^{a} &= \frac{1}{2}\sum_{efmn}\check{\lambda}_{ef}^{mn}\check{t}_{\check{m}\check{n}i}^{\check{e}\check{f}a} + \frac{1}{6}\sum_{efgmno}\check{\lambda}_{efg}^{mno}\check{t}_{\check{m}\check{n}\check{o}i}^{\check{e}\check{f}\check{g}a} \\ &\quad - \sum_{emn}\tilde{\tilde{\check{\Gamma}}}_{ei}^{mn}\check{t}_{\check{m}n}^{\check{e}a} \end{aligned} \tag{B.13}$$

$$\begin{aligned} \check{D}_{i}^{a} &= \tilde{\check{D}}_{i}^{a} + \check{t}_{i}^{a} + \sum_{em}\check{\lambda}_{e}^{m}\left(\check{t}_{\check{m}i}^{\check{e}a} - \check{t}_{i}^{e}\check{t}_{m}^{a}\right) + \sum_{e}\tilde{\check{D}}_{e}^{a}\check{t}_{i}^{e} - \sum_{m}\tilde{\check{D}}_{i}^{m}\check{t}_{m}^{a} \\ &\quad + 2\sum_{emn}\tilde{\tilde{\check{\Gamma}}}_{ei}^{mn}\check{t}_{\check{m}n}^{\check{e}a} - \sum_{emn}\tilde{\check{\Gamma}}_{ei}^{mn}\check{t}_{\check{m}n}^{\check{e}a} + \sum_{efm}\tilde{\check{\Gamma}}_{ef}^{ma}\check{t}_{\check{m}i}^{\check{e}f} \end{aligned} \tag{B.14}$$

$$\check{\Gamma}_{ab}^{ij} = \check{\lambda}_{ab}^{ij} \tag{B.15}$$

$$\tilde{\tilde{\check{\Gamma}}}_{ka}^{ij} = \sum_{efm}\check{\lambda}_{\check{e}fa}^{\check{m}ij}\check{t}_{mk}^{ef} \tag{B.16}$$

$$\tilde{\check{\Gamma}}_{ka}^{ij} = \tilde{\tilde{\check{\Gamma}}}_{ka}^{ij} + \frac{1}{2}\sum_{efgmn}\check{\lambda}_{\check{e}\check{f}ga}^{\check{m}\check{n}ij}\check{t}_{mnk}^{efg} \tag{B.17}$$

$$\check{\Gamma}_{ka}^{ij} = \tilde{\check{\Gamma}}_{ka}^{ij} + \sum_{e}\check{\lambda}_{ea}^{ij}\check{t}_{k}^{e} \tag{B.18}$$

$$\tilde{\check{\Gamma}}^{ai}_{bc} = -\sum_{emn} \check{\lambda}^{\check{m}ni}_{\check{e}bc} \check{t}^{ea}_{mn} - \frac{1}{2} \sum_{efmno} \check{\lambda}^{\check{m}\check{n}oi}_{\check{e}\check{f}bc} \check{t}^{efa}_{mno} \tag{B.19}$$

$$\check{\Gamma}^{ai}_{bc} = \tilde{\check{\Gamma}}^{ai}_{bc} - \sum_{m} \check{\lambda}^{mi}_{bc} \check{t}^{a}_{m} \tag{B.20}$$

$$\check{H}^{ai}_{bj} = -\sum_{em} \check{\lambda}^{mi}_{be} \left(\frac{1}{2} \check{t}^{ea}_{jm} + \check{t}^{e}_{j} \check{t}^{a}_{m} \right) \tag{B.21}$$

$$\begin{aligned} \check{H}^{ai}_{jb} = {} & \frac{1}{2} \sum_{em} \check{\lambda}^{\check{m}i}_{\check{e}b} \left(\frac{1}{2} \check{t}^{e\check{a}}_{m\check{\jmath}} - \check{t}^{e}_{j} \check{t}^{a}_{m} \right) \\ & - \frac{1}{2} \sum_{em} \check{\lambda}^{mi}_{be} \left(\frac{1}{2} \check{t}^{ea}_{jm} + \check{t}^{e}_{j} \check{t}^{a}_{m} \right) \end{aligned} \tag{B.22}$$

$$\begin{aligned} \tilde{\tilde{\check{\Gamma}}}^{ai}_{bj} = {} & -\sum_{efmn} \check{\lambda}^{\check{n}mi}_{\check{f}be} \check{t}^{fea}_{njm} - \frac{1}{2} \sum_{efgmno} \check{\lambda}^{\check{n}\check{o}mi}_{\check{f}\check{g}be} \check{t}^{fgea}_{nojm} \\ & - \sum_{emn} \tilde{\check{\Gamma}}^{\check{n}mi}_{\check{f}bj} \check{t}^{fa}_{nm} \end{aligned} \tag{B.23}$$

$$\begin{aligned} \tilde{\tilde{\check{\Gamma}}}^{ai}_{jb} = {} & \frac{1}{2} \tilde{\tilde{\check{\Gamma}}}^{ai}_{bj} + \frac{1}{4} \sum_{efmn} \check{\lambda}^{\check{n}\check{m}i}_{\check{f}\check{e}b} \check{t}^{fe\check{a}}_{nm\check{\jmath}} + \frac{1}{12} \sum_{efgmno} \check{\lambda}^{\check{n}\check{o}\check{m}i}_{\check{f}\check{g}\check{e}b} \check{t}^{fge\check{a}}_{nom\check{\jmath}} \\ & - \frac{1}{2} \sum_{emn} \tilde{\check{\Gamma}}^{\check{n}\check{m}i}_{\check{f}\check{\jmath}b} \check{t}^{fa}_{nm} \end{aligned} \tag{B.24}$$

$$\tilde{\check{\Gamma}}^{ai}_{bj} = \tilde{\tilde{\check{\Gamma}}}^{ai}_{bj} - \sum_{em} \check{\lambda}^{mi}_{be} \check{t}^{ea}_{jm} \tag{B.25}$$

$$\tilde{\check{\Gamma}}^{ai}_{jb} = \tilde{\tilde{\check{\Gamma}}}^{ai}_{jb} + \frac{1}{2} \sum_{em} \check{\lambda}^{\check{m}i}_{\check{e}b} \check{t}^{e\check{a}}_{m\check{\jmath}} - \frac{1}{2} \sum_{em} \check{\lambda}^{mi}_{be} \check{t}^{ea}_{jm} \tag{B.26}$$

$$\check{\Gamma}^{ai}_{bj} = \tilde{\check{\Gamma}}^{ai}_{bj} - \sum_{m} \check{\Gamma}^{mi}_{bj} \check{t}^{a}_{m} + \sum_{e} \tilde{\check{\Gamma}}^{ai}_{be} \check{t}^{e}_{j} \tag{B.27}$$

$$\check{\Gamma}^{ai}_{jb} = \tilde{\check{\Gamma}}^{ai}_{jb} + \check{\lambda}^{i}_{b} \check{t}^{a}_{j} - \sum_{m} \check{\Gamma}^{mi}_{jb} \check{t}^{a}_{m} + \sum_{e} \tilde{\check{\Gamma}}^{ai}_{eb} \check{t}^{e}_{j} \tag{B.28}$$

$$\tilde{\check{\Gamma}}^{ij}_{kl} = \sum_{efgm} \check{\lambda}^{\check{m}ij}_{\check{e}fg} \check{t}^{efg}_{mkl} + \frac{1}{2} \sum_{efghmn} \check{\lambda}^{\check{m}\check{n}ij}_{\check{e}\check{f}gh} \check{t}^{efgh}_{mnkl} + \sum_{efm} \tilde{\check{\Gamma}}^{\check{m}ij}_{\check{e}fl} \check{t}^{ef}_{mk} \tag{B.29}$$

$$\check{\Gamma}^{ij}_{kl} = \tilde{\check{\Gamma}}^{ij}_{kl} + \sum_{ef} \check{\lambda}^{ij}_{ef} \tau^{ef}_{kl} + \left(1 + P^{ik}_{jl}\right) \sum_{e} \tilde{\check{\Gamma}}^{ij}_{ke} \check{t}^{e}_{l} \tag{B.30}$$

$$\begin{aligned}\tilde{\check{\Gamma}}^{ab}_{cd} &= \sum_{emno}\check{\lambda}^{\check{m}no}_{\check{e}cd}\check{t}^{eab}_{mno} + \frac{1}{2}\sum_{efmnop}\check{\lambda}^{\check{m}\check{n}op}_{\check{e}\check{f}cd}\check{t}^{efab}_{mnop} \\ &\quad - \sum_{emn}\tilde{\check{\Gamma}}^{\check{m}nb}_{\check{e}cd}\check{t}^{ea}_{mn}\end{aligned} \tag{B.31}$$

$$\check{\Gamma}^{ab}_{cd} = \tilde{\check{\Gamma}}^{ab}_{cd} + \sum_{mn}\check{\lambda}^{mn}_{cd}\tau^{ab}_{mn} - (1+P^{ac}_{bd})\sum_{m}\tilde{\check{\Gamma}}^{am}_{cd}\check{t}^{b}_{m} \tag{B.32}$$

$$\tilde{\check{\Gamma}}^{ia}_{jk} = \frac{1}{2}\sum_{efgmn}\check{\lambda}^{mni}_{efg}\check{t}^{\check{e}\check{f}ga}_{\check{m}\check{n}jk} \tag{B.33}$$

$$\begin{aligned}\tilde{\tilde{\check{\Gamma}}}^{ia}_{jk} &= \tilde{\check{\Gamma}}^{ia}_{jk} + \frac{1}{2}\sum_{em}\tilde{\check{\Gamma}}^{\check{m}i}_{\check{e}j}\check{t}^{\check{e}a}_{\check{m}k} - \left(\frac{1}{2}+P^{j}_{k}\right)\sum_{em}\tilde{\check{\Gamma}}^{mi}_{je}\check{t}^{ea}_{km} \\ &\quad + \sum_{efgm}\tilde{\check{\Gamma}}^{mia}_{efg}\check{t}^{\check{e}fg}_{\check{m}jk} - \frac{1}{4}\sum_{efmn}\tilde{\check{\Gamma}}^{\check{m}\check{n}i}_{\check{e}\check{f}j}\check{t}^{ef\check{a}}_{mn\check{k}} \\ &\quad + \left(\frac{1}{2}+P^{j}_{k}\right)\sum_{efmn}\tilde{\check{\Gamma}}^{\check{m}ni}_{\check{e}jf}\check{t}^{efa}_{mkn}\end{aligned} \tag{B.34}$$

$$\begin{aligned}\check{\Gamma}^{ia}_{jk} &= \tilde{\tilde{\check{\Gamma}}}^{ia}_{jk} + \sum_{e}\check{\lambda}^{i}_{e}\check{t}^{ea}_{jk} + \sum_{efm}\check{\lambda}^{mi}_{ef}\check{t}^{\check{e}fa}_{\check{m}jk} + \tilde{\check{D}}^{i}_{j}\check{t}^{a}_{k} - \sum_{m}\tilde{\check{\Gamma}}^{im}_{jk}\check{t}^{a}_{m} \\ &\quad + \sum_{ef}\check{\Gamma}^{ia}_{ef}\check{t}^{ef}_{jk} + \sum_{e}\check{\Gamma}^{ia}_{je}\check{t}^{e}_{k} + \sum_{e}\check{\Gamma}^{ia}_{ek}\check{t}^{e}_{j}\end{aligned} \tag{B.35}$$

$$\tilde{\check{\Gamma}}^{ab}_{ci} = -\frac{1}{2}\sum_{efmno}\check{\lambda}^{mno}_{efc}\check{t}^{\check{e}\check{f}ab}_{\check{m}\check{n}oi} \tag{B.36}$$

$$\begin{aligned}\tilde{\tilde{\check{\Gamma}}}^{ab}_{ci} &= \tilde{\check{\Gamma}}^{ab}_{ci} + \frac{1}{2}\sum_{em}\tilde{\check{\Gamma}}^{\check{m}a}_{\check{e}c}\check{t}^{\check{e}b}_{\check{m}i} - \left(\frac{1}{2}+P^{a}_{b}\right)\sum_{em}\tilde{\check{\Gamma}}^{ma}_{ce}\check{t}^{eb}_{im} \\ &\quad - \sum_{emno}\tilde{\check{\Gamma}}^{mno}_{eci}\check{t}^{\check{e}ab}_{\check{m}no} + \frac{1}{4}\sum_{efmn}\tilde{\check{\Gamma}}^{\check{m}\check{n}a}_{\check{e}\check{f}c}\check{t}^{ef\check{b}}_{mn\check{i}} \\ &\quad - \left(\frac{1}{2}+P^{a}_{b}\right)\sum_{efmn}\tilde{\check{\Gamma}}^{\check{m}na}_{\check{e}cf}\check{t}^{efb}_{min}\end{aligned} \tag{B.37}$$

$$\begin{aligned}\check{\Gamma}^{ab}_{ci} &= \tilde{\tilde{\check{\Gamma}}}^{ab}_{ci} - \sum_{m}\check{\lambda}^{m}_{c}\check{t}^{ab}_{mi} - \sum_{emn}\check{\lambda}^{mn}_{ec}\check{t}^{\check{e}ab}_{\check{m}ni} + \tilde{\check{D}}^{a}_{c}\check{t}^{b}_{i} + \sum_{e}\tilde{\check{\Gamma}}^{ab}_{ce}\check{t}^{e}_{i} \\ &\quad + \sum_{mn}\check{\Gamma}^{mn}_{ci}\check{t}^{ab}_{mn} - \sum_{m}\check{\Gamma}^{am}_{ci}\check{t}^{b}_{m} - \sum_{m}\check{\Gamma}^{mb}_{ci}\check{t}^{a}_{m}\end{aligned} \tag{B.38}$$

$$\begin{aligned}
\check{\Gamma}_{ij}^{ab} \quad &= \quad \left(1 + P_{bj}^{ai}\right) \left\{ \frac{1}{2}\tau_{ij}^{ab} + \frac{1}{2}\sum_{em} \check{\lambda}_{e}^{m} \check{t}_{\check{m}ij}^{\check{e}ab} + \frac{1}{4} \sum_{efmn} \check{\lambda}_{ef}^{mn} \check{t}_{\check{m}\check{n}ij}^{\check{e}\check{f}ab} \right. \\
&\quad + \sum_{e} \tilde{\tilde{\check{\Gamma}}}_{ej}^{ab} \check{t}_{i}^{e} - \sum_{m} \tilde{\tilde{\check{\Gamma}}}_{ij}^{mb} \check{t}_{m}^{a} + \frac{1}{2}\sum_{em} \check{H}_{\check{e}i}^{\check{m}a} \check{t}_{\check{m}j}^{\check{e}b} \\
&\quad - \left(\frac{1}{2} + P_{j}^{i}\right) \sum_{em} \check{H}_{ie}^{ma} \check{t}_{jm}^{eb} + \sum_{e} \check{D}_{e}^{a} \check{t}_{ij}^{eb} - \sum_{m} \check{D}_{i}^{m} \check{t}_{mj}^{ab} \\
&\quad + \frac{1}{2}\sum_{em} \tilde{\tilde{\check{\Gamma}}}_{\check{e}i}^{\check{m}a} \left(\check{t}_{\check{m}j}^{\check{e}b} - \check{t}_{j}^{e}\check{t}_{m}^{b}\right) - \left(\frac{1}{2} + P_{j}^{i}\right) \sum_{em} \tilde{\tilde{\check{\Gamma}}}_{ie}^{ma} \tau_{jm}^{eb} \\
&\quad + \sum_{efm} \check{\Gamma}_{ef}^{ma} \check{t}_{\check{m}ij}^{\check{e}fb} - \sum_{emn} \check{\Gamma}_{ei}^{mn} \check{t}_{\check{m}nj}^{\check{e}ab} + \left(\check{D}_{i}^{a} - \check{t}_{i}^{a}\right) \check{t}_{j}^{b} \Lambda \\
&\quad \frac{1}{2}\sum_{mn} \check{D}_{ij}^{mn} \tau_{mn}^{ab} && \text{(B.39)} \\
\tilde{\check{\Gamma}}_{lab}^{ijk} \quad &= \quad \sum_{efm} \check{\lambda}_{\check{e}fab}^{\check{m}ijk} \check{t}_{ml}^{ef} && \text{(B.40)} \\
\tilde{\check{\Gamma}}_{abc}^{dij} \quad &= \quad -\sum_{emn} \check{\lambda}_{\check{e}abc}^{\check{m}nij} \check{t}_{mn}^{ed} && \text{(B.41)}
\end{aligned}$$

With these equations and the proper integrals, the gradient of the coupled cluster energy and any first-order molecular properties can be evaluated.

Bibliography

[1] Čížek, J. *J. Chem. Phys.* **1966**, *45*, 4256–4266.

[2] Čížek, J. In *Advances in Chemical Physics*; LeFebvre, R., Moser, C., Eds.; John Wiley & Sons, Inc., 1969; pp 35–89.

[3] Bartlett, R. J. *J. Phys. Chem.* **1989**, *93*, 1697–1708.

[4] Feller, D.; Dixon, D. A. *J. Chem. Phys.* **2001**, *115*, 3484–3496.

[5] Heckert, M.; Kállay, M.; Gauss, J. *Mol. Phys.* **2005**, *103*, 2109–2115.

[6] Bartlett, R. J.; Musiał, M. *Rev. Mod. Phys.* **2007**, *79*, 291–352.

[7] Urban, M.; Noga, J.; Cole, S. J.; Bartlett, R. J. *J. Chem. Phys.* **1985**, *83*, 4041.

[8] Raghavachari, K.; Trucks, G. W.; Pople, J. A.; Head-Gordon, M. *Chem. Phys. Lett.* **1989**, *157*, 479–483.

[9] Peterson, K. A.; Dunning, T. H. *J. Phys. Chem.* **1995**, *99*, 3898–3901.

[10] Bak, K. L.; Jørgensen, P.; Olsen, J.; Helgaker, T.; Klopper, W. *J. Chem. Phys.* **2000**, *112*, 9229–9242.

[11] Mukherjee, D.; Moitra, R. K.; Mukhopadhyay, A. *Mol. Phys.* **1975**, *30*, 1861–1888.

[12] Jeziorski, B.; Monkhorst, H. J. *Phys. Rev. A* **1981**, *24*, 1668–1681.

[13] Jeziorski, B.; Paldus, J. *J. Chem. Phys.* **1988**, *88*, 5673–5687.

[14] Piecuch, P.; Oliphant, N.; Adamowicz, L. *J. Chem. Phys.* **1993**, *99*, 1875–1900.

[15] Mahapatra, U. S.; Datta, B.; Mukherjee, D. *J. Chem. Phys.* **1999**, *110*, 6171–6188.

[16] Kállay, M.; Szalay, P. G.; Surján, P. R. *J. Chem. Phys.* **2002**, *117*, 980–990.

[17] Evangelista, F. A.; Allen, W. D.; Schaefer III, H. F. *J. Chem. Phys.* **2007**, *127*, 024102.

[18] Musiał, M.; Perera, A.; Bartlett, R. J. *J. Chem. Phys.* **2011**, *134*, 114108.

[19] Köhn, A.; Hanauer, M.; Mück, L. A.; Jagau, T.-C.; Gauss, J. *WIREs Comput. Mol. Sci.* **2013**, *3*, 176–197.

[20] Shirley, W. A.; Petersson, G. A. *Chem. Phys. Lett.* **1991**, *181*, 588–590.

[21] Kucharski, S. A.; Bartlett, R. J. *J. Chem. Phys.* **1999**, *110*, 8233–8235.

[22] Martin, J. M. *Mol. Phys.* **2014**, *112*, 785–793.

[23] Hu, C. H.; Shen, M.; Schaefer III, H. F. *J. Am. Chem. Soc.* **1993**, *115*, 2923–2929.

[24] Barrows, S. E.; Storer, J. W.; Cramer, C. J.; French, A. D.; Truhlar, D. G. *J. Comput. Chem.* **1998**, *19*, 1111–1129.

[25] Zhao, Y.; Tishchenko, O.; Gour, J. R.; Li, W.; Lutz, J. J.; Piecuch, P.; Truhlar, D. G. *J. Phys. Chem. A* **2009**, *113*, 5786–5799.

[26] Yang, J.; Hu, W.; Uysvat, D.; Matthews, D.; Schütz, M.; Chan, G. K.-L. *Science* **2014**, Accepted.

[27] Feller, D.; Dixon, D. A. *J. Phys. Chem. A* **2003**, *107*, 9641–9651.

[28] Hopkins, B. W.; Tschumper, G. S. *J. Phys. Chem. A* **2004**, *108*, 2941–2948.

[29] Klopper, W.; Bachorz, R. A.; Tew, D. P.; Aguilera-Iparraguirre, J.; Carissan, Y.; Hättig, C. *J. Phys. Chem. A* **2009**, *113*, 11679–11684.

[30] Nguyen, T. L.; Li, J.; Dawes, R.; Stanton, J. F.; Guo, H. *J. Phys. Chem. A* **2013**, *117*, 8864–8872.

[31] Itano, W. M. *Phys. Rev. A* **2006**, *73*, 022510.

[32] van der Tak, F.; Müller, H.; Harding, M.; Gauss, J. *arXiv:0909.0390 [astro-ph]* **2009**, arXiv: 0909.0390.

[33] Cheng, L.; Stopkowicz, S.; Stanton, J. F.; Gauss, J. *J. Chem. Phys.* **2012**, *137*, 224302.

[34] Crawford, T. D.; Tam, M. C.; Abrams, M. L. *J. Phys. Chem. A* **2007**, *111*, 12057–12068.

[35] Pedersen, T. B.; Kongsted, J.; Crawford, T. D. *Chirality* **2009**, *21*, E68–E75.

[36] Bartlett, R. J. *Annu. Rev. Phys. Chem.* **1981**, *32*, 359–401.

[37] Crawford, T. D.; Schaefer III, H. F. *Rev. Comp. Chem.* **2000**, *14*, 33.

[38] Shavitt, I.; Bartlett, R. J. *Many-Body Methods in Chemistry and Physics: MBPT and Coupled-Cluster Theory*, 1st ed.; Cambridge University Press: Cambridge ; New York, 2009.

[39] Wick, G. C. *Phys. Rev.* **1950**, *80*, 268–272.

[40] Boys, S. F. *Proc. R. Soc. London* **1950**, *A200*, 542–554.

[41] Slater, J. C. *Phys. Rev.* **1951**, *81*, 385–390.

[42] Slater, J. C. *Phys. Rev.* **1953**, *91*, 528–530.

[43] Pople, J. A.; Nesbet, R. K. *J. Chem. Phys.* **1954**, *22*, 571.

[44] Brueckner, K. A. *Phys. Rev.* **1955**, *100*, 36–45.

[45] Goldstone, J. *Proc. R. Soc. Lond. A* **1957**, *239*, 267–279.

[46] BRANDOW, B. H. *Rev. Mod. Phys.* **1967**, *39*, 771–828.

[47] Tajti, A.; Szalay, P. G.; Császár, A. G.; Kállay, M.; Gauss, J.; Valeev, E. F.; Flowers, B. A.; Vázquez, J.; Stanton, J. F. *J. Chem. Phys.* **2004**, *121*, 11599–11613.

[48] Bomble, Y. J.; Vázquez, J.; Kállay, M.; Michauk, C.; Szalay, P. G.; Császár, A. G.; Gauss, J.; Stanton, J. F. *J. Chem. Phys.* **2006**, *125*, 064108.

[49] Harding, M. E.; Vázquez, J.; Ruscic, B.; Wilson, A. K.; Gauss, J.; Stanton, J. F. *J. Chem. Phys.* **2008**, *128*, 114111.

[50] Karton, A.; Rabinovich, E.; Martin, J. M. L.; Ruscic, B. *J. Chem. Phys.* **2006**, *125*, 144108.

[51] Karton, A.; Taylor, P. R.; Martin, J. M. L. *J. Chem. Phys.* **2007**, *127*, 064104.

[52] Karton, A.; Martin, J. M. L. *J. Chem. Phys.* **2010**, *133*, 144102.

[53] Kucharski, S. A.; Bartlett, R. J. *J. Chem. Phys.* **1992**, *97*, 4282–4288.

[54] Kucharski, S. A.; Kolaski, M.; Bartlett, R. J. *J. Chem. Phys.* **2001**, *114*, 692–700.

[55] Robinson, D. *J. Comput. Chem.* **2013**, *34*, 2625–2634.

[56] Yang, K. R.; Jalan, A.; Green, W. H.; Truhlar, D. G. *J. Chem. Theory Comput.* **2013**, *9*, 418–431.

[57] Bomble, Y. J.; Stanton, J. F.; Kállay, M.; Gauss, J. *J. Chem. Phys.* **2005**, *123*, 4101.

[58] Kállay, M.; Gauss, J. *J. Chem. Phys.* **2005**, *123*, 214105–214105–13.

[59] Stanton, J. F.; Bartlett, R. J. *J. Chem. Phys.* **1993**, *98*, 7029.

[60] Krylov, A. I. *Acc. Chem. Res.* **2006**, *39*, 83–91.

[61] Paldus, J.; Čížek, J.; Shavitt, I. *Phys. Rev. A* **1972**, *5*, 50–67.

[62] Scuseria, G. E.; Scheiner, A. C.; Lee, T. J.; Rice, J. E.; Schaefer III, H. F. *J. Chem. Phys.* **1987**, *86*, 2881–2890.

[63] Lee, T. J.; Rice, J. E. *Chem. Phys. Lett.* **1988**, *150*, 406–415.

[64] Scuseria, G. E.; Janssen, C. L.; Schaefer III, H. F. *J. Chem. Phys.* **1988**, *89*, 7382–7387.

[65] Szabo, A.; Ostlund, N. S. *Modern Quantum Chemistry: Introduction to Advanced Electronic Structure Theory*, new edition edition ed.; Dover Publications: Mineola, N.Y, 1996.

[66] Kucharski, S. A.; Bartlett, R. J. *Theor. Chim. Acta* **1991**, *80*, 387–405.

[67] Stanton, J. F. *Chem. Phys. Lett.* **1997**, *281*, 130.

[68] Handy, N. C.; Schaefer III, H. F. *J. Chem. Phys.* **1984**, *81*, 5031–5033.

[69] Fitzgerald, G. *J. Chem. Phys.* **1986**, *85*, 5143.

[70] Scheiner, A. C.; Scuseria, G. E.; Rice, J. E.; Lee, T. J.; Schaefer III, H. F. *J. Chem. Phys.* **1987**, *87*, 5361.

[71] Monkhorst, H. J. *Int. J. Quant. Chem.* **1977**, *12*, 421–432.

[72] Stanton, J. F. et al. CFOUR, Coupled-Cluster techniques for Computational Chemistry, a quantum-chemical program package with the integral packages MOLECULE (J. Almlöf and P. R. Taylor), PROPS (P. R. Taylor), ABACUS (T. Helgaker, H. J. Jensen, P. Jørgensen and J. Olsen), and ECP routines by A. V. Mitin and C. van Wüllen. For the current version, see http://www.cfour.de.

[73] Matthews, D. A.; Gauss, J.; Stanton, J. F. *J. Chem. Theory Comput.* **2013**, *9*, 2567–2572.

[74] Adams, B. G.; Paldus, J. *Phys. Rev. A* **1979**, *20*, 1.

[75] Lawson, C. L.; Hanson, R. J.; Kincaid, D. R.; Krogh, F. T. *ACM Trans. Math. Softw.* **1979**, *5*, 308–323.

[76] Dongarra, J. J.; Du Croz, J.; Hammarling, S.; Hanson, R. J. *ACM Trans. Math. Softw.* **1988**, *14*, 1–17.

[77] Dongarra, J. J.; Du Croz, J.; Hammarling, S.; Duff, I. S. *ACM Trans. Math. Softw.* **1990**, *16*, 1–17.

[78] Stanton, J. F.; Gauss, J.; Watts, J. D.; Bartlett, R. J. *J. Chem. Phys.* **1991**, *94*, 4334–4345.

[79] Gauss, J.; Stanton, J. F.; Bartlett, R. J. *J. Chem. Phys.* **1991**, *95*, 2623.

[80] Kállay, M.; Surján, P. R. *J. Chem. Phys.* **2000**, *113*, 1359.

[81] Kállay, M.; Surján, P. R. *J. Chem. Phys.* **2001**, *115*, 2945.

[82] Van Zee, F. G.; van de Geijn, R. A. *ACM Trans. Math. Softw.* **2013**, Accepted.

[83] Van Zee, F. G.; Smith, T.; Igual, F. D.; Smelyanskiy, M.; Zhang, X.; Kistler, M.; Austel, V.; Gunnels, J.; Low, T. M.; Marker, B.; Killough, L.; van de Geijn, R. A. *ACM Trans. Math. Softw.* **2013**, Accepted pending minor modifications.

[84] Smith, T. M.; van de Geijn, R. A.; Smelyanskiy, M.; Hammond, J. R.; Van Zee, F. G. Anatomy of High-Performance Many-Threaded Matrix Multiplication. 28th IEEE International Parallel & Distributed Processing Symposium (IPDPS 2014). 2014.